EUROPEAN ORGANISATION FOR NUCLEAR RESEARCH (CERN)

JHEP 10 (2023) 001
DOI: 10.1007/JHEP10(2023)001

CERN-EP-2023-033
24th October 2023

Search for leptoquarks decaying into the bτ final state in pp collisions at $\sqrt{s} = 13$ TeV with the ATLAS detector

The ATLAS Collaboration

A search for leptoquarks decaying into the $b\tau$ final state is performed using Run 2 proton–proton collision data from the Large Hadron Collider, corresponding to an integrated luminosity of 139 fb^{-1} at $\sqrt{s}$ = 13 TeV recorded by the ATLAS detector. The benchmark models considered in this search are vector leptoquarks with electric charge of 2/3e and scalar leptoquarks with an electric charge of 4/3e. No significant excess above the Standard Model prediction is observed, and 95% confidence level upper limits are set on the cross-section times branching fraction of leptoquarks decaying into $b\tau$. For the vector leptoquark production two models are considered: the Yang–Mills and Minimal coupling models. In the Yang–Mills (Minimal coupling) scenario, vector leptoquarks with a mass below 1.58 (1.35) TeV are excluded for a gauge coupling of 1.0 and below 2.05 (1.99) TeV for a gauge coupling of 2.5. In the case of scalar leptoquarks, masses below 1.28 (1.53) TeV are excluded for a Yukawa coupling of 1.0 (2.5). Finally, an interpretation of the results with minimal model dependence is performed for each of the signal region categories, and limits on the visible cross-section for beyond the Standard Model processes are provided.

Contents

1 Introduction **2**

2 The ATLAS Detector **5**

3 Data and Monte Carlo Samples **6**

4 Object Reconstruction and Identification **8**

5 Event Selection **10**

6 Background Estimation **11**
6.1 $\tau_{\text{lep}}\,\tau_{\text{had}}$ channel 11
6.2 $\tau_{\text{had}}\,\tau_{\text{had}}$ channel 15

7 Systematic Uncertainties **18**

8 Results **19**

9 Conclusion **27**

1 Introduction

The existing similarities between the structure of the quark and lepton sectors in the Standard Model (SM) suggest the possibility of a new underlying symmetry in particle physics. Leptoquarks (LQs) that couple to both quarks and leptons, with non-zero baryon and lepton numbers, and fractional electric charges are predicted by several beyond the SM theories that attempt to unify the fundamental interactions, such as technicolour [1–3], composite models [4], and grand unification [5–7].

Recent results reported by BaBar [8, 9], Belle [10] and LHCb [11] show hints of deviations from lepton-flavour universality in B-meson decays into final states with $D^{(*)}$ mesons, which could be caused by the existence of LQs. The 4.2 standard deviation disagreement with respect to the SM prediction observed in the anomalous muon magnetic moment measurement [12], though significantly reduced when updated lattice quantum chromodynamics (QCD) calculations [13] are considered, could be caused by LQ contributions to the muon magnetic moment [14].

In light of the lepton-flavour universality anomalies observed in the B-meson decays into $D^{(*)}\tau\nu$ final states, the couplings of LQs to third-generation quarks and leptons are expected to be large [15]. At the LHC, third-generation LQs can be produced singly via quark–gluon fusion and quark–gluon scattering or in pairs via the gluon–gluon fusion process, as shown in the Feynman diagrams in Figure 1. The search presented in this paper is optimised for the single production of third-generation LQ via the $bg \to \text{LQ}\tau \to b\tau\tau$ channel, while LQ pair and non-resonant production processes are also considered since they can also contribute to the $b\tau\tau$ final state. The single LQ production contribution becomes larger than that from LQ pair production at high LQ mass and coupling values. The results are obtained from proton–proton collision data at a centre-of-mass energy of $\sqrt{s}$ = 13 TeV collected by the ATLAS detector [16, 17] at

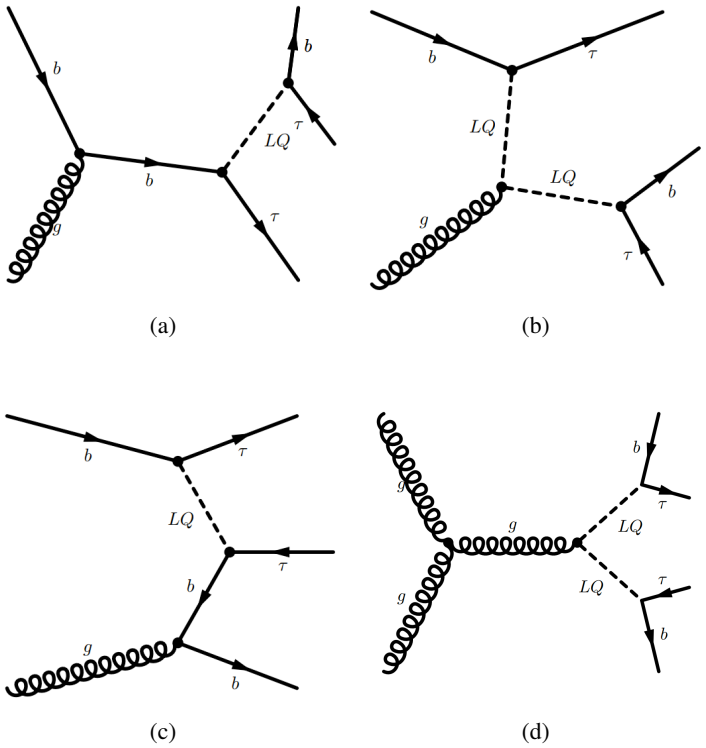

Figure 1: Illustrative Feynman diagrams of (a,b) single LQ production, (c) non-resonant LQ production, and (d) LQ pair production.

the LHC [18] during Run 2 between 2015 and 2018, corresponding to a total integrated luminosity of 139 fb^{-1}.

The vector LQ model chosen for this search is the U_1 model [19], a SU(2)$_{\mathrm{L}}$ singlet with fermion number $F = 3B + L = 0$, where B and L are the baryon and lepton numbers respectively, and an electric charge of $2/3e$. The interaction part of U_1 model Lagrangian is:

$$\mathcal{L}_{U_1} \supset -ig_s(1-\kappa)U^{\dagger}_{1\mu}T^a U_{1\nu}G^{a\mu\nu} + \frac{g_U}{\sqrt{2}}[U^{\mu}_1(\beta^{ij}_{\mathrm{L}}\bar{q}^i_{\mathrm{L}}\gamma_\mu \ell^j_{\mathrm{L}} + \beta^{ij}_{\mathrm{R}}\bar{d}^i_{\mathrm{R}}\gamma_\mu e^j_{\mathrm{R}}) + \mathrm{h.c.}],$$

where $T^a = \lambda^a/2$ with $\lambda^a (a = 1,\cdots,8)$ are the Gell-Mann matrices, g_s is the QCD coupling, q_{L} (ℓ_{L}) denotes the left-handed quark (lepton) doublets and d_{R} (e_{R}) denotes the right-handed down-type quark (charged-lepton) singlets. The i and j indices represent the flavour generation. A summation over the colour indices is performed and omitted for clarity. The term $-ig_s(1-\kappa)U^{\dagger}_{1\mu}T^a U_{1\nu}G^{a\mu\nu}$ describes the interaction between U_1 leptoquarks and SM gluon gauge fields $G^{a\mu\nu}$. In this analysis, two vector LQ scenarios are considered: the Yang–Mills (U_1^{YM}) coupling scenario, $\kappa = 0$, and the Minimal (U_1^{MIN}) coupling scenario, $\kappa = 1$. The β^{ij}_{L} and β^{ij}_{R} parameters describe the coupling between U_1 leptoquarks and left-handed or right-handed charged leptons and quarks, respectively. In the framework of the U_1^{YM} and U_1^{MIN} scenarios, the probability to decay into the b-quark and τ-lepton final state is predicted to be the same as to decay into the top-quark and neutrino final state. Hence, the branching fraction $\mathcal{B}$ of the LQ decays into a b-quark and a τ-lepton is set to 0.5. In this search, all of β^{ij}_{R} are set to zero, β^{33}_{L} is set to one

and other β_{L}^{ij} are set to zero, such that each LQ decays into a b-quark and a τ-lepton or into a top-quark and a neutrino. Due to these choices, the gauge coupling (λ) between U_1 leptoquarks and third-generation charged leptons and quarks can be written as $\lambda = g_U \beta_{\mathrm{L}}^{33}/\sqrt{2}$.

The scalar LQ model $\widetilde{S_1}$ is also considered, with $F = 3B + L = -2$ and electric charge of $4/3e$ [20, 21]. There are three parameters in this model: the branching fraction $\mathcal{B}$ into charged leptons, the LQ to τb Yukawa coupling parameter λ, and the mass term of the LQ. Following Ref. [21], the Lagrangian terms for $\widetilde{S_1}$ LQs related to this analysis are:

$$\mathcal{L}_{\widetilde{S_1}} \supset +\lambda^{ij} \bar{d}_{\mathrm{R}}^{Ci} \widetilde{S_1} e_{\mathrm{R}}^{j} + \text{h.c.},$$

where C in the superscript stands for the charge conjugation operation. The terms e_{R} and d_{R} are the right-handed charged leptons and down-type quarks and λ^{ij} represents the Yukawa couplings between $\widetilde{S_1}$, charged leptons, and quarks, where the ij refers to the generations of the quark and charged lepton. In the framework of the $\widetilde{S_1}$ model, the only non-zero Yukawa coupling considered in this paper is the coupling to a b-quark and a τ-lepton. Since only the coupling to the third-generation charged lepton and quark is considered, $\lambda^{33} = \lambda$ is assumed to be different from zero, while the rest of the λ^{ij} are set to zero.

Most of the previous searches for LQs performed by the ATLAS [22–28] and CMS [29–32] collaborations have been conducted on different final states compared to this search. For third generation LQs, the CMS Collaboration has recently published results of searches for LQs decaying into $t\nu$ and $b\tau$ [33]. The ATLAS Collaboration performed a search for pair produced scalar LQs in $b\tau b\tau$ final states with 36 fb^{-1} of proton–proton collision data at $\sqrt{s} = 13$ TeV that excluded scalar LQs with masses below 1 TeV, assuming a LQ to $b\tau$ branching fraction equal to one [34].

The analysis described in this paper is the first search by the ATLAS Collaboration for singly produced LQs decaying into $b\tau$. The search is performed over a LQ mass (m_{LQ}) in the range of 0.4 TeV to 2.5 TeV. The λ range is chosen to be between 0.5 and 2.5 to cover possible regions where LQs could explain the anomalies observed in the B-meson decay and is extended to large λ where the single LQ production channel provides a significant contribution compared to the pair-production process. In the case of the vector LQ production, the contribution from LQs decaying into $t\nu$ is neglected.

The analysis starts from the selection of a pair of oppositely charged τ-leptons produced in association with a jet identified as containing a b-hadron (b-jet). The main backgrounds to the search are the $t\bar{t}$ and tW production processes. Two signatures are considered, containing either a $\tau_{\mathrm{lep}}\tau_{\mathrm{had}}$ or $\tau_{\mathrm{had}}\tau_{\mathrm{had}}$ pair, where τ_{had} (τ_{lep}) refers to a τ-lepton decaying into hadrons and a neutrino (two neutrinos and an electron or a muon). In each of these two analysis channels, events are classified, based on the transverse momentum (p_{T}) of the b-jet, in two categories of low and high b-jet p_{T}. The search for LQs is only performed in the high b-jet p_{T} category, where the effect from the interference of non-resonant LQ production with SM processes is expected to be small [35]. The non-resonant contribution can be significantly modified by the interference contribution, which depends on the signal model parameters [35, 36]. The effect of the interference with SM diagrams, such as those from $Z/\gamma^*(\rightarrow \tau\tau) + b$-jet, is neglected. Due to the lack of detailed studies of the interference effect, an additional search is performed considering both high and low b-jet p_{T} categories and not relying on a specific LQ model choice for its signal description (henceforth called 'model-independent'), and covering a wider range of beyond-SM signatures. For this search, the results are expressed in terms of the visible cross-section of the beyond-SM signal.

The next sections discuss the ATLAS detector in Section 2, data and simulated samples in Section 3, followed by the object reconstruction and definitions in Section 4. Section 5 discusses the overall analysis

strategy and event selection, then Section 6 goes into more details of the background estimation methods. The systematic uncertainties are discussed in Section 7 followed by the results in Section 8, with the conclusion in Section 9.

2 The ATLAS Detector

The ATLAS detector [16] at the LHC covers nearly the entire solid angle around the collision point.[1] It consists of an inner tracking detector surrounded by a thin superconducting solenoid, electromagnetic and hadron calorimeters, and a muon spectrometer incorporating three large superconducting air-core toroidal magnets.

The inner-detector system (ID) is immersed in a 2 T axial magnetic field and provides charged-particle tracking in the range of $|\eta| < 2.5$. The high-granularity silicon pixel detector covers the vertex region and typically provides four measurements per track, the first hit normally being in the insertable B-layer installed before Run 2 [17, 37]. It is followed by the silicon microstrip tracker, which usually provides eight measurements per track. These silicon detectors are complemented by the transition radiation tracker (TRT), which enables radially extended track reconstruction up to $|\eta| = 2.0$. The TRT also provides electron identification information based on the fraction of hits (typically 30 in total) above a higher energy-deposit threshold corresponding to transition radiation.

The calorimeter system covers the pseudorapidity range of $|\eta| < 4.9$. Within the region $|\eta| = 3.2$, electromagnetic calorimetry is provided by barrel and endcap high-granularity lead/liquid-argon (LAr) calorimeters, with an additional thin LAr presampler covering $|\eta| < 1.8$ to correct for energy loss in material upstream of the calorimeters. Hadron calorimetry is provided by the steel/scintillator-tile calorimeter, segmented into three barrel structures within $|\eta| = 1.7$, and two copper/LAr hadron endcap calorimeters. The solid angle coverage is completed by forward copper/LAr and tungsten/LAr calorimeter modules optimised for electromagnetic and hadronic energy measurements respectively.

The muon spectrometer (MS) comprises separate trigger and high-precision tracking chambers measuring the deflection of muons in a magnetic field generated by the superconducting air-core toroidal magnets. The field integral of the toroids ranges between 2.0 and 6.0 T m across most of the detector. A set of precision chambers covers the region $|\eta| < 2.7$ with three layers of monitored drift tubes, complemented by cathode-strip chambers in the forward region, where the background is highest. The muon trigger system covers the range of $|\eta| < 2.4$ with resistive-plate chambers in the barrel, and thin-gap chambers in the endcap regions.

Interesting events are selected by the first-level trigger system implemented in custom hardware, followed by selections made by algorithms implemented in software in the high-level trigger [38]. The first-level trigger accepts events from the 40 MHz bunch crossings at a rate below 100 kHz, which the high-level trigger reduces in order to record events to disk at about 1 kHz.

An extensive software suite [39] is used in data simulation, in the reconstruction and analysis of real and simulated data, in detector operations, and in the trigger and data acquisition systems of the experiment.

[1] ATLAS uses a right-handed coordinate system with its origin at the nominal interaction point (IP) in the centre of the detector and the z-axis along the beam pipe. The x-axis points from the IP to the centre of the LHC ring, and the y-axis points upwards. Cylindrical coordinates (r, ϕ) are used in the transverse plane, ϕ being the azimuthal angle around the z-axis. The pseudorapidity is defined in terms of the polar angle θ as $\eta = -\ln\tan(\theta/2)$. Angular distance is measured in units of $\Delta R \equiv \sqrt{(\Delta\eta)^2 + (\Delta\phi)^2}$.

3 Data and Monte Carlo Samples

The data were collected using unprescaled single-lepton and single τ_{had} triggers. A more detailed description of the triggers used in the analysis for each data-taking period is given in Section 5. Quality criteria are applied to events to ensure that the data were not affected by any hardware- or software-related issues [40].

Monte Carlo (MC) simulated events of single LQs decaying into $b\tau$ were produced for masses ranging from 0.4 TeV to 2.5 TeV. The signal samples were produced at leading order (LO) in QCD in the five-flavour scheme using the MadGraph5_aMC@NLO 2.8.1 [41] generator with the NNPDF3.0nnlo [42] parton distribution function (PDF) followed by parton shower (PS) and hadronisation with Pythia 8.244 [43] using the A14 set of tuned parameters (tune) [44] and the NNPDF2.3lo PDF set. Single scalar and vector LQ signal samples were produced with coupling parameters λ from 0.5 to 2.5. The intrinsic width of the LQs increases quadratically with λ and linearly as a function of m_{LQ}. In the considered range of parameters, the LQ width is 16% or less of the LQ mass. The simulated signal events do not include interference effects with the SM processes. For the vector LQ signal two samples were produced for each λ, one with Yang–Mills coupling ($\kappa = 0$) and the other with minimal coupling ($\kappa = 1$). The implementation of the signal model is based on that described in Refs. [20, 21, 45].

Simulated events with pair produced scalar LQs were generated at next-to-leading order (NLO) in QCD with MadGraph5_aMC@NLO 2.6.0, using the LQ model described in Ref. [46], which adds PS to the fixed-order NLO QCD calculations [47, 48] interfaced to Pythia 8.230 for the PS and hadronisation. Parton luminosities are provided by the five-flavour scheme NNPDF3.0nlo PDF set with a value of the strong coupling constant $\alpha_s = 0.118$, and the underlying event was modelled with the A14 tune. The LQ pair-production cross-sections were obtained from the calculation of direct top-squark pair production assuming that all other supersymmetric particles are heavier, since the production modes of this process are the same as the LQ pair production. The cross-sections were computed at approximate next-to-next-to-leading order (NNLO) in QCD with resummation of next-to-next-to-leading logarithmic (NNLL) soft gluon terms [49–52]. The cross-sections do not include lepton t-channel contributions, which are neglected in Ref. [46] and may lead to corrections at the percent level [53].

Simulated events with pair-produced vector LQs were generated with MadGraph5_aMC@NLO 2.6.0 at LO in QCD, using the LQ model of Ref. [19] and the NNPDF3.0nlo PDF set with $\alpha_s = 0.118$. Decays of the LQs were performed with MadSpin, while PS and hadronisation were simulated using Pythia 8.244 with the A14 tune. Since no higher-order cross-sections are available for this model, the LO MadGraph5_aMC@NLO cross-sections were used.

Several simulation samples are used to model the expected background processes. These include $t\bar{t}$, single top-quark, Z and W bosons produced in association with jets (Z+jets and W+jets), and diboson events.

The production of $t\bar{t}$ simulated events was performed with the Powheg Box v2 [54–57] generator at NLO with the NNPDF3.0nlo PDF set [58] and the h_{damp} parameter[2] set to 1.5 m_{top} [59], with $m_{\text{top}} = 172.5$ GeV. The events were interfaced to Pythia 8.230 [43] to model the PS, hadronisation, and underlying event, with parameters set according to the A14 tune and using the NNPDF2.3lo set of PDFs. The $t\bar{t}$ sample was normalised to the cross-section prediction at NNLO in QCD including the resummation of NNLL calculated using Top++ 2.0 [60–66].

[2] The h_{damp} parameter is a resummation damping factor and one of the parameters that controls the matching of Powheg matrix elements to the PS and thus effectively regulates the high-p_{T} radiation against which the $t\bar{t}$ system recoils.

Single top-quark s-channel (t-channel) production was simulated using the POWHEG BOX v2 generator at NLO in QCD in the five-flavour (four-flavour) scheme with the NNPDF3.0NLO set of PDFs. The events were interfaced with PYTHIA 8.230 using the A14 tune and the NNPDF2.3LO PDF set. The samples were normalised to the theory prediction calculated at NLO in QCD with HATHOR 2.1 [67, 68]. Similarly, the associated production of top quarks with W bosons (tW) was modelled by the POWHEG BOX v2 generator at NLO in QCD using the five-flavour scheme and the NNPDF3.0NLO set of PDFs. The diagram removal scheme [69] was used to remove interference and overlap with $t\bar{t}$ production. The related uncertainty is estimated by comparison with an alternative sample generated using the diagram subtraction scheme [59, 69]. The events were interfaced to PYTHIA 8.230 using the A14 tune and the NNPDF2.3LO set of PDFs.

For the production of Z/γ^* sample, the POWHEG BOX v1 [55–57, 70] generator was used for the simulation at NLO accuracy of the hard-scattering processes of Z boson production and decay into the electron, muon, and τ-lepton channels. It was interfaced to PYTHIA 8.186 [71] for the modelling of the PS, hadronisation, and underlying event, with parameters set according to the AZNLO tune [72]. The CT10NLO PDF set [73] was used for the hard-scattering processes, whereas the CTEQ6L1 PDF set [74] was used for the PS. The effect of QED final-state radiation was simulated with PHOTOS++ 3.52 [75, 76].

The production of W+jets events was generated with SHERPA 2.2.1 [77]. In this set-up, NLO-accurate matrix elements for up to two partons and LO-accurate matrix elements for up to four partons were calculated with the Comix [78] and OPENLOOPS [79–81] libraries. The default SHERPA PS [82] based on Catani–Seymour dipole factorisation and the cluster hadronisation model [83] were used. They employed the dedicated set of tuned parameters developed by the SHERPA authors and the NNPDF3.0NNLO PDF set [58]. The NLO matrix elements for a given jet multiplicity were matched to the PS using a colour-exact variant of the MC@NLO algorithm [84]. Different jet multiplicities were then merged into an inclusive sample using an improved CKKW matching procedure [85, 86] that is extended to NLO accuracy using the MEPS@NLO prescription [87].

Diboson production was simulated with the SHERPA 2.2.1 or 2.2.2 generator depending on the process. Fully leptonic final states and semileptonic final states, where one boson decays leptonically and the other hadronically, were generated using matrix elements at NLO accuracy in QCD for up to one additional parton emission and at LO accuracy for up to three additional parton emissions. Samples for the loop-induced processes $gg \to VV$ were generated using LO-accurate matrix elements for up to one additional parton emission for both the fully leptonic and semileptonic final states. The matrix element calculations were matched and merged with the SHERPA PS based on Catani–Seymour dipole factorisation using the MEPS@NLO prescription. The virtual QCD corrections were provided by the OPENLOOPS library. The NNPDF3.0NNLO set of PDFs were used, along with the dedicated set of tuned PS parameters developed by the SHERPA authors. The samples were normalised to a NLO prediction.

A summary of all the features used for the simulation of the signal and background processes is shown in Table 1. In all samples except those produced with SHERPA 2.2.1 or SHERPA 2.2.2, decays of heavy-flavour hadrons were modelled with EVTGEN 1.2.0 or EVTGEN 1.6.0 program [88], depending on the process. All samples of simulated events were processed through the ATLAS detector simulation [89] based on GEANT4 [90]. The effects of multiple interactions in the same and nearby bunch crossings (pile-up) were modelled by overlaying minimum-bias events simulated using the soft QCD processes of PYTHIA 8.186 [71] with the A3 tune [91] and the NNPDF2.3LO PDF set.

Table 1: Overview of the MC generators used for the main signal and background samples. The last column specifies the order in QCD for the cross-section calculation used for the normalisation of the simulated samples.

Process	Generator		PDF set		Tune	Normalisation
	ME	PS	ME	PS		
LQ→ $b\tau$	MadGraph5_aMC@NLO	Pythia 8.244	NNPDF3.0nnlo	NNPDF2.3lo	A14	LO
Scalar LQLQ→ $b\tau b\tau$	MadGraph5_aMC@NLO	Pythia 8.230	NNPDF3.0nnlo	NNPDF2.3lo	A14	NNLO + NNLL
Vector LQLQ→ $b\tau b\tau$	MadGraph5_aMC@NLO	Pythia 8.244	NNPDF3.0nnlo	NNPDF2.3lo	A14	LO
$t\bar{t}$	Powheg Box v2	Pythia 8.230	NNPDF3.0nnlo	NNPDF2.3lo	A14	NNLO + NNLL
Single top	Powheg Box v2	Pythia 8.230	NNPDF3.0nnlo	NNPDF2.3lo	A14	NLO
Z/γ^*	Powheg Box v1	Pythia 8.186	CT10nlo	CTEQ6L1	AZNLO	NLO
W+jets	Sherpa 2.2.1		NNPDF3.0nnlo		Sherpa	NNLO
Diboson	Sherpa 2.2.1/Sherpa 2.2.2		NNPDF3.0nnlo		Sherpa	NLO

4 Object Reconstruction and Identification

Tracks measured in the ID are used to reconstruct the interaction vertices [92]. The primary vertex of the hard interaction is chosen as the proton–proton vertex candidate with the highest sum of the squared transverse momenta of the associated tracks.

Electrons are reconstructed from topological clusters of energy deposits in the electromagnetic calorimeter that are matched to a track reconstructed in the ID [93]. In the $\tau_{\text{lep}}\tau_{\text{had}}$ ($\tau_{\text{had}}\tau_{\text{had}}$) final state, the selected (rejected) electrons are required to satisfy the 'medium' ('loose') identification criteria and have $p_{\text{T}} > 20\,\text{GeV}$ (15 GeV). Moreover, electrons are required to be within $|\eta_{\text{cluster}}| = 2.47$ with the exclusion of the region between the barrel and endcap calorimeters ($1.37 < |\eta_{\text{cluster}}| < 1.52$). An additional 'loose' isolation criterion [93] is also required, which has an efficiency of 90% for candidates with $p_{\text{T}} > 15\,\text{GeV}$, increasing to more than 98% for candidates with $p_{\text{T}} > 30\,\text{GeV}$.

Muons are reconstructed from signals in the MS matched with tracks inside the ID. In the $\tau_{\text{lep}}\tau_{\text{had}}$ final state, the selected muons are required to satisfy the 'medium' identification criteria with an average efficiency of 97%, and have $p_{\text{T}} > 25\,\text{GeV}$ and $|\eta| < 2.5$. In the $\tau_{\text{had}}\tau_{\text{had}}$ chanel, muons having $p_{\text{T}} > 7\,\text{GeV}$ are rejected if they satisfy the 'loose' identification criteria. A 'tight' isolation criterion [94] based on track information and having an average efficiency of 89% is also applied.

Jets are reconstructed with a particle-flow algorithm, which combines energy deposits in the calorimeter with ID tracks [95], using the anti-k_t algorithm [96, 97] with a radius parameter $R = 0.4$. Only jets with $|\eta| < 2.5$ and $p_{\text{T}} > 25\,\text{GeV}$ are considered. The 'tight' working point of the jet vertex tagger (JVT) [98] algorithm is selected to remove jets with $p_{\text{T}} < 60\,\text{GeV}$ and $|\eta| < 2.4$ that are identified as not being associated with the primary vertex of the hard interaction. Jets containing b-hadrons are identified using the DL1r b-tagging algorithm [99, 100]. A 70% efficiency working point is used, with the efficiencies being measured in simulated $t\bar{t}$ events. The corresponding rejection factors (defined as the reciprocal of the efficiency values) for b-tagged jets initiated by c-quarks and light partons are 9.4 and 390 respectively.

The τ_{had} decays are composed of a neutrino and a set of visible decay products, most frequently one or three charged pions and up to two neutral pions. The visible decay products of the τ_{had} decay are denoted by $\tau_{\text{had-vis}}$. The reconstruction of the $\tau_{\text{had-vis}}$ is seeded by jets reconstructed by the anti-k_t algorithm [96], using calibrated topological clusters [101] as inputs, with a radius parameter of $R = 0.4$ [102]. Reconstructed tracks are matched to $\tau_{\text{had-vis}}$ candidates and a multivariate discriminant is used to assess whether these tracks are likely to have been produced by the charged τ_{had} decay products, rejecting tracks originating from other interactions, nearby jets, photon conversions or misreconstructed tracks. The $\tau_{\text{had-vis}}$ objects

are required to have one or three associated charged-particle tracks selected by this discriminant. Their charge (q) is defined as the sum of the measured electric charges of these associated tracks and is required to be $|q| = 1$. The $\tau_{\text{had-vis}}$ objects are also required to satisfy $p_{\text{T}} > 20\,\text{GeV}$ and $|\eta| < 2.5$, excluding the region $1.37 < |\eta| < 1.52$. To separate the $\tau_{\text{had-vis}}$ candidates produced by hadronic τ-lepton decays from those due to jets initiated by quarks or gluons, a recurrent neural network (RNN) identification algorithm [103] (τ_{had}-ID) is constructed using information from reconstructed charged-particle tracks and calorimeter-energy clusters associated with $\tau_{\text{had-vis}}$ candidates. This analysis uses two τ_{had}-ID working points: 'medium', which has a 75% (60%) acceptance efficiency and a background rejection of 35 (240) and 'loose', which has a 85% (75%) acceptance efficiency and a background rejection of 21 (90) for τ_{had} with one (three) charged-particle tracks. A 'very loose' working point, having a 95% acceptance efficiency, is also used for background estimation. A separate boosted decision tree discriminant ('eBDT') is also used to reject backgrounds arising from electrons misidentified as $\tau_{\text{had-vis}}$. This discriminant is built using information from the calorimeter and the ID, most notably transition radiation information from the TRT system and variables sensitive to the ratio of the energy deposited in the calorimeter to the visible momentum measured from the reconstructed tracks.

The reconstructed objects used in this analysis are not built from disjoint sets of tracks or calorimetric clusters. It is therefore possible that two different objects share most of their constituents. An overlap removal procedure is applied to resolve this ambiguity. This procedure is summarised in Table 2.

The missing transverse momentum vector, $\vec{E}_{\text{T}}^{\text{miss}}$, is reconstructed as the negative vector sum of the transverse momenta of leptons, $\tau_{\text{had-vis}}$ and jets, and a 'soft-term' [104]. The soft-term is calculated as the vectorial sum of the $\vec{p}_{\text{T}}$ of tracks matched to the primary vertex but not associated with a reconstructed lepton, $\tau_{\text{had-vis}}$ or jet. The magnitude of $\vec{E}_{\text{T}}^{\text{miss}}$ is referred to as the missing transverse energy, $E_{\text{T}}^{\text{miss}}$.

Table 2: Criteria applied to overlapping reconstructed objects. The criteria are listed in the order they are applied.

Object to keep	Object to remove	Criteria
Electron	Electron	If they share the same track, the electron with the highest transverse momentum is kept.
Electron	$\tau_{\text{had-vis}}$	If $\Delta R < 0.2$, the electron is kept.
Muon	$\tau_{\text{had-vis}}$	If $\Delta R < 0.2$, the muon is kept.
Muon	Electron	If they share a track, the electron is removed if the muon is associated with a signature in the MS, otherwise the muon is removed.
Electron	Jet	Any jet within $\Delta R = 0.2$ of an electron is removed.
Muon	Jet	Any jet within $\Delta R = 0.2$ of a muon is removed if it has fewer than three associated tracks.
Jet	Electron	Any electron within $\Delta R = 0.4$ of a jet is removed.
Jet	Muon	Any muon within $\Delta R = 0.4$ of a jet is removed.
$\tau_{\text{had-vis}}$	Jet	Any jet within $\Delta R = 0.2$ of a $\tau_{\text{had-vis}}$ is removed.

5 Event Selection

Events are required to contain at least one primary vertex with at least two associated tracks.

For the $\tau_{\text{lep}}\tau_{\text{had}}$ channel events were selected by single-lepton triggers. In 2015 single-electron triggers were simultaneously active with p_{T} thresholds of 24, 60 and 120 GeV [105]. For data from 2016 onward the p_{T} thresholds are 26, 60 and 140 GeV. Similarly to the single-electron triggers, the single-muon triggers had p_{T} thresholds of 20 and 50 GeV for 2015, and 26 and 50 GeV from 2016 [106]. The trigger thresholds were raised to keep the trigger rates sufficiently low as the luminosity was increased. The lowest p_{T} threshold electron and muon triggers also have an isolation requirement. The lepton isolation and identification requirements loosen as the trigger p_{T} thresholds increase. Events must contain at least one τ_{had} candidate and exactly one electron or one muon. The electron or muon must be isolated and satisfy the medium lepton identification. Events with more than one lepton satisfying the medium identification are rejected, considering electrons (muons) with a p_{T} greater than 15 (7) GeV. This helps to reject $Z/\gamma^* \to ee/\mu\mu$ events and $Z/\gamma^* \to \tau_{\text{lep}}\tau_{\text{lep}}$. Furthermore, the electron and muon candidates are required to have $p_{\text{T}} > 30$ GeV, and be matched to the trigger object that caused the event to be selected. The τ_{had} candidate is required to have $p_{\text{T}} > 50$ GeV, satisfy the medium τ_{had}-ID selection and have $|\eta| < 2.3$. The pseudorapidity selection requirement rejects events with τ_{had} candidates in a region with a higher background contamination and large uncertainties in the determination of the rate of electrons misidentified as τ_{had}.

In the $\tau_{\text{had}}\tau_{\text{had}}$ channel, events were selected by a single τ_{had} trigger [107]. For 2015 and 2016, three single τ_{had} triggers were available with p_{T} thresholds of 80, 125 and 160 GeV. In 2017 and 2018, due to higher instantaneous luminosity, only the $p_{\text{T}} > 160$ GeV trigger threshold was used. The τ_{had} identification requirements become less stringent as the trigger p_{T} thresholds rise. Events must contain at least two τ_{had} candidates where the leading τ_{had} candidate in p_{T} must be matched to the trigger within an angular distance of $\Delta R = 0.2$ and have p_{T} that is at least 5 GeV above the trigger threshold. The subleading-p_{T} τ_{had} candidate is required to have $p_{\text{T}} > 65$ GeV. Identification requirements are applied to both τ_{had} candidates; the leading-p_{T} τ_{had} must satisfy the medium selection and the subleading-p_{T} τ_{had} the loose selection. Events that contain any electron or muon that satisfies the loose identification requirements are rejected, which ensures orthogonality to the $\tau_{\text{lep}}\tau_{\text{had}}$ channel.

Events passing the previous requirements are then selected with criteria that are similar between the two channels. The two τ_{had} or the electron/muon (denoted by ℓ) and τ_{had} must have opposite electric charges and at least one b-tagged jet is required. The invariant mass of the visible decay products of the two τ-leptons, $m_{\text{vis}}(\ell, \tau_{\text{had}})$ or $m_{\text{vis}}(\tau_{\text{had}}, \tau_{\text{had}})$, is required to be above 100 GeV, which is effective at reducing the $Z/\gamma^* \to \tau\tau$ background. An additional requirement $\Delta\phi(\ell, E_{\text{T}}^{\text{miss}}) < 1.5$ is applied in the $\tau_{\text{lep}}\tau_{\text{had}}$ channel to reduce single top and $t\bar{t}$ events.

The variable S_{T} is defined as the scalar p_{T} sum of the two $\tau_{\text{had-vis}}$ (or ℓ and $\tau_{\text{had-vis}}$) and the leading-p_{T} b-jet. A minimum requirement of $S_{\text{T}} > 300$ GeV is applied, as there is almost no improvement in the expected results of the analysis, discussed in Section 8, by adding events with lower S_{T} values.

The selection criteria described above define the signal region (SR) of the analysis. The signal acceptance times efficiency of the event selection varies between 3% and 10%, depending on the LQ mass and coupling. The efficiency is defined as the ratio of events passing the selection in each channel with respect to the signal events of the $b\tau_{\text{lep}}\tau_{\text{had}}$ and $b\tau_{\text{had}}\tau_{\text{had}}$ final states, respectively. Events in the SR of each channel are assigned to two categories of low (< 200 GeV) and high (> 200 GeV) transverse momentum of the leading-p_{T} b-jet. The two categories are called high and low b-jet p_{T} SRs, respectively. The high b-jet

p_{T} SR is found to perform better for low-mass singly produced LQs, where the resonant contribution is dominant. Conversely, the low b-jet p_{T} SR has a better acceptance for high mass signals, where the non-resonant contribution is dominant for signals with $m_{\mathrm{LQ}} \geq 0.9$ TeV. This split into two categories improves the expected results of the analysis, discussed in Section 8, by up to 30%.

Alternative selections define the control regions (CR), used to evaluate the contribution of the main background processes in the SR, and the validation regions (VR), used to verify the good modelling of the backgrounds. The selection requirements used for the signal regions are summarised in Table 3. The use of the control and validation regions in the background estimation methods is discussed in Section 6.

Table 3: Definition of signal regions (SR) used in the $\tau_{\mathrm{lep}}\tau_{\mathrm{had}}$ and $\tau_{\mathrm{had}}\tau_{\mathrm{had}}$ channel. The symbol ℓ represents the selected electron or muon candidate and $\tau_{\text{had-vis}}$ represents the leading $\tau_{\text{had-vis}}$ candidate. The symbol τ_1 (τ_2) represents the leading (sub-leading) $\tau_{\text{had-vis}}$ candidate.

$\tau_{\mathrm{lep}}\tau_{\mathrm{had}}$ Signal Regions	Selection
SR	ℓ (trigger, isolated), $\tau_{\text{had-vis}}$ (medium τ_{had}-ID), $q(\ell) \times q(\tau_{\text{had-vis}}) < 0$, $\Delta\phi(\ell, E_{\mathrm{T}}^{\mathrm{miss}}) < 1.5$, $m_{\mathrm{vis}}(\ell, \tau_{\text{had-vis}}) > 100$ GeV, $S_{\mathrm{T}} > 300$ GeV, at least one b-jet
High b-jet p_{T} SR	SR selection, leading b-jet $p_{\mathrm{T}} > 200$ GeV
Low b-jet p_{T} SR	SR selection, leading b-jet $p_{\mathrm{T}} < 200$ GeV
$\tau_{\mathrm{had}}\tau_{\mathrm{had}}$ Signal Regions	Selection
SR	τ_1 (trigger, medium τ_{had}-ID), τ_2 (loose τ_{had}-ID), $q(\tau_1) \times q(\tau_2) < 0$, $m_{\mathrm{vis}}(\tau_1, \tau_2) > 100$ GeV, $S_{\mathrm{T}} > 300$ GeV, at least one b-jet
High b-jet p_{T} SR	SR selection, leading b-jet $p_{\mathrm{T}} > 200$ GeV
Low b-jet p_{T} SR	SR selection, leading b-jet $p_{\mathrm{T}} < 200$ GeV

6 Background Estimation

6.1 $\tau_{\mathrm{lep}}\,\tau_{\mathrm{had}}$ channel

Control and validation regions are used in the analysis to estimate and study the modelling of the main background processes. The selection requirements used for the CR and VR in the $\tau_{\mathrm{lep}}\tau_{\mathrm{had}}$ channel are summarised in Table 4.

In the $\tau_{\mathrm{lep}}\tau_{\mathrm{had}}$ channel the dominant background contributions are from $t\bar{t}$ and single top-quark events. Processes involving top quarks can produce real τ-leptons, or jets that are misidentified as τ_{had}, and are estimated by using simulation with data-driven corrections. The $t\bar{t}$ and tW contributions are treated as one combined top-quark background due to their similar kinematics and final states. In the low (high) b-jet p_{T} SR, $t\bar{t}$ accounts for 90% (86%) of all top-quark processes and 96% (97%) of the single top-quarks are from tW. To ensure that this background is accurately modelled, a top-quark control region (Top-CR) is defined. With respect to the SR selection, the requirements on the leading b-jet p_{T} and the S_{T} are removed, and the condition $\Delta\phi(\ell, E_{\mathrm{T}}^{\mathrm{miss}}) < 1.5$ is replaced by $\Delta\phi(\ell, E_{\mathrm{T}}^{\mathrm{miss}}) > 2.5$. This results in a region with a purity of 91% in top-quark processes and negligible signal contamination. Out of all top-quark events in the Top-CR, 91% are from $t\bar{t}$ processes and ~97% of the single top-quark events are from tW, which is compatible with the composition of the SRs.

Table 4: Definition of the background-enriched control regions (CR) and validation regions (VR) used in the $\tau_{\text{lep}}\tau_{\text{had}}$ channel. The symbol ℓ represents the selected electron or muon candidate and $\tau_{\text{had-vis}}$ represents the leading $\tau_{\text{had-vis}}$ candidate.

$\tau_{\text{lep}}\tau_{\text{had}}$ Control/Validation Regions	Selection	Purpose
Multijet-CR	ℓ (trigger, pass/fail offline isolation), $m_{\text{T}}(\ell, E_{\text{T}}^{\text{miss}}) < 30$ GeV, one b-jet, τ_{had}-ID score < 0.01, $E_{\text{T}}^{\text{miss}} < 50$ GeV	Measure lepton fake-factor
Top-CR	Satisfy SR except: $\Delta\phi(\ell, E_{\text{T}}^{\text{miss}}) > 2.5$, no S_{T} and lead. b-jet p_{T} req.	Derive top correction
SS-CR	Satisfy SR except: $q(\ell) \times q(\tau_{\text{had-vis}}) > 0$, no $\Delta\phi(\ell, E_{\text{T}}^{\text{miss}})$, and S_{T} req.	Measure jet$\rightarrow\tau$ background scale factor
High b-jet p_{T} VR	Satisfy high b-jet p_{T} SR except: $1.5 < \Delta\phi(\ell, E_{\text{T}}^{\text{miss}}) < 2.5$, 300 GeV $< S_{\text{T}} <$ 600 GeV	Background modelling validation
Low b-jet p_{T} VR	Satisfy low b-jet p_{T} SR except: $1.5 < \Delta\phi(\ell, E_{\text{T}}^{\text{miss}}) < 2.5$, 300 GeV $< S_{\text{T}} <$ 600 GeV	Background modelling validation
b-jet Z-CR	Satisfy SR except: 45 GeV $< m_{\text{vis}}(\ell, \tau_{\text{had-vis}}) <$ 80 GeV, $p_{\text{T}}(\ell)/p_{\text{T}}(b\text{-jet}) > 0.8$, $\lvert\Delta\phi(\ell, \tau_{\text{had-vis}})\rvert > 2.4$, no S_{T} req.	Z+heavy-flavour jets normalisation factor

A discrepancy between the data and simulation prediction is observed in the Top-CR, with the simulation overestimating the background contribution. Recent measurements of differential cross-sections have demonstrated that the current simulations of $t\bar{t}$ processes overestimate the upper tail of the top-quark p_{T} spectrum [108, 109]. The discrepancy varies depending on S_{T}; for this reason, a correction is derived as a function of S_{T} in this region based on the ratio between data and simulation. A top-quark correction scale factor is defined in Eq. (1) and is applied to all $t\bar{t}$ and single top-quark simulated events. The comparison between data and the background prediction in the Top-CR and the derived correction as a function of S_{T} are shown in Figure 2, where $t\bar{t}$ and tW events with a generated lepton reconstructed as a lepton (a 'true' lepton) and a jet misidentified as a τ_{had} are included under the *Jet*$\rightarrow\tau$ *fake* contribution. This demonstrates that the Top-CR is dominated by $t\bar{t}$ and tW events with true leptons and τ_{had} in the final state, thus this correction does not account for mismodelling due to jets being misidentified as τ_{had}. The modelling of events with a true lepton and jet misidentified as a τ_{had} in the final state is discussed later in this section.

The top-quark correction scale factor is defined as a function of S_{T}:

$$SF_{\text{Top}}(S_{\text{T}}) = \frac{(N_{\text{data}} - N_{\text{non-Top}})(S_{\text{T}})}{N_{\text{Top}}(S_{\text{T}})}, \tag{1}$$

where N_{data} and N_{Top} represent respectively the number of data events and of $t\bar{t}$ plus single top-quark events predicted by simulation, N_{Top} includes events with both true and misidentified τ_{had} in the final state and $N_{\text{non-Top}}$ includes all the other backgrounds estimated by using simulation. The resulting correction is well fitted by a linear function, which is used to derive the correction scale factors. The correction is also derived with an alternative logarithmic function: $SF_{\text{Top}}(S_{\text{T}}) = a\ln(S_{\text{T}}) + b$, and the difference between the two corrections is taken as an uncertainty on the correction. Additional uncertainties related to the cross-section and acceptance of the top-quark processes, as well as the statistical and cross-section uncertainties related to the subtraction of the contribution from the other processes, are applied to account for the slight difference between the fractions of top-quark events that are due to $t\bar{t}$ production in the Top-CR and SRs and for the extrapolation to the SR. The scale factor is applied at the per-event level to the $t\bar{t}$ plus single top-quark events passing the selections of the signal, control or validation regions. The total uncertainty in the scale factor varies between 4% and 7% for S_{T} in the range of 300–700 GeV. Different

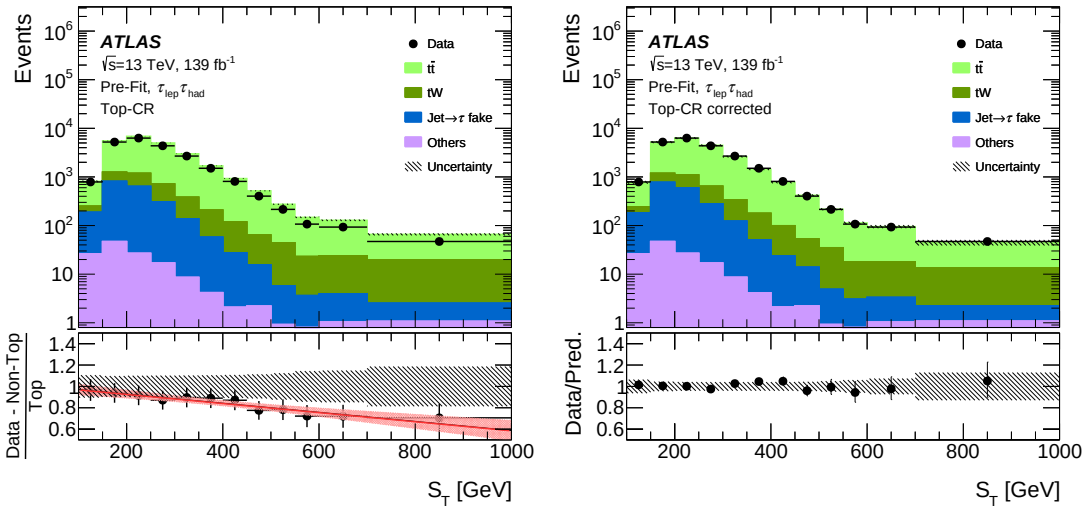

(a) (b)

Figure 2: (a) Comparison between data and the background prediction for the S_{T} distribution in the Top-CR in the $\tau_{\mathrm{lep}}\tau_{\mathrm{had}}$ channel. The $t\bar{t}$ and tW contributions only include events with true leptons and τ_{had} in the final state. The label *Jet→ τ fake* corresponds to events with a lepton and a quark- or gluon-initiated jet misidentified as τ_{had}; this contribution is estimated by using simulation. The bottom panel shows the ratio of the data to the prediction where the uncertainty shown by both the points and hatched band includes the statistical uncertainty in the data and background predictions, the theoretical uncertainty in the MC simulation predictions, and the MC subtraction uncertainty. Finally, the line and the cross dashed band show the resulting fit and the associated uncertainty. The label 'Top' in the bottom panel denotes the sum of $t\bar{t}$ and tW processes, while 'Non-Top' refers to all other processes considered. Entries with values above the x-axis range are included in the last bin of the distribution. (b) Shows the same distribution after the top-quark correction scale factor is applied to the $t\bar{t}$ and tW simulated events. Only the uncertainty associated to the top-quark correction and the statistical uncertainty on data and simulation are considered.

binning choices for the S_{T} distribution were also considered, but the impact on the $SF_{\mathrm{Top}}(S_{\mathrm{T}})$ uncertainty is found to be below 5% and therefore not considered as an additional source of uncertainty.

Another source of background in the $\tau_{\mathrm{lep}}\,\tau_{\mathrm{had}}$ channel stems from multi-jet events, where jets can mimic both the τ_{lep} and τ_{had}. This type of background from multi-jet events is estimated via a data-driven fake-factor method by deriving a lepton fake-factor. The lepton fake-factor is measured in the multi-jet control region (multijet-CR) that is enriched in multi-jet events, but is similar kinematically to the SR. The events are still required to satisfy the single lepton trigger and to have exactly one b-jet, but the identification algorithm to reject jets misidentified as τ_{had} is instead used to select multi-jet events by requiring an extremely low value for τ_{had} RNN identification score (corresponding to only 1% acceptance for true τ_{had}). Additional selection criteria on $m_{\mathrm{T}}(\ell, E_{\mathrm{T}}^{\mathrm{miss}}) < 30$ GeV and $E_{\mathrm{T}}^{\mathrm{miss}} < 50$ GeV are applied to increase the purity of multi-jet events relative to other backgrounds. The fake-factor is measured with a requirement on the leading b-jet $p_{\mathrm{T}} > 25$ GeV and is defined as:

$$FF_{\mathrm{lep}}(p_{\mathrm{T}}(\tau_{\mathrm{lep}}), \eta(\tau_{\mathrm{lep}})) = \frac{(N_{\mathrm{data}} - N_{\mathrm{MC}})^{\mathrm{pass-iso}}(p_{\mathrm{T}}(\tau_{\mathrm{lep}}), \eta(\tau_{\mathrm{lep}}))}{(N_{\mathrm{data}} - N_{\mathrm{MC}})^{\mathrm{fail-iso}}(p_{\mathrm{T}}(\tau_{\mathrm{lep}}), \eta(\tau_{\mathrm{lep}}))}.$$

The variable N_{data} is the total number of data events and N_{MC} is the number of background events predicted

by simulation that contain a true τ_{lep}. Events are split between the numerator and denominator based on whether the τ_{lep} satisfied the lepton isolation requirement or not. The fake-factor is parameterised as a function of the τ_{lep} p_{T} and split into central ($|\eta| < 1.52$) and forward ($|\eta| > 1.52$) regions. The statistical uncertainty on the $FF_{\text{lep}}(p_{\text{T}}(\tau_{\text{lep}}), \eta(\tau_{\text{lep}}))$ fake-factor and simulation-related uncertainties on N_{MC} are considered as systematic uncertainties and propagated to the estimate of the multi-jet background. The uncertainties are in the range of 6–230% as a function of the $\tau_{\text{had-vis}}$ η and p_{T}. A control region is defined by having the same selection as the SR, except that the lepton isolation requirement inverted. Applying the fake-factor at the per-event level, the multi-jet estimate in each SR is then obtained by scaling the distribution in the corresponding control region where the isolation criteria are not satisfied.

An additional source of background are events where a lepton is produced in association with a jet that is misidentified as a τ_{had} (*Jet*$\rightarrow \tau$ *fake*). These contribute approximately 20% to the expected background in the SR and are mostly from $t\bar{t}$ with contributions from W+jets, Z+jets, and diboson events. To ensure that these are well modelled, a 'same-sign' control region (SS-CR) is defined by taking the same selection as the SR, but with a light lepton with the same electric charge as τ_{had}. The requirements on $\Delta\phi(\ell, E_{\text{T}}^{\text{miss}})$, S_{T} and the leading b-jet p_{T} are removed to increase the number of events in the CR. The top-quark correction scale factor derived in Eq. (1) is applied to top-quark events in this region (approximately 81% of the total). As the Top-CR used to derive that scale factor is dominated by $t\bar{t}$ and tW events with true τ-leptons in the final state, it does not correct for mismodelling of jets that are misidentified as a τ_{had}. As a difference between the simulation prediction and the data is still observed, another scale factor is derived to account for any remaining differences from those backgrounds with a lepton and misidentified τ_{had} (approximately 60% of the events in this region). The remaining events contain true τ_{had} and are subtracted, before calculating the scale factor, by applying the top-quark correction scale factor. Then, the scale factor for events with a lepton and a jet misidentified as a τ_{had} is defined as:

$$SF_{\text{fake}-\tau}(p_{\text{T}}(\tau_{\text{had-vis}}), n_{\text{track}}) = \frac{(N_{\text{data}} - N_{\text{true}-\tau})(p_{\text{T}}(\tau_{\text{had-vis}}), n_{\text{track}})}{N_{\text{fake}-\tau}(p_{\text{T}}(\tau_{\text{had-vis}}), n_{\text{track}})},$$

where $N_{\text{true}-\tau}$ is the total number of events predicted by simulation where both the τ_{had} and τ_{lep} are true and $N_{\text{fake}-\tau}$ is the number of predicted events with a jet misidentified as a τ_{had} and a true τ_{lep}. The scale factor is parameterised as a function of $p_{\text{T}}(\tau_{\text{had-vis}})$ and the number of charged-particle tracks (n_{track}). It is applied to any MC background event with a true lepton and a jet misidentified as a τ_{had}. The correction is derived in the SS-CR of the $\tau_\mu\tau_{\text{had}}$ channel and then applied to both $\tau_e\tau_{\text{had}}$ and $\tau_\mu\tau_{\text{had}}$, because the $\tau_e\tau_{\text{had}}$ SS-CR contains events with misidentified electrons, which are not well modelled by simulation. The $SF_{\text{fake}-\tau}$ correction values are in the range of 1–1.2 (1–1.5) for τ_{had} with one (three) charged-particle tracks. The statistical uncertainty on the $SF_{\text{fake}-\tau}$ correction and the simulation-related uncertainties affecting $N_{\text{true}-\tau}$ and $N_{\text{fake}-\tau}$ are propagated to the background estimate as systematic uncertainties. As a function of the $\tau_{\text{had-vis}}$ p_{T}, the uncertainties amount to 15–20% (22–140%) for $\tau_{\text{had-vis}}$ candidates with one (three) associated charged-particle track.

To validate the background modelling in a region depleted in signal, high and low b-jet p_{T} validation regions (high and low b-jet p_{T} VR) are defined by applying the SR requirements, with the exceptions of the $\Delta\phi(\ell, E_{\text{T}}^{\text{miss}}) < 1.5$ and the $S_{\text{T}} > 300$ GeV criteria, that are modified into $1.5 < \Delta\phi(\ell, E_{\text{T}}^{\text{miss}}) < 2.5$ and $300 < S_{\text{T}} < 600$ GeV. The low (high) b-jet p_{T} VR consists of 82% (80%) $t\bar{t}$ events, of 8% (10%) single top-quark events, and of 9% (9%) of events where a jet is misidentified as a τ_{had}. Good modelling of the background is found in the validation regions; the background estimate agrees with data within the total uncertainty, as shown in Figure 3.

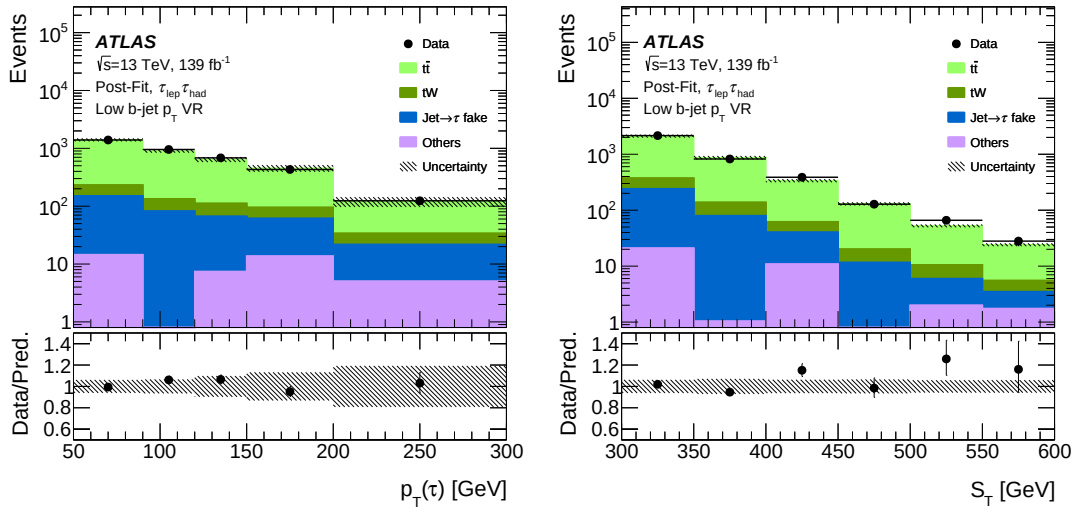

(a) (b)

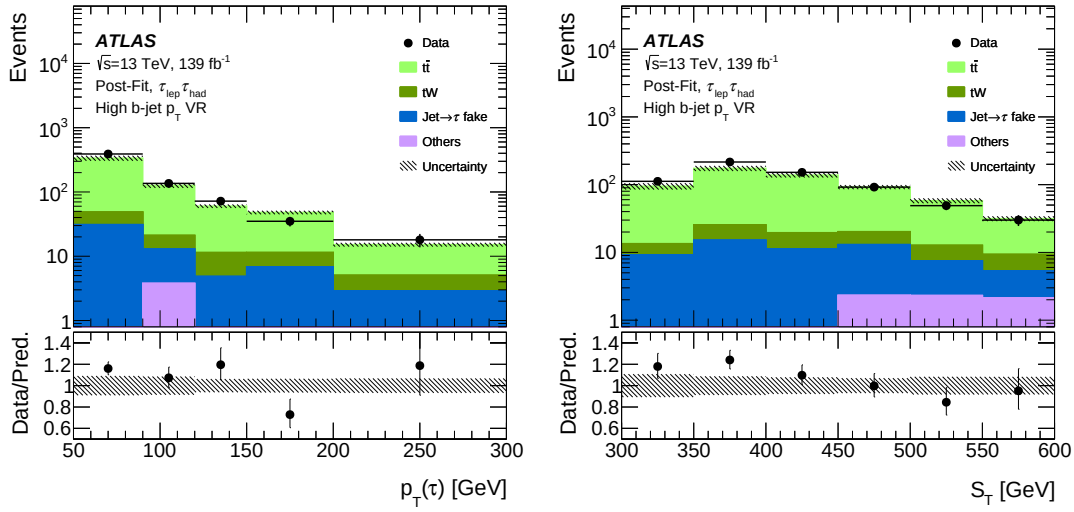

(c) (d)

Figure 3: Comparison between data and the background prediction for the $\tau_{\text{lep}}\,\tau_{\text{had}}$ channel validation regions after applying the scale factors discussed in Section 6.1. (a) and (b) show the $p_{\text{T}}(\tau)$ and S_{T} respectively for the low b-jet p_{T} category, (c) and (d) show the same for the high b-jet p_{T} category. The uncertainty band includes both statistical and systematic uncertainties evaluated in the fit described in Section 8. Entries with values above the x-axis range are included in the last bin of each distribution. The lower panels show the ratio of the data to the predictions.

6.2 $\tau_{\text{had}}\,\tau_{\text{had}}$ channel

In the $\tau_{\text{had}}\tau_{\text{had}}$ channel, the main background sources are $Z/\gamma^* \rightarrow \tau_{\text{had}}\tau_{\text{had}}$ events, as well as top-quark processes, with W bosons decaying to τ_{had}, or to electrons, muons or jets misidentified as τ_{had}. Both $Z/\gamma^* \rightarrow \tau_{\text{had}}\tau_{\text{had}}$ and top-quark backgrounds are estimated using simulation with data-driven corrections, which are discussed further below. The selection requirements used to define the CR and VR in the $\tau_{\text{had}}\tau_{\text{had}}$

channel are summarised in Table 5.

Table 5: Definition of the background-enriched control regions (CR) and validation regions (VR) used in the $\tau_{\text{had}}\tau_{\text{had}}$ channel. The symbol τ_1 (τ_2) represents the leading (sub-leading) $\tau_{\text{had-vis}}$ candidate.

$\tau_{\text{had}}\tau_{\text{had}}$ Control/Validation Regions	Selection	Purpose
Dijet-CR	Satisfy SR except: τ_1 and τ_2 satisfy very loose τ_{had}-ID, τ_1 fail medium τ_{had}-ID	Measure $\tau_{\text{had-vis}}$ fake-factor
CR-1	Satisfy SR except: τ_2 fail loose τ_{had}-ID	Apply $\tau_{\text{had-vis}}$ fake-factor
SS-VR	Satisfy SR except: $q(\tau_1) \times q(\tau_2) > 0$	Multijet modelling check
Z+light flavour jets VR	Satisfy SR except: 0 b-jets, $\Delta\phi(\tau_1, \tau_2) > 0.25$, $m_{\text{vis}}(\tau_1, \tau_2) < 100$ GeV, $E_{\text{T}}^{\text{miss}} > 60$ GeV	Z+light jets modelling

As the mismodelling of the kinematic distributions observed in the $\tau_{\text{lep}}\tau_{\text{had}}$ channel originates from the underlying top-quark process rather than the τ_{had} decay, it is also expected to be present in the $\tau_{\text{had}}\tau_{\text{had}}$ channel. However, due to small number of events in the $\tau_{\text{had}}\tau_{\text{had}}$ channel the statistical uncertainty in the top-quark processes is comparable with the expected mismodelling. This makes it difficult to select a $\tau_{\text{had}}\tau_{\text{had}}$-only control region to quantify this mismodelling. Therefore, the S_{T}-dependent top-quark correction scale factor from Eq. (1) derived in the $\tau_{\text{lep}}\tau_{\text{had}}$ channel is also applied to the $\tau_{\text{had}}\tau_{\text{had}}$ channel. The shape of the S_{T} distribution is checked and found to be compatible between the $\tau_{\text{lep}}\tau_{\text{had}}$ and $\tau_{\text{had}}\tau_{\text{had}}$ channels.

The $Z/\gamma^* \rightarrow \tau_{\text{had}}\tau_{\text{had}}$ background is also modelled using simulation. Due to a known discrepancy in the simulation compared with the data for $Z(\rightarrow \tau\tau)$ + heavy-flavour jets with at least one b- or c-jet (Z+HF) [110], a correction factor for the normalisation of this background is derived in the τ_{lep} τ_{had} b-jet Z-CR, defined in Table 4, which has a purity of around 60% for the Z+HF processes and is inclusive in p_{T} of the leading b-jet. A comparison between the data and the prediction from the simulation in the b-jet Z-CR before deriving the correction factor is shown in Figure 4.

The scale factor is derived by subtracting backgrounds estimated from simulation that are not from the Z+HF process ($N_{\text{non-ZHF}}$):

$$SF_{\text{ZHF}} = \frac{N_{\text{data}} - N_{\text{non-ZHF}}}{N_{\text{ZHF}}},$$

where N_{ZHF} is the number of Z+HF events predicted by simulation.

The scale factor is applied as a normalisation to the total Z+HF contribution, with a value of 1.13 ± 0.23 obtained from the control region. The uncertainty includes the statistical uncertainty, the uncertainty in the subtraction of the simulation events and the extrapolation uncertainty from the control region to the SRs. The extrapolation uncertainty is obtained by repeating the scale factor calculation in the $\tau_{\text{lep}}\tau_{\text{had}}$ channel using selection criteria for the control and signal regions equivalent to the ones used in the $\tau_{\text{had}}\tau_{\text{had}}$ channel.

For $Z(\rightarrow \tau\tau)$ + light-flavour jets (Z+LF, no b- or c-jets), the modelling is validated in a b-veto region (Z+LF VR). This region has the same event selection as the SR, except that zero b-jets are required. In addition, the requirements $m_{\text{vis}} < 100$ GeV, $E_{\text{T}}^{\text{miss}} > 60$ GeV and $\Delta\phi(\tau, \tau) > 0.25$ are applied to ensure a

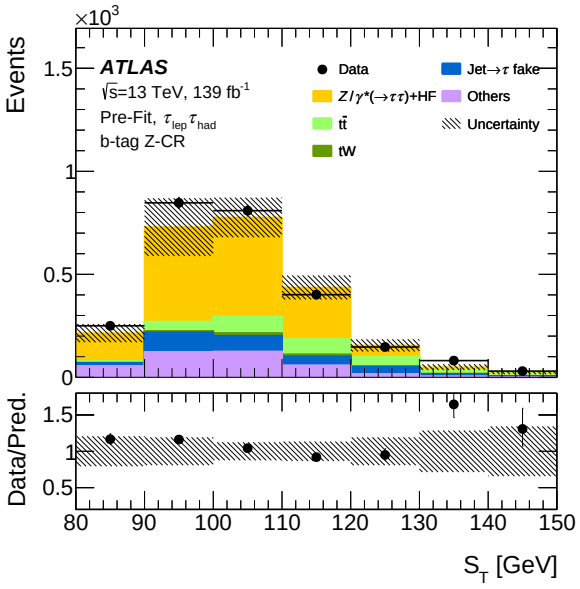

Figure 4: Comparison between data and the background prediction for the S_{T} distribution in the control region used for correcting the $Z(\rightarrow \tau\tau)$ + heavy-flavour jets process. The uncertainty band includes both statistical and systematic components. Entries with values above the x-axis range are included in the last bin of the distribution. The lower panel shows the ratio of the data to the predictions.

high Z+LF purity. The data is found to be in agreement with the simulation within the statistical uncertainty in the data.

Finally the background originating from multi-jet events, where jets are misidentified as τ_{had}, is estimated by using a data-driven fake-factor method. A control region dominated by multi-jet events, called Dijet-CR, is defined by taking events that satisfy one of the single-jet triggers (with thresholds between 15 and 420 GeV). The leading $\tau_{\text{had-vis}}$ candidate is required to not satisfy the medium τ_{had} identification and the subleading $\tau_{\text{had-vis}}$ candidate is used as a probe. Both $\tau_{\text{had-vis}}$ candidates are still required to pass the very loose τ_{had} identification requirement. As for the $\tau_{\mathrm{lep}}\tau_{\mathrm{had}}$ channel, the fake-factor is measured inclusively in the leading b-jet p_{T}. The leading and subleading $\tau_{\text{had-vis}}$ candidates are required to have opposite electric charges and have a $p_{\mathrm{T}} > 65$ GeV. At least one additional b-tagged jet is required, but no selection is made on the leading b-jet p_{T}. Then, the fake-factor is defined as:

$$f_{\tau_{\mathrm{had}}-\mathrm{ID}}(p_{\mathrm{T}}, N_{\mathrm{track}}) \equiv \left.\frac{(N_{\mathrm{data}} - N_{\mathrm{MC}})^{\text{pass } \tau_{\mathrm{had}}-\mathrm{ID}}(p_{\mathrm{T}}, N_{\mathrm{track}})}{(N_{\mathrm{data}} - N_{\mathrm{MC}})^{\text{fail } \tau_{\mathrm{had}}-\mathrm{ID}}(p_{\mathrm{T}}, N_{\mathrm{track}})}\right|_{\mathrm{dijet}},$$

where N_{MC} includes all simulated background events. The pass or fail τ_{had}-ID superscript refers to whether the subleading $\tau_{\text{had-vis}}$ candidate satisfies the loose τ_{had}-ID or not, while still satisfying the very loose requirement. For each of the SRs, the multi-jet estimate is then obtained from the a control region, called CR-1, composed of events in which the subleading $\tau_{\text{had-vis}}$ candidate fails the loose τ_{had}-ID, using the fake-factor:

$$N_{\mathrm{multi-jet}}(p_{\mathrm{T}}, N_{\mathrm{track}}) = f_{\tau_{\mathrm{had}}-\mathrm{ID}}(p_{\mathrm{T}}, N_{\mathrm{track}}) \times (N_{\mathrm{data}} - N_{\mathrm{MC}})^{\text{fail } \tau_{\mathrm{had}}-\mathrm{ID}}(p_{\mathrm{T}}, N_{\mathrm{track}}).$$

The fake-factor is parameterised as a function of the p_{T} and number of charged-particle tracks of the subleading $\tau_{\text{had-vis}}$ candidate. The statistical uncertainty on the $f_{\tau_{\text{had}}-\text{ID}}(p_{\mathrm{T}}, N_{\text{track}})$ fake-factor is considered as systematic uncertainty, and it varies in the range of 4–15% as a function of the $\tau_{\text{had-vis}}$ p_{T}, for $\tau_{\text{had-vis}}$ candidates with both one and three associated charged-particle tracks. For this method to be accurate, it is important that the fail-τ_{had}-ID and multi-jet control regions have a similar composition of quark- and gluon-initiated jets. This is obtained by inspecting the shape of subleading τ_{had} identification scores in the two regions, which depends on the quark–gluon fraction. A lower threshold than the very loose requirement is applied on this score, which ensures that the shapes of the distributions are compatible.

After the selection, the multi-jet contribution to the SR is expected to be small. The modelling of the multi-jet background is verified in the same-sign validation regions (SS-VR). The SS-VR has the same selection as the SR, but the electric charges of the τ_{had} candidates are required to be the same. For key distributions in the low b-jet p_{T} category, the data is found to agree with the background prediction, with approximately half of the events being from $t\bar{t}$ and half from multi-jet background. The selection in the high b-jet p_{T} SS-VR leads to low statistics with 2.8 expected events (mostly from $t\bar{t}$) and 4 observed data events.

7 Systematic Uncertainties

Systematic uncertainties arise from the reconstruction of the various physics objects and from theoretical or modelling uncertainties affecting the predictions for both the backgrounds and signals. These uncertainties manifest themselves in both the overall yield and shape of the final observable, and can be divided into two main groups: the experimental uncertainties and the modelling uncertainties.

The experimental uncertainties include the uncertainties related to the trigger, reconstruction, calibration and identification of electrons [93], muons [94], taus [102] and jets [98, 99, 111]; for electron and muons, additional uncertainties in the lepton isolation are considered. Uncertainties related to background with misidentified τ-leptons are described in Section 6. Another source of experimental uncertainties is given by the luminosity measurement, whose primary measurement is obtained using the LUCID-2 detector [112]. An uncertainty value of 1.7% [113] is assigned for the combined 2015–2018 integrated luminosity.

Among the experimental uncertainties, the ones with the highest impact on the analysis sensitivity are the $\tau_{\text{had-vis}}$ related uncertainties, with an impact on the results in the range of 30–40% depending on the LQ coupling and mass values considered. The uncertainties in the $\tau_{\text{had-vis}}$ identification efficiency are in the range of 2% to 6%, while the eBDT efficiency uncertainties are of the order of 1% to 2%. These uncertainties are parameterised as a function of the $\tau_{\text{had-vis}}$ p_{T} and the number of associated tracks for the $\tau_{\text{had-vis}}$ identification efficiency, and as a function of the τ_{had} decay mode for the eBDT efficiency. In both cases, the uncertainties are derived in dedicated tag and probe measurements [102]. The $\tau_{\text{had-vis}}$ reconstruction efficiency uncertainty is derived from comparisons between simulations using different detector geometries or GEANT4 physics lists; this uncertainty is parameterised as a function of true $\tau_{\text{had-vis}}$ p_{T} and is between 1% and 1.5%. For the $\tau_{\text{had-vis}}$ energy scale, the total uncertainty is in the range of 1% to 4% of the $\tau_{\text{had-vis}}$ p_{T}, arising from a combination of measurements: a direct measurement with $Z \to \tau\tau \to \mu\tau_{\text{had-vis}} + 3\,\nu$ events, measurements of the calorimeter response to single particles, and comparisons between simulations using different detector geometries or GEANT4 physics lists. This uncertainty is also parameterised as a function of the $\tau_{\text{had-vis}}$ p_{T} and the number of associated tracks.

The uncertainties in the background modelling include uncertainties in the top-quark, Z+jets and diboson backgrounds, as well as multijet events in which quark- or gluon-initiated jets are misidentified as a τ_{had}. Among the background modelling uncertainties, the ones related to the top-quark background have the largest impact on the analysis sensitivity, with an impact on the results in the range of 40–50% depending on the LQ coupling and mass values. This uncertainty is extracted by comparing nominal and alternative $t\bar{t}$ and single top-quark MC samples in the phase space of the SR and Top-CR. For each sample, a dedicated data-driven S_{T}-dependent correction is applied before the comparison. The difference between the nominal and alternative samples in the S_{T} distribution is taken as the uncertainty in the top-quark processes. The alternative samples have variations of the initial/final-state radiation, matrix element and PS compared to the nominal sample. To derive the initial/final-state radiation uncertainty, the generator parameters used to produce the nominal samples are varied. The matrix element to PS NLO matching uncertainty is derived by comparing the MadGraph5_aMC@NLO and Powheg predictions while keeping the same generator for the PS component. For the PS, the uncertainty is derived by a comparison with an alternative sample generated by using Herwig for the PS while keeping the same generator for the hard-scattering simulation component. The uncertainties in the background modelling originating from the PDF and α_S uncertainties are found to be less than 1% and are neglected. Finally, an uncertainty in the tW interference for the single top-quark background is estimated by comparing the nominal sample, where the diagram removal scheme is applied, to an alternative sample that uses the diagram subtraction scheme [114].

The uncertainties in the signal modelling include those from the signal cross-section and acceptance due to renormalisation scale (μ_R) and factorisation scale (μ_F) variations, PDF and α_S. The μ_R and μ_F uncertainties are estimated through an envelope of the variations obtained from scaling μ_R and μ_F by a factor between 0.5 and 2, while keeping their ratio between 0.5 and 2. The uncertainties due to the NNPDF3.0nlo PDF set and α_S are evaluated following the PDF4LHC recommendation [115].

8 Results

The distribution of the S_{T} variable for the events of the signal regions defined in Table 3 for the $\tau_{\text{lep}}\tau_{\text{had}}$ and $\tau_{\text{had}}\tau_{\text{had}}$ channels, is used as final discriminant between the leptoquark signal and the background. The statistical analysis of the data is performed using the profile likelihood ratio method [116], to test whether a model can be rejected given the observed data. As the model under test is a signal plus background hypothesis, the chosen parameter of interest is the signal strength, μ, defined as the ratio of the observed to the predicted value of the signal cross-section times branching fraction. The likelihood function $\mathcal{L}(\mu, \theta)$ is then constructed as a product of Poisson probability terms for each bin of the distributions. It depends on μ and on the nuisance parameters θ, which encode systematic uncertainties that can affect the signal and background distributions and are constrained using Gaussian probability density functions. The asymptotic approximation is used when constructing the test statistic $\tilde{q}_u$ [117] from the likelihood ratio, defined as $\tilde{q}_\mu = -2\ln(\mathcal{L}(\mu, \hat{\hat{\theta}})/\mathcal{L}(\hat{\mu}, \hat{\theta}))$ where $\hat{\mu}$ and $\hat{\theta}$ are the parameters that define the global maximum-likelihood function and $\hat{\hat{\theta}}$ are the nuisance parameters that give the maximum likelihood for a given value of μ. To ensure a reliable estimation of the backgrounds in the fit model, the binning in S_{T} is optimised so that sufficient background events (greater than 10) are present in each bin of the pre-fit distribution. No significant excess above the background expectations is observed and corresponding limits on production cross-sections of the LQ signals are set.

For the LQ results interpretation, only the high b-jet p_{T} signal regions from the $\tau_{\text{lep}}\tau_{\text{had}}$ and $\tau_{\text{had}}\tau_{\text{had}}$ channels are considered and fit simultaneously. For the high b-jet p_{T} signal regions, the contribution from

the non-resonant LQ production process is small. Therefore the interference between the LQ non-resonant processes and the SM processes is not expected to be substantial in these SRs, and it is neglected. By setting $\mu = 0$ in the profile likelihood ratio, the test statistic can be used to check for compatibility with the background-only hypothesis. The data are first fit under the background-only hypothesis and the resulting post-fit distributions are found to be in good agreement with the data, as shown in Figure 5. Table 6 shows the yields for the $\tau_{\text{lep}}\tau_{\text{had}}$ and $\tau_{\text{had}}\tau_{\text{had}}$ channels, respectively.

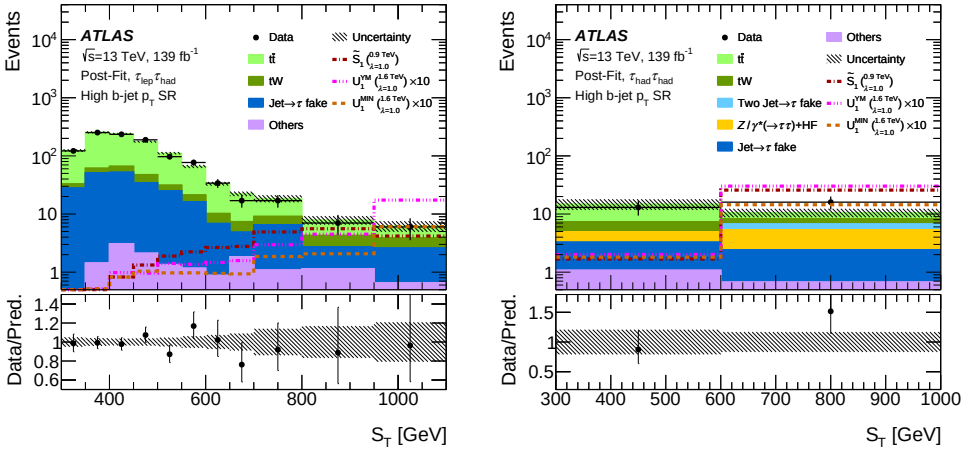

(a) (b)

Figure 5: Post-fit distributions of the discriminating variable S_{T} in the high b-jet p_{T} signal region for the (a) $\tau_{\text{lep}}\tau_{\text{had}}$ and (b) $\tau_{\text{had}}\tau_{\text{had}}$ channels. The two channels are fit simultaneously considering the background-only hypothesis. The lower panels show the ratio of the data to the predictions, where the uncertainty band includes both statistical and systematic post-fit errors. Entries with values above the x-axis range are included in the last bin of each distribution. For illustrative purposes, the dotted lines show the expectation from three singly produced scalar and vector LQ signals.

As good agreement is found between the data and the background expectation, upper limits are set on the cross-section assuming that the branching fraction $\mathcal{B}(\text{LQ} \to b\tau)$ is 100% in the case of the $\widetilde{S}_1$ model and 50% for the U_1^{YM} and U_1^{MIN} scenarios. This is performed using the frequentist CL_s method [116]. A production cross-section for a given signal scenario is excluded at the 95% confidence level (CL) when $\text{CL}_\text{s} < 0.05$.

The results are interpreted considering all LQ production modes in the U_1 model. Several values of the coupling λ are considered, each one with a value of the coupling parameter κ of 0 or 1. The exclusion limits for the single plus non-resonant plus pair vector LQ production are shown in Figure 6. The behaviour of the upper limits as a function of m_{LQ} reflects the signal acceptance times efficiency of the analysis. Figure 7 shows the vector LQ limits in the $\lambda - m_{\text{LQ}}$ plane for each of the κ coupling values considered.

The same procedure is used to interpret the results for single, non-resonant and pair production of scalar LQs from the $\widetilde{S}_1$ model. The single $\widetilde{S}_1$ production and the combined single plus non-resonant plus pair $\widetilde{S}_1$ production are considered. The 95% CL_s limits on the $\widetilde{S}_1$ production cross-section are derived as a function of LQ mass for various assumptions on the coupling λ value. The single plus non-resonant plus pair $\widetilde{S}_1$ production result is shown in Figure 8. The exclusion limits in the $\lambda - m_{\text{LQ}}$ plane are shown in Figure 9.

The observed and expected limits on the LQ mass for the various signal production modes considered are

Table 6: Post-fit background yields in the high b-jet p_{T} signal region of $\tau_{\mathrm{lep}}\tau_{\mathrm{had}}$ and $\tau_{\mathrm{had}}\tau_{\mathrm{had}}$ channels. 'Jet$\rightarrow \tau$ *fake*' indicates the events with a true lepton and a quark- or gluon-initiated jet misidentified as a τ_{had}. The 'Two jet$\rightarrow \tau$ *fake*' indicates the events where two jets are misidentified as τ_{had}. 'Others' in $\tau_{\mathrm{lep}}\tau_{\mathrm{had}}$ includes $Z(\rightarrow \tau\tau)$+LF jets, diboson, W+jets and $Z(\rightarrow ee,\mu\mu)$+jets while 'Others' in $\tau_{\mathrm{had}}\tau_{\mathrm{had}}$ includes $Z(\rightarrow \tau\tau)$+LF jets, diboson and W+jets. The results are extracted from a fit assuming the background-only hypothesis.

Process	$\tau_{\mathrm{lep}}\tau_{\mathrm{had}}$	$\tau_{\mathrm{had}}\tau_{\mathrm{had}}$
$t\bar{t}$	764 ± 82	9.9 ± 2.6
Single top	65 ± 35	3.9 ± 1.0
Jet$\rightarrow \tau$ *fake*	215 ± 79	3.9 ± 1.0
Two jet$\rightarrow \tau$ *fake*	–	1.34 ± 0.27
$Z(\rightarrow \tau\tau)$+HF jets	5.5 ± 0.4	4.6 ± 1.1
Others	9.7 ± 1.0	1.75 ± 0.30
Total	1059 ± 51	25.4 ± 4.9
Data	1053	29

Table 7: Observed (expected) 95% lower limits on the LQ mass in high b-jet p_{T} signal region for the singly plus non-resonant and singly plus non-resonant plus pair produced LQs. All limits are reported in TeV.

Model	$\lambda = 1.0$	$\lambda = 1.7$	$\lambda = 2.5$
Single+non-resonant U_1^{YM} production	1.31 (1.43)	1.59 (1.73)	2.03 (2.27)
Single+non-resonant U_1^{MIN} production	1.15 (1.24)	1.45 (1.58)	1.98 (2.26)
Single+non-resonant+pair U_1^{YM} production	1.58 (1.64)	1.70 (1.81)	2.05 (2.28)
Single+non-resonant+pair U_1^{MIN} production	1.35 (1.44)	1.52 (1.63)	1.99 (2.26)
Single+non-resonant $\widetilde{S}_1$ production	1.04 (1.11)	1.26 (1.38)	1.49 (1.62)
Single+non-resonant+pair $\widetilde{S}_1$ production	1.28 (1.37)	1.38 (1.49)	1.53 (1.67)

reported in Table 7. This analysis is the first ATLAS result for the search of singly produced LQs in the $b\tau\tau$ final state. Vector LQs in the U_1 Yang-Mills (Minimal coupling) model are excluded below masses of 1.56 (1.29) TeV for all λ values; $\widetilde{S}_1$ masses below 1.26 TeV are excluded for all λ values. The observed limits obtained are less stringent than the expected limits, which is mostly driven by the higher data yields relative to the predicted yields in the highest S_{T} bin in the $\tau_{\mathrm{had}}\tau_{\mathrm{had}}$ channel. Overall the $\tau_{\mathrm{had}}\tau_{\mathrm{had}}$ channel is more sensitive than the $\tau_{\mathrm{lep}}\tau_{\mathrm{had}}$ channel due to the smaller background and the larger signal to background ratio in the last S_{T} bin. This difference arises from the larger $t\bar{t}$ background for the $b\tau_{\mathrm{lep}}\tau_{\mathrm{had}}$ final state in the most sensitive part of the S_{T} spectrum.

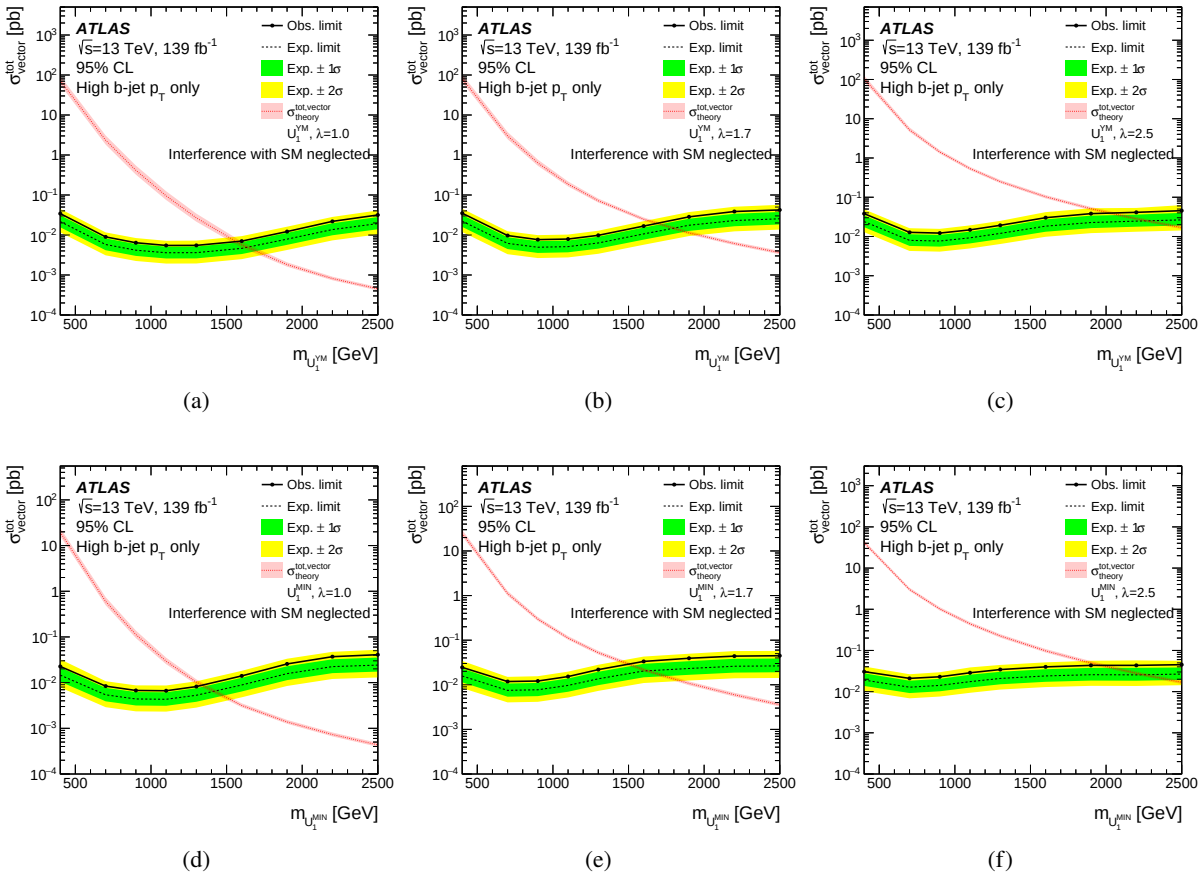

Figure 6: Observed (solid line) and expected (dashed line) 95% CL upper limits on the cross-section of single plus non-resonant plus pair vector LQ production from the combination of the high b-jet p_{T} signal region for the $\tau_{\mathrm{lep}}\tau_{\mathrm{had}}$ and $\tau_{\mathrm{had}}\tau_{\mathrm{had}}$ channels. The dotted curve indicates the total theoretical predictions for singly, non-resonant and pair-produced vector LQ at LO. The top row shows the U_1^{YM} model ($\kappa = 0$) with (a) $\lambda = 1.0$, (b) $\lambda = 1.7$ and (c) $\lambda = 2.5$. The bottom row shows the U_1^{MIN} model ($\kappa = 1$) with (d) $\lambda = 1.0$, (e) $\lambda = 1.7$ and (f) $\lambda = 2.5$. The interference of the non-resonant LQ production with SM processes is expected to be small in the high b-jet p_{T} category and it is neglected.

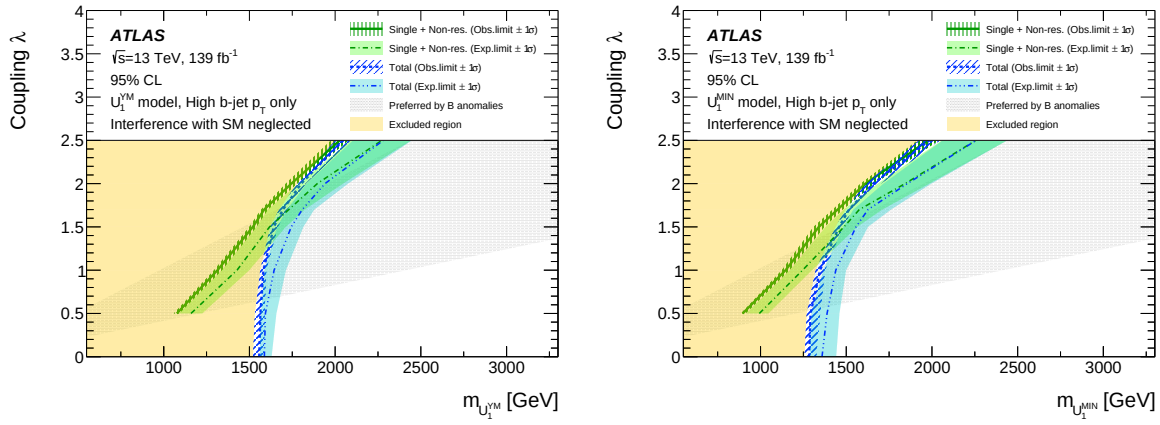

(a) (b)

Figure 7: The two-dimensional 95% CL exclusion limits in the $\lambda - m_{\mathrm{LQ}}$ plane for singly plus non-resonant produced vector LQ (green lines) and for the sum, referred as *Total*, of single plus non-resonant plus pair vector LQ production (blue lines), with (a) showing the case with $\kappa = 0$ and (b) the case with $\kappa = 1$. Regions to the left of the lines are excluded. The dotted area shows the preferred region where the chosen LQ model can explain observed B anomalies [118]. The interference of the non-resonant LQ production with SM processes is expected to be small in the high b-jet p_{T} category and it is neglected.

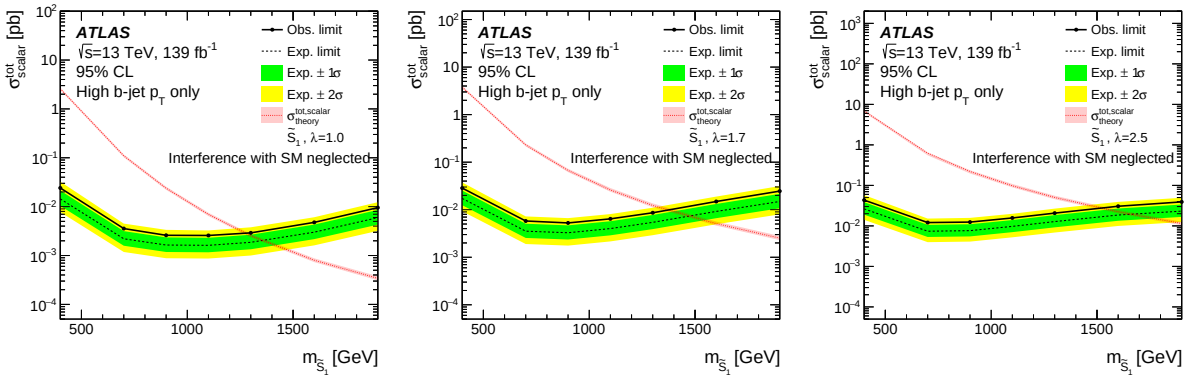

(a) (b) (c)

Figure 8: Observed (solid line) and expected (dashed line) 95% CL upper limits for (a) $\lambda = 1.0$, (b) $\lambda = 1.7$ and (c) $\lambda = 2.5$ on the cross-section of single plus non-resonant plus pair $\widetilde{S_1}$ production hypotheses from the combination of the high b-jet p_{T} signal region for the $\tau_{\mathrm{lep}}\tau_{\mathrm{had}}$ and $\tau_{\mathrm{had}}\tau_{\mathrm{had}}$ channels. The dotted curve indicates the total theoretical predictions for singly, non-resonant and pair-produced scalar LQ. The prediction for singly plus non-resonant produced $\widetilde{S_1}$ (pair-produced $\widetilde{S_1}$) is calculated at LO (NNLO+NNLL). The interference of the non-resonant LQ production with SM processes is expected to be small in the high b-jet p_{T} category and it is neglected.

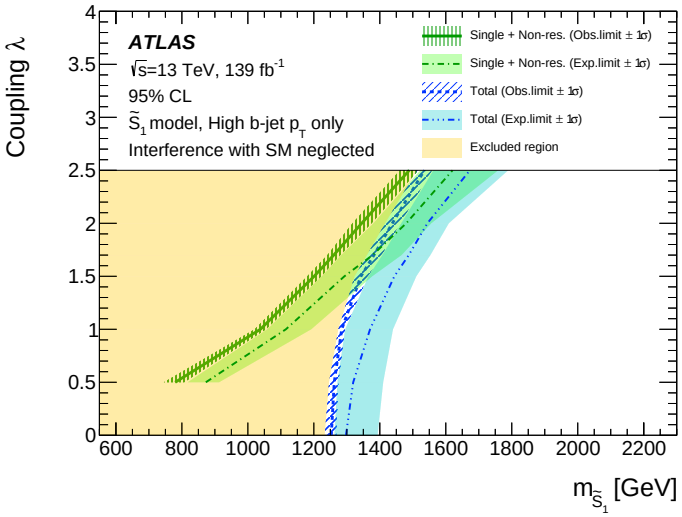

Figure 9: The two-dimensional 95% CL exclusion limits in the $\lambda - m_{\mathrm{LQ}}$ plane for singly plus non-resonant produced $\widetilde{S_1}$ (green lines) and for the sum, referred as *Total*, of single plus non-resonant plus pair vector LQ production (blue lines). Regions to the left of the lines are excluded. The interference of the non-resonant LQ production with SM processes is expected to be small in the high b-jet p_{T} category and it is neglected.

An additional model-independent search considering both the high and low b-jet p_{T} signal regions in the $\tau_{\mathrm{lep}}\tau_{\mathrm{had}}$ and $\tau_{\mathrm{had}}\tau_{\mathrm{had}}$ channels is performed. For each of these regions, the events with $S_{\mathrm{T}} < 600$ GeV form a sideband region, while a signal region is defined by counting the number of events with a S_{T} value above a variable threshold. First the four sideband regions, one for each channel and for each b-jet p_{T} signal region, are fit simultaneously considering the background-only hypothesis. Then, the fit results are used to scale the predicted background contribution in the signal regions. In each signal region, the signal is obtained by counting the number of observed data events after subtracting the background prediction. Figure 10 shows the post-fit distributions of the S_{T} variable in the sideband region and the background composition in each channel as a function of the S_{T} lower bound threshold used to define the signal regions.

Since no significant excess is observed in any of the signal regions, a signal-plus-background fit is performed considering a generic signal in the signal region. As for the LQs search, the parameter of interest of the statistical analysis is the signal strength μ, and the results are translated into upper limits on the number of signal events and, dividing them by the integrated luminosity, they can be expressed in terms of upper limits on the visible cross-section, σ_{vis}. Figure 11 shows the limit values of the visible cross-section as a function of S_{T} lower bound threshold in each signal category. The visible cross-section limits can be reinterpreted as limits on specific physics models as long as the selection efficiency and acceptance of the model (including any uncertainties in these values) for a specific signal region definition used in this analysis is known. By dividing the visible cross-section limits given here by this efficiency and acceptance, upper limits on the cross-section can be derived.

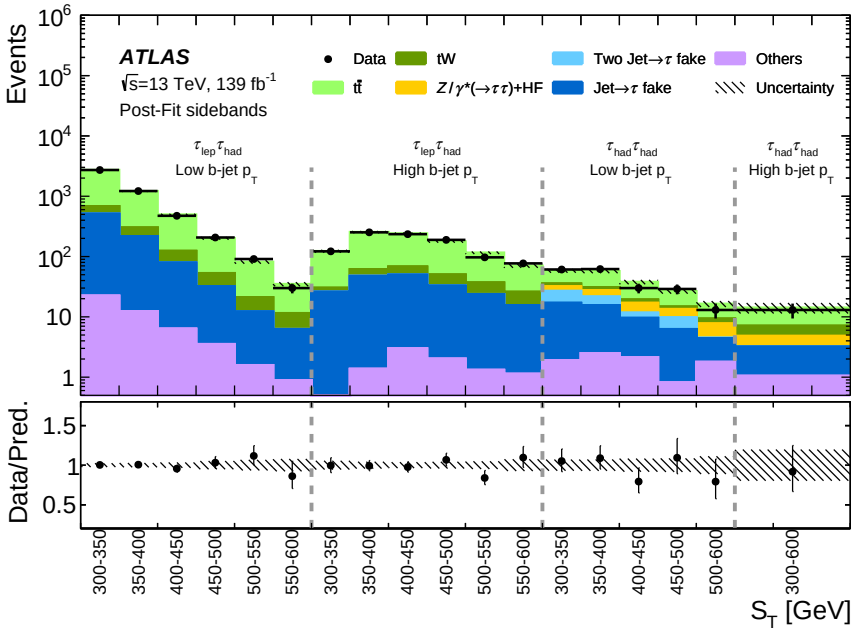

(a)

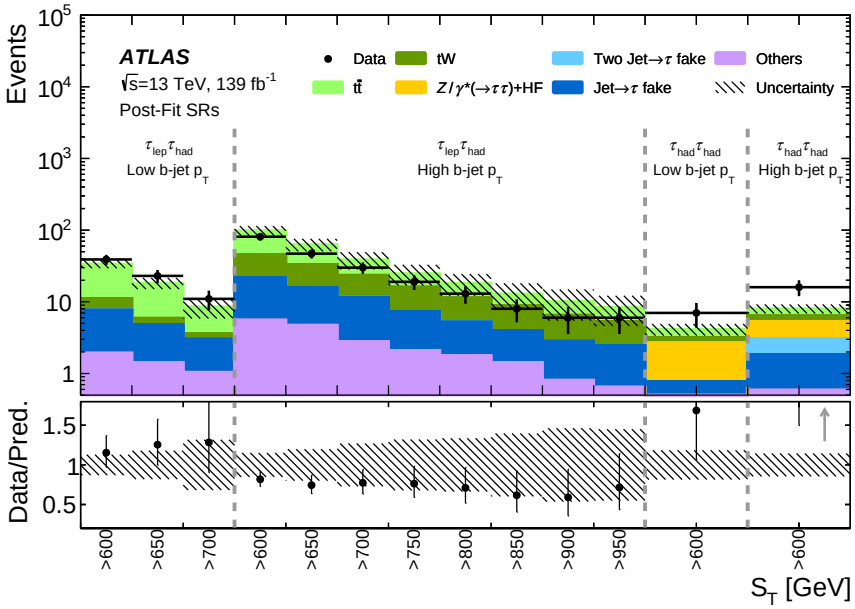

(b)

Figure 10: (a) Post-fit distributions of the discriminating variable S_{T} in the sideband regions for the high and low b-jet p_{T} signal regions for the $\tau_{\mathrm{lep}}\tau_{\mathrm{had}}$ and $\tau_{\mathrm{had}}\tau_{\mathrm{had}}$ channels. The distributions are fit simultaneously considering the background-only hypothesis. (b) Observed and predicted yields of the background as a function of the S_{T} threshold used to define the signal regions for the high and low b-jet p_{T} signal regions of the $\tau_{\mathrm{lep}}\tau_{\mathrm{had}}$ and $\tau_{\mathrm{had}}\tau_{\mathrm{had}}$ channels. The background predictions in the signal regions have been extracted by projecting the results from the fit of the sideband regions, assuming the background-only hypothesis in the context of the model-independent search. The lower panel shows the ratio of the data to the background predictions.

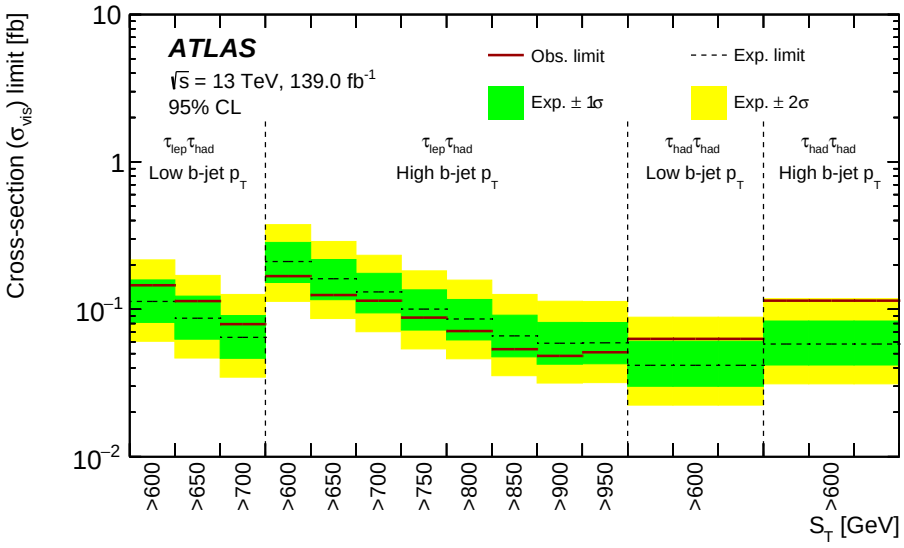

Figure 11: Observed (solid line) and expected (dashed line) 95% upper limits on the visible cross-section, σ_{vis}, obtained from the model-independent search by a signal-plus-background fit in the high and low b-jet p_{T} signal regions for the $\tau_{\text{lep}}\tau_{\text{had}}$ and $\tau_{\text{had}}\tau_{\text{had}}$ channels.

9 Conclusion

A search for scalar and vector leptoquarks is performed in the $b\tau\tau$ final state using pp collision data at $\sqrt{s} = 13$ TeV recorded by the ATLAS detector at the LHC from 2015 to 2018 corresponding to an integrated luminosity of 139 fb^{-1}. Final states including one leptonic and one hadronic τ-lepton decay or two hadronic τ-leptons decays are considered. In each of these two final states, events are classified, based on the p_{T} of the b-jet, in two signal regions of low and high b-jet p_{T}. The benchmark model is U_1 for vector leptoquarks in the Yang–Mills or Minimal coupling scenarios with λ between 0.5 and 2.5. For scalar leptoquarks the benchmark model is $\widetilde{S_1}$, with values of the λ parameter ranging between 0.5 and 2.5.

Upper limits at 95% CL on the cross-section for leptoquarks produced via either single plus non-resonant production, or considering all production modes (including pair production), and decaying into $b\tau$ are set. The results have been extracted considering only the high b-jet signal region and the combination of both final states. For the Yang–Mills coupling, the observed (expected) lower limits on the leptoquark mass are 1.58 (1.64) TeV for $\lambda = 1.0$, 1.70 (1.81) TeV for $\lambda = 1.7$, and 2.05 (2.28) TeV for $\lambda = 2.5$, considering all leptoquark production modes. In the Minimal coupling case, considering all leptoquark production modes, the lower limits are 1.35 (1.44) TeV for $\lambda = 1.0$, 1.52 (1.63) TeV for $\lambda = 1.7$ and 1.99 (2.26) TeV for $\lambda = 2.5$. The observed (expected) lower limits, considering all leptoquark production modes in the $\widetilde{S_1}$ model, are 1.28 (1.37) TeV for $\lambda = 1.0$, 1.38 (1.49) TeV for $\lambda = 1.7$ and 1.53 (1.67) TeV for $\lambda = 2.5$.

An interpretation of the results in a model-independent scenario is also performed for each of the signal region categories. The 95% confidence level limits on the visible cross-section vary between 0.17 fb and $4.8 \cdot 10^{-2}$ fb as a function of the event variable S_{T} ranging from $S_{\text{T}} > 600$ GeV to $S_{\text{T}} > 950$ GeV.

Acknowledgements

We thank CERN for the very successful operation of the LHC, as well as the support staff from our institutions without whom ATLAS could not be operated efficiently.

We acknowledge the support of ANPCyT, Argentina; YerPhI, Armenia; ARC, Australia; BMWFW and FWF, Austria; ANAS, Azerbaijan; CNPq and FAPESP, Brazil; NSERC, NRC and CFI, Canada; CERN; ANID, Chile; CAS, MOST and NSFC, China; Minciencias, Colombia; MEYS CR, Czech Republic; DNRF and DNSRC, Denmark; IN2P3-CNRS and CEA-DRF/IRFU, France; SRNSFG, Georgia; BMBF, HGF and MPG, Germany; GSRI, Greece; RGC and Hong Kong SAR, China; ISF and Benoziyo Center, Israel; INFN, Italy; MEXT and JSPS, Japan; CNRST, Morocco; NWO, Netherlands; RCN, Norway; MEiN, Poland; FCT, Portugal; MNE/IFA, Romania; MESTD, Serbia; MSSR, Slovakia; ARRS and MIZŠ, Slovenia; DSI/NRF, South Africa; MICINN, Spain; SRC and Wallenberg Foundation, Sweden; SERI, SNSF and Cantons of Bern and Geneva, Switzerland; MOST, Taiwan; TENMAK, Türkiye; STFC, United Kingdom; DOE and NSF, United States of America. In addition, individual groups and members have received support from BCKDF, CANARIE, Compute Canada and CRC, Canada; PRIMUS 21/SCI/017 and UNCE SCI/013, Czech Republic; COST, ERC, ERDF, Horizon 2020 and Marie Skłodowska-Curie Actions, European Union; Investissements d'Avenir Labex, Investissements d'Avenir Idex and ANR, France; DFG and AvH Foundation, Germany; Herakleitos, Thales and Aristeia programmes co-financed by EU-ESF and the Greek NSRF, Greece; BSF-NSF and MINERVA, Israel; Norwegian Financial Mechanism 2014-2021, Norway; NCN and NAWA, Poland; La Caixa Banking Foundation, CERCA Programme Generalitat de Catalunya and PROMETEO and GenT Programmes Generalitat Valenciana, Spain; Göran Gustafssons Stiftelse, Sweden; The Royal Society and Leverhulme Trust, United Kingdom.

The crucial computing support from all WLCG partners is acknowledged gratefully, in particular from CERN, the ATLAS Tier-1 facilities at TRIUMF (Canada), NDGF (Denmark, Norway, Sweden), CC-IN2P3 (France), KIT/GridKA (Germany), INFN-CNAF (Italy), NL-T1 (Netherlands), PIC (Spain), ASGC (Taiwan), RAL (UK) and BNL (USA), the Tier-2 facilities worldwide and large non-WLCG resource providers. Major contributors of computing resources are listed in Ref. [119].

References

[1] S. Dimopoulos and L. Susskind, *Mass without scalars*, Nucl. Phys. B **155** (1979) 237.

[2] S. Dimopoulos, *Technicolored signatures*, Nucl. Phys. B **168** (1980) 69, ed. by A. Zichichi.

[3] E. Farhi and L. Susskind, *Technicolour*, Phys. Rept. **74** (1981) 277.

[4] B. Schrempp and F. Schrempp, *Light leptoquarks*, Phys. Lett. B **153** (1985) 101.

[5] J. C. Pati and A. Salam,
Unified Lepton-Hadron Symmetry and a Gauge Theory of the Basic Interactions,
Phys. Rev. D **8** (1973) 1240.

[6] J. C. Pati and A. Salam, *Lepton number as the fourth "color"*, Phys. Rev. D **10** (1974) 275.

[7] H. Georgi and S. L. Glashow, *Unity of All Elementary-Particle Forces*,
Phys. Rev. Lett. **32** (1974) 438.

[8] BaBar Collaboration, *Evidence for an Excess of $\bar{B} \to D^{(*)}\tau^-\bar{\nu}_\tau$ Decays*,
Phys. Rev. Lett. **109** (2012) 101802, arXiv: 1205.5442 [hep-ex].

[9] BaBar Collaboration,
Measurement of an excess of $\bar{B} \to D^{(*)}\tau^-\bar{\nu}_\tau$ decays and implications for charged Higgs bosons,
Phys. Rev. D **88** (2013) 072012, arXiv: 1303.0571 [hep-ex].

[10] Belle Collaboration, *Measurement of the branching ratio of $\bar{B} \to D^{(*)}\tau^-\bar{\nu}_\tau$ relative to $\bar{B} \to D^{(*)}\ell^-\bar{\nu}_\ell$ decays with hadronic tagging at Belle*, Phys. Rev. D **92** (2015) 072014,
arXiv: 1507.03233 [hep-ex].

[11] LHCb Collaboration,
Measurement of the Ratio of Branching Fractions $\mathcal{B}(\bar{B}^0 \to D^{*+}\tau^-\bar{\nu}_\tau)/\mathcal{B}(\bar{B}^0 \to D^{*+}\mu^-\bar{\nu}_\mu)$,
Phys. Rev. Lett. **115** (2015) 111803, arXiv: 1506.08614 [hep-ex],
Erratum: Phys. Rev. Lett. **115** (2015) 159901.

[12] Muon g-2 Collaboration,
Measurement of the Positive Muon Anomalous Magnetic Moment to 0.46 ppm,
Phys. Rev. Lett. **126** (2021).

[13] S. Borsanyi et al., *Leading hadronic contribution to the muon magnetic moment from lattice QCD*,
Nature **593** (2021) 51, arXiv: 2002.12347 [hep-lat].

[14] A. Greljo, P. Stangl and A. E. Thomsen, *A model of muon anomalies*,
Phys. Lett. B **820** (2021) 136554, arXiv: 2103.13991 [hep-ph].

[15] D. Buttazzo, A. Greljo, G. Isidori and D. Marzocca,
B-physics anomalies: a guide to combined explanations, JHEP **11** (2017) 044.

[16] ATLAS Collaboration, *The ATLAS Experiment at the CERN Large Hadron Collider*,
JINST **3** (2008) S08003.

[17] B. Abbott et al., *Production and integration of the ATLAS Insertable B-Layer*,
JINST **13** (2018) T05008, arXiv: 1803.00844 [physics.ins-det].

[18] L. Evans and P. Bryant, *LHC Machine*, JINST **3** (2008) S08001.

[19] M. J. Baker, J. Fuentes-Martin, G. Isidori and M. Konig,
High-p_T signatures in vector–leptoquark models, Eur. Phys. J. C **79** (2019) 334,
arXiv: 1901.10480 [hep-ph].

[20] W. Buchmuller, R. Ruckl and D. Wyler, *Leptoquarks in lepton-quark collisions*, Phys. Lett. B **191** (1987) 442, Erratum: Phys. Lett. B **448** (1999) 320.

[21] I. Doršner, S. Fajfer, A. Greljo, J. F. Kamenik and N. Košnik, *Physics of leptoquarks in precision experiments and at particle colliders*, Phys. Rep. **641** (2016) 1.

[22] ATLAS Collaboration, *Search for a scalar partner of the top quark in the all-hadronic $t\bar{t}$ plus missing transverse momentum final state at $\sqrt{s} = 13$ TeV with the ATLAS detector*, Eur. Phys. J. C **80** (2020) 737, arXiv: 2004.14060 [hep-ex].

[23] ATLAS Collaboration, *Search for new phenomena in final states with b-jets and missing transverse momentum in $\sqrt{s} = 13$ TeV pp collisions with the ATLAS detector*, JHEP **05** (2021) 093, arXiv: 2101.12527 [hep-ex].

[24] ATLAS Collaboration, *Search for new phenomena in pp collisions in final states with tau leptons, b-jets, and missing transverse momentum with the ATLAS detector*, Phys. Rev. D **104** (2021) 112005, arXiv: 2108.07665 [hep-ex].

[25] ATLAS Collaboration, *Search for pairs of scalar leptoquarks decaying into quarks and electrons or muons in $\sqrt{s} = 13$ TeV pp collisions with the ATLAS detector*, JHEP **10** (2020) 112, arXiv: 2006.05872 [hep-ex].

[26] ATLAS Collaboration, *Search for pair production of third-generation scalar leptoquarks decaying into a top quark and a τ-lepton in pp collisions at $\sqrt{s} = 13$ TeV with the ATLAS detector*, JHEP **06** (2021) 179, arXiv: 2101.11582 [hep-ex].

[27] ATLAS Collaboration, *Search for pair production of scalar leptoquarks decaying into first- or second-generation leptons and top quarks in proton–proton collisions at $\sqrt{s} = 13$ TeV with the ATLAS detector*, Eur. Phys. J. C **81** (2021) 313, arXiv: 2010.02098 [hep-ex].

[28] ATLAS Collaboration, *Search for pair production of third-generation leptoquarks decaying into a bottom quark and a τ-lepton with the ATLAS detector*, (2023), arXiv: 2303.01294 [hep-ex].

[29] CMS Collaboration, *Search for Leptoquarks Coupled to Third-Generation Quarks in Proton–Proton Collisions at $\sqrt{s} = 13$ TeV*, Phys. Rev. Lett. **121** (2018) 241802, arXiv: 1809.05558 [hep-ex].

[30] CMS Collaboration, *Search for third-generation scalar leptoquarks decaying to a top quark and a τ lepton at $\sqrt{s} = 13$ TeV*, Eur. Phys. J. C **78** (2018) 707, arXiv: 1803.02864 [hep-ex].

[31] CMS Collaboration, *Search for dark matter in events with a leptoquark and missing transverse momentum in proton–proton collisions at 13 TeV*, Phys. Lett. B **795** (2019) 76, arXiv: 1811.10151 [hep-ex].

[32] CMS Collaboration, *Search for heavy neutrinos and third-generation leptoquarks in hadronic states of two τ leptons and two jets in proton–proton collisions at $\sqrt{s} = 13$ TeV*, JHEP **03** (2019) 170, arXiv: 1811.00806 [hep-ex].

[33] CMS Collaboration, *Search for singly and pair-produced leptoquarks coupling to third-generation fermions in proton–proton collisions at $\sqrt{s} = 13$ TeV*, Phys. Lett. B **819** (2021) 136446, arXiv: 2012.04178 [hep-ex].

[34] ATLAS Collaboration, *Searches for third-generation scalar leptoquarks in $\sqrt{s} = 13$ TeV pp collisions with the ATLAS detector*, JHEP **06** (2019) 144, arXiv: 1902.08103 [hep-ex].

[35] T. Mandal, S. Mitra and S. Raz, *$R_{D^{(*)}}$ motivated S_1 leptoquark scenarios: Impact of interference on the exclusion limits from LHC data*, Phys. Rev. D **99** (5 2019) 055028, arXiv: 1811.03561.

[36] A. Bessaa and S. Davidson,
Constraints on t -channel leptoquark exchange from LHC contact interaction searches,
Eur. Phys. J. C **75** (2015) 97, arXiv: 1409.2372 [hep-ph].

[37] ATLAS Collaboration, *ATLAS Insertable B-Layer: Technical Design Report*,
ATLAS-TDR-19; CERN-LHCC-2010-013, 2010,
URL: https://cds.cern.ch/record/1291633, Addendum: ATLAS-TDR-19-ADD-1;
CERN-LHCC-2012-009, 2012, URL: https://cds.cern.ch/record/1451888.

[38] ATLAS Collaboration, *Performance of the ATLAS trigger system in 2015*,
Eur. Phys. J. C **77** (2017) 317, arXiv: 1611.09661 [hep-ex].

[39] ATLAS Collaboration, *The ATLAS Collaboration Software and Firmware*,
ATL-SOFT-PUB-2021-001, 2021, URL: https://cds.cern.ch/record/2767187.

[40] ATLAS Collaboration,
ATLAS data quality operations and performance for 2015–2018 data-taking,
JINST **15** (2020) P04003, arXiv: 1911.04632 [physics.ins-det].

[41] J. Alwall et al., *The automated computation of tree-level and next-to-leading order differential cross sections, and their matching to parton shower simulations*, JHEP **07** (2014) 079,
arXiv: 1405.0301 [hep-ph].

[42] NNPDF Collaboration, R. D. Ball et al., *Parton distributions with LHC data*,
Nucl. Phys. B **867** (2013) 244, arXiv: 1207.1303 [hep-ph].

[43] T. Sjöstrand et al., *An introduction to PYTHIA 8.2*, Comput. Phys. Commun. **191** (2015) 159,
arXiv: 1410.3012 [hep-ph].

[44] ATLAS Collaboration, *ATLAS Pythia 8 tunes to 7 TeV data*, ATL-PHYS-PUB-2014-021, 2014,
URL: https://cds.cern.ch/record/1966419.

[45] I. Doršner and A. Greljo, *Leptoquark toolbox for precision collider studies*, JHEP **05** (2018) 126,
arXiv: 1801.07641 [hep-ph].

[46] T. Mandal, S. Mitra and S. Seth,
Pair production of scalar leptoquarks at the LHC to NLO parton shower accuracy,
Phys. Rev. D **93** (2016) 035018, arXiv: 1506.07369 [hep-ph].

[47] M. Krämer, T. Plehn, M. Spira and P. M. Zerwas,
Pair production of scalar leptoquarks at the CERN LHC, Phys. Rev. D **71** (2005) 057503,
arXiv: hep-ph/0411038.

[48] M. Krämer, T. Plehn, M. Spira and P. M. Zerwas,
Pair Production of Scalar Leptoquarks at the Fermilab Tevatron, Phys. Rev. Lett. **79** (1997) 341,
arXiv: hep-ph/9704322.

[49] W. Beenakker, C. Borschensky, M. Krämer, A. Kulesza and E. Laenen,
NNLL-fast: predictions for coloured supersymmetric particle production at the LHC with threshold and Coulomb resummation, JHEP **12** (2016) 133, arXiv: 1607.07741 [hep-ph].

[50] W. Beenakker, M. Krämer, T. Plehn, M. Spira and P. M. Zerwas,
Stop production at hadron colliders, Nucl. Phys. B **515** (1998) 3, arXiv: hep-ph/9710451.

[51] W. Beenakker et al., *Supersymmetric top and bottom squark production at hadron colliders*, JHEP **08** (2010) 098, arXiv: 1006.4771 [hep-ph].

[52] W. Beenakker et al., *NNLL resummation for stop pair-production at the LHC*, JHEP **05** (2016) 153, arXiv: 1601.02954 [hep-ph].

[53] C. Borschensky, B. Fuks, A. Kulesza and D. Schwartländer, *Scalar leptoquark pair production at hadron colliders*, Phys. Rev. D **101** (2020) 115017, arXiv: 2002.08971 [hep-ph].

[54] S. Frixione, G. Ridolfi and P. Nason, *A positive-weight next-to-leading-order Monte Carlo for heavy flavour hadroproduction*, JHEP **09** (2007) 126, arXiv: 0707.3088 [hep-ph].

[55] P. Nason, *A new method for combining NLO QCD with shower Monte Carlo algorithms*, JHEP **11** (2004) 040, arXiv: hep-ph/0409146.

[56] S. Frixione, P. Nason and C. Oleari, *Matching NLO QCD computations with parton shower simulations: the POWHEG method*, JHEP **11** (2007) 070, arXiv: 0709.2092 [hep-ph].

[57] S. Alioli, P. Nason, C. Oleari and E. Re, *A general framework for implementing NLO calculations in shower Monte Carlo programs: the POWHEG BOX*, JHEP **06** (2010) 043, arXiv: 1002.2581 [hep-ph].

[58] The NNPDF Collaboration, R. D. Ball et al., *Parton distributions for the LHC run II*, JHEP **04** (2015) 040, arXiv: 1410.8849 [hep-ph].

[59] ATLAS Collaboration, *Studies on top-quark Monte Carlo modelling for Top2016*, ATL-PHYS-PUB-2016-020, 2016, URL: https://cds.cern.ch/record/2216168.

[60] M. Beneke, P. Falgari, S. Klein and C. Schwinn, *Hadronic top-quark pair production with NNLL threshold resummation*, Nucl. Phys. B **855** (2012) 695, arXiv: 1109.1536 [hep-ph].

[61] M. Cacciari, M. Czakon, M. Mangano, A. Mitov and P. Nason, *Top-pair production at hadron colliders with next-to-next-to-leading logarithmic soft-gluon resummation*, Phys. Lett. B **710** (2012) 612, arXiv: 1111.5869 [hep-ph].

[62] P. Bärnreuther, M. Czakon and A. Mitov, *Percent-Level-Precision Physics at the Tevatron: Next-to-Next-to-Leading Order QCD Corrections to $q\bar{q} \to t\bar{t} + X$*, Phys. Rev. Lett. **109** (2012) 132001, arXiv: 1204.5201 [hep-ph].

[63] M. Czakon and A. Mitov, *NNLO corrections to top-pair production at hadron colliders: the all-fermionic scattering channels*, JHEP **12** (2012) 054, arXiv: 1207.0236 [hep-ph].

[64] M. Czakon and A. Mitov, *NNLO corrections to top pair production at hadron colliders: the quark-gluon reaction*, JHEP **01** (2013) 080, arXiv: 1210.6832 [hep-ph].

[65] M. Czakon, P. Fiedler and A. Mitov, *Total Top-Quark Pair-Production Cross Section at Hadron Colliders Through $O(\alpha_S^4)$*, Phys. Rev. Lett. **110** (2013) 252004, arXiv: 1303.6254 [hep-ph].

[66] M. Czakon and A. Mitov, *Top++: A program for the calculation of the top-pair cross-section at hadron colliders*, Comput. Phys. Commun. **185** (2014) 2930, arXiv: 1112.5675 [hep-ph].

[67] M. Aliev et al., *HATHOR – HAdronic Top and Heavy quarks crOss section calculatoR*, Comput. Phys. Commun. **182** (2011) 1034, arXiv: 1007.1327 [hep-ph].

[68] P. Kant et al., *HatHor for single top-quark production: Updated predictions and uncertainty estimates for single top-quark production in hadronic collisions*, Comput. Phys. Commun. **191** (2015) 74, arXiv: 1406.4403 [hep-ph].

[69] S. Frixione, E. Laenen, P. Motylinski, C. White and B. R. Webber, *Single-top hadroproduction in association with a W boson*, JHEP **07** (2008) 029, arXiv: 0805.3067 [hep-ph].

[70] S. Alioli, P. Nason, C. Oleari and E. Re, *NLO vector-boson production matched with shower in POWHEG*, JHEP **07** (2008) 060, arXiv: 0805.4802 [hep-ph].

[71] T. Sjöstrand, S. Mrenna and P. Skands, *A brief introduction to PYTHIA 8.1*, Comput. Phys. Commun. **178** (2008) 852, arXiv: 0710.3820 [hep-ph].

[72] ATLAS Collaboration, *Measurement of the Z/γ^* boson transverse momentum distribution in pp collisions at $\sqrt{s} = 7$ TeV with the ATLAS detector*, JHEP **09** (2014) 145, arXiv: 1406.3660 [hep-ex].

[73] H.-L. Lai et al., *New parton distributions for collider physics*, Phys. Rev. D **82** (2010) 074024, arXiv: 1007.2241 [hep-ph].

[74] J. Pumplin et al., *New Generation of Parton Distributions with Uncertainties from Global QCD Analysis*, JHEP **07** (2002) 012, arXiv: hep-ph/0201195.

[75] P. Golonka and Z. Was, *PHOTOS Monte Carlo: a precision tool for QED corrections in Z and W decays*, Eur. Phys. J. C **45** (2006) 97, arXiv: hep-ph/0506026.

[76] N. Davidson, T. Przedzinski and Z. Was, *PHOTOS Interface in C++: Technical and physics documentation*, Comput. Phys. Commun. **199** (2016) 86, arXiv: 1011.0937 [hep-ph].

[77] E. Bothmann et al., *Event generation with Sherpa 2.2*, SciPost Phys. **7** (2019) 034, arXiv: 1905.09127 [hep-ph].

[78] T. Gleisberg and S. Höche, *Comix, a new matrix element generator*, JHEP **12** (2008) 039, arXiv: 0808.3674 [hep-ph].

[79] F. Buccioni et al., *OpenLoops 2*, Eur. Phys. J. C **79** (2019) 866, arXiv: 1907.13071 [hep-ph].

[80] F. Cascioli, P. Maierhöfer and S. Pozzorini, *Scattering Amplitudes with Open Loops*, Phys. Rev. Lett. **108** (2012) 111601, arXiv: 1111.5206 [hep-ph].

[81] A. Denner, S. Dittmaier and L. Hofer, *Collier: A fortran-based complex one-loop library in extended regularizations*, Comput. Phys. Commun. **212** (2017) 220, arXiv: 1604.06792 [hep-ph].

[82] S. Schumann and F. Krauss, *A parton shower algorithm based on Catani–Seymour dipole factorisation*, JHEP **03** (2008) 038, arXiv: 0709.1027 [hep-ph].

[83] J.-C. Winter, F. Krauss and G. Soff, *A modified cluster-hadronisation model*, Eur. Phys. J. C **36** (2004) 381, arXiv: hep-ph/0311085.

[84] S. Höche, F. Krauss, M. Schönherr and F. Siegert,
A critical appraisal of NLO+PS matching methods, JHEP **09** (2012) 049,
arXiv: 1111.1220 [hep-ph].

[85] S. Catani, F. Krauss, B. R. Webber and R. Kuhn, *QCD Matrix Elements + Parton Showers*,
JHEP **11** (2001) 063, arXiv: hep-ph/0109231.

[86] S. Höche, F. Krauss, S. Schumann and F. Siegert, *QCD matrix elements and truncated showers*,
JHEP **05** (2009) 053, arXiv: 0903.1219 [hep-ph].

[87] S. Höche, F. Krauss, M. Schönherr and F. Siegert,
QCD matrix elements + parton showers. The NLO case, JHEP **04** (2013) 027,
arXiv: 1207.5030 [hep-ph].

[88] D. J. Lange, *The EvtGen particle decay simulation package*,
Nucl. Instrum. Meth. A **462** (2001) 152.

[89] ATLAS Collaboration, *The ATLAS Simulation Infrastructure*, Eur. Phys. J. C **70** (2010) 823,
arXiv: 1005.4568 [physics.ins-det].

[90] S. Agostinelli et al., *GEANT4 – a simulation toolkit*, Nucl. Instrum. Meth. A **506** (2003) 250.

[91] ATLAS Collaboration, *The Pythia 8 A3 tune description of ATLAS minimum bias and inelastic measurements incorporating the Donnachie–Landshoff diffractive model*,
ATL-PHYS-PUB-2016-017, 2016, URL: https://cds.cern.ch/record/2206965.

[92] ATLAS Collaboration, *Vertex Reconstruction Performance of the ATLAS Detector at* $\sqrt{s} = 13$ *TeV*,
ATL-PHYS-PUB-2015-026, 2015, URL: https://cds.cern.ch/record/2037717.

[93] ATLAS Collaboration, *Electron and photon performance measurements with the ATLAS detector using the 2015–2017 LHC proton–proton collision data*, JINST **14** (2019) P12006,
arXiv: 1908.00005 [hep-ex].

[94] ATLAS Collaboration, *Muon reconstruction and identification efficiency in ATLAS using the full Run 2 pp collision data set at* $\sqrt{s} = 13$ *TeV*, Eur. Phys. J. C **81** (2021) 578,
arXiv: 2012.00578 [hep-ex].

[95] ATLAS Collaboration,
Jet reconstruction and performance using particle flow with the ATLAS Detector,
Eur. Phys. J. C **77** (2017) 466, arXiv: 1703.10485 [hep-ex].

[96] M. Cacciari, G. P. Salam and G. Soyez, *The anti-k_t jet clustering algorithm*, JHEP **04** (2008) 063,
arXiv: 0802.1189 [hep-ph].

[97] M. Cacciari, G. P. Salam and G. Soyez, *FastJet user manual*, Eur. Phys. J. C **72** (2012) 1896,
arXiv: 1111.6097 [hep-ph].

[98] ATLAS Collaboration, *Performance of pile-up mitigation techniques for jets in pp collisions at* $\sqrt{s} = 8$ *TeV using the ATLAS detector*, Eur. Phys. J. C **76** (2016) 581,
arXiv: 1510.03823 [hep-ex].

[99] ATLAS Collaboration, *ATLAS flavour-tagging algorithms for the LHC Run 2 pp collision dataset*,
(2022), arXiv: 2211.16345 [physics.data-an].

[100] ATLAS Collaboration, *Optimisation and performance studies of the ATLAS b-tagging algorithms for the 2017-18 LHC run*, ATL-PHYS-PUB-2017-013, 2017,
URL: https://cds.cern.ch/record/2273281.

[101] ATLAS Collaboration,
Topological cell clustering in the ATLAS calorimeters and its performance in LHC Run 1,
Eur. Phys. J. C **77** (2017) 490, arXiv: 1603.02934 [hep-ex].

[102] ATLAS Collaboration, *Measurement of the tau lepton reconstruction and identification performance in the ATLAS experiment using pp collisions at $\sqrt{s} = 13$ TeV*,
ATLAS-CONF-2017-029, 2017, URL: https://cds.cern.ch/record/2261772.

[103] ATLAS Collaboration,
Identification of hadronic tau lepton decays using neural networks in the ATLAS experiment,
ATL-PHYS-PUB-2019-033, 2019, URL: https://cds.cern.ch/record/2688062.

[104] ATLAS Collaboration, *Performance of missing transverse momentum reconstruction with the ATLAS detector using proton–proton collisions at $\sqrt{s} = 13$ TeV*, Eur. Phys. J. C **78** (2018) 903,
arXiv: 1802.08168 [hep-ex].

[105] ATLAS Collaboration, *Performance of electron and photon triggers in ATLAS during LHC Run 2*,
Eur. Phys. J. C **80** (2020) 47, arXiv: 1909.00761 [hep-ex].

[106] ATLAS Collaboration, *Performance of the ATLAS muon triggers in Run 2*,
JINST **15** (2020) P09015, arXiv: 2004.13447 [hep-ex].

[107] ATLAS Collaboration, *The ATLAS Tau Trigger in Run 2*, ATLAS-CONF-2017-061, 2017,
URL: https://cds.cern.ch/record/2274201.

[108] ATLAS Collaboration, *Measurements of top-quark pair differential and double-differential cross-sections in the ℓ+jets channel with pp collisions at $\sqrt{s} = 13$ TeV using the ATLAS detector*,
Eur. Phys. J. C **79** (2019) 1028, arXiv: 1908.07305 [hep-ex],
Erratum: Eur. Phys. J. C **80** (2020) 1092.

[109] ATLAS Collaboration, *Measurement of the $t\bar{t}$ production cross-section and lepton differential distributions in $e\mu$ dilepton events from pp collisions at $\sqrt{s} = 13$ TeV with the ATLAS detector*,
Eur. Phys. J. C **80** (2020) 528, arXiv: 1910.08819 [hep-ex].

[110] ATLAS Collaboration, *ATLAS simulation of boson plus jets processes in Run 2*,
ATL-PHYS-PUB-2017-006, 2017, URL: https://cds.cern.ch/record/2261937.

[111] ATLAS Collaboration, *Jet energy scale and resolution measured in proton–proton collisions at $\sqrt{s} = 13$ TeV with the ATLAS detector*, Eur. Phys. J. C **81** (2021) 689,
arXiv: 2007.02645 [hep-ex].

[112] G. Avoni et al., *The new LUCID-2 detector for luminosity measurement and monitoring in ATLAS*,
JINST **13** (2018) P07017.

[113] ATLAS Collaboration,
Luminosity determination in pp collisions at $\sqrt{s} = 13$ TeV using the ATLAS detector at the LHC,
ATLAS-CONF-2019-021, 2019, URL: https://cds.cern.ch/record/2677054.

[114] C. D. White, S. Frixione, E. Laenen and F. Maltoni, *Isolating Wt production at the LHC*,
JHEP **11** (2009) 074, arXiv: 0908.0631.

[115] J. Butterworth et al., *PDF4LHC recommendations for LHC Run II*, J. Phys. G **43** (2016) 023001,
arXiv: 1510.03865 [hep-ph].

[116] A. L. Read, *Presentation of search results: the CL_S technique*, J. Phys. G **28** (2002) 2693.

[117] G. Cowan, K. Cranmer, E. Gross and O. Vitells,
Asymptotic formulae for likelihood-based tests of new physics, Eur. Phys. J. C **71** (2011) 1554, arXiv: 1007.1727 [physics.data-an], Erratum: Eur. Phys. J. C **73** (2013) 2501.

[118] J. Aebischer, G. Isidori, M. Pesut, B. A. Stefanek and F. Wilsch,
Confronting the vector leptoquark hypothesis with new low- and high-energy data,
Eur. Phys. J. C **83** (2023) 153, arXiv: 2210.13422.

[119] ATLAS Collaboration, *ATLAS Computing Acknowledgements*, ATL-SOFT-PUB-2021-003, 2021,
URL: https://cds.cern.ch/record/2776662.

The ATLAS Collaboration

G. Aad [90b], B. Abbott [120], K. Abeling [55], N.J. Abicht [49], S.H. Abidi [29], A. Aboulhorma [35e], H. Abramowicz [151], H. Abreu [150], Y. Abulaiti [117], A.C. Abusleme Hoffman [137a], B.S. Acharya [69a,69b,p], C. Adam Bourdarios [4], L. Adamczyk [85a], L. Adamek [155], S.V. Addepalli [26], M.J. Addison [102], J. Adelman [115], A. Adiguzel [21c], T. Adye [134], A.A. Affolder [136], Y. Afik [36], M.N. Agaras [13], J. Agarwala [73a,73b], A. Aggarwal [101], C. Agheorghiesei [27c], A. Ahmad [36], F. Ahmadov [38,ad], W.S. Ahmed [104], S. Ahuja [96], X. Ai [62a], G. Aielli [76a,76b], M. Ait Tamlihat [35e], B. Aitbenchikh [35a], I. Aizenberg [169], M. Akbiyik [101], T.P.A. Åkesson [99], A.V. Akimov [37], D. Akiyama [168], N.N. Akolkar [24], K. Al Khoury [41], G.L. Alberghi [23b], J. Albert [165], P. Albicocco [53], G.L. Albouy [60], S. Alderweireldt [52], M. Aleksa [36], I.N. Aleksandrov [38], C. Alexa [27b], T. Alexopoulos [10], A. Alfonsi [114], F. Alfonsi [23b], M. Algren [56], M. Alhroob [120], B. Ali [132], H.M.J. Ali [92], S. Ali [148], S.W. Alibocus [93], M. Aliev [37], G. Alimonti [71a], W. Alkakhi [55], C. Allaire [66], B.M.M. Allbrooke [146], J.F. Allen [52], C.A. Allendes Flores [137f], P.P. Allport [20], A. Aloisio [72a,72b], F. Alonso [91], C. Alpigiani [138], M. Alvarez Estevez [100], A. Alvarez Fernandez [101], M.G. Alviggi [72a,72b], M. Aly [102], Y. Amaral Coutinho [82b], A. Ambler [104], C. Amelung[36], M. Amerl [102], C.G. Ames [109], D. Amidei [106], S.P. Amor Dos Santos [130a], K.R. Amos [163], V. Ananiev [125], C. Anastopoulos [139], T. Andeen [11], J.K. Anders [36], S.Y. Andrean [47a,47b], A. Andreazza [71a,71b], S. Angelidakis [9], A. Angerami [41,ag], A.V. Anisenkov [37], A. Annovi [74a], C. Antel [56], M.T. Anthony [139], E. Antipov [145], M. Antonelli [53], D.J.A. Antrim [17a], F. Anulli [75a], M. Aoki [83], T. Aoki [153], J.A. Aparisi Pozo [163], M.A. Aparo [146], L. Aperio Bella [48], C. Appelt [18], N. Aranzabal [36], C. Arcangeletti [53], A.T.H. Arce [51], E. Arena [93], J-F. Arguin [108], S. Argyropoulos [54], J.-H. Arling [48], A.J. Armbruster [36], O. Arnaez [4], H. Arnold [114], Z.P. Arrubarrena Tame[109], G. Artoni [75a,75b], H. Asada [111], K. Asai [118], S. Asai [153], N.A. Asbah [61], J. Assahsah [35d], K. Assamagan [29], R. Astalos [28a], S. Atashi [160], R.J. Atkin [33a], M. Atkinson[162], N.B. Atlay [18], H. Atmani[62b], P.A. Atmasiddha [106], K. Augsten [132], S. Auricchio [72a,72b], A.D. Auriol [20], V.A. Austrup [102], G. Avolio [36], K. Axiotis [56], G. Azuelos [108,ak], D. Babal [28b], H. Bachacou [135], K. Bachas [152,t], A. Bachiu [34], F. Backman [47a,47b], A. Badea [61], P. Bagnaia [75a,75b], M. Bahmani [18], A.J. Bailey [163], V.R. Bailey [162], J.T. Baines [134], L. Baines [95], C. Bakalis [10], O.K. Baker [172], E. Bakos [15], D. Bakshi Gupta [8], R. Balasubramanian [114], E.M. Baldin [37], P. Balek [85a], E. Ballabene [23b,23a], F. Balli [135], L.M. Baltes [63a], W.K. Balunas [32], J. Balz [101], E. Banas [86], M. Bandieramonte [129], A. Bandyopadhyay [24], S. Bansal [24], L. Barak [151], M. Barakat [48], E.L. Barberio [105], D. Barberis [57b,57a], M. Barbero [90b], G. Barbour[97], K.N. Barends [33a], T. Barillari [110], M-S. Barisits [36], T. Barklow [143], P. Baron [122], D.A. Baron Moreno [102], A. Baroncelli [62a], G. Barone [29], A.J. Barr [126], J.D. Barr [97], L. Barranco Navarro [47a,47b], F. Barreiro [100], J. Barreiro Guimarães da Costa [14a], U. Barron [151], M.G. Barros Teixeira [130a], S. Barsov [37], F. Bartels [63a], R. Bartoldus [143], A.E. Barton [92], P. Bartos [28a], A. Basan [101], M. Baselga [49], A. Bassalat [66,b], M.J. Basso [156a], C.R. Basson [102], R.L. Bates [59], S. Batlamous[35e], J.R. Batley [32], B. Batool [141], M. Battaglia [136], D. Battulga [18], M. Bauce [75a,75b], M. Bauer [36], P. Bauer [24], L.T. Bazzano Hurrell [30], J.B. Beacham [51], T. Beau [127], P.H. Beauchemin [158], F. Becherer [54], P. Bechtle [24], H.P. Beck [19,s], K. Becker [167], A.J. Beddall [21d], V.A. Bednyakov [38], C.P. Bee [145], L.J. Beemster[15], T.A. Beermann [36], M. Begalli [82d], M. Begel [29], A. Behera [145], J.K. Behr [48], J.F. Beirer [55], F. Beisiegel [24], M. Belfkir [159], G. Bella [151], L. Bellagamba [23b], A. Bellerive [34], P. Bellos [20], K. Beloborodov [37], N.L. Belyaev [37], D. Benchekroun [35a], F. Bendebba [35a],

Y. Benhammou [151], M. Benoit [29], J.R. Bensinger [26], S. Bentvelsen [114], L. Beresford [48], M. Beretta [53], E. Bergeaas Kuutmann [161], N. Berger [4], B. Bergmann [132], J. Beringer [17a], G. Bernardi [5], C. Bernius [143], F.U. Bernlochner [24], F. Bernon [36,90b], T. Berry [96], P. Berta [133], A. Berthold [50], I.A. Bertram [92], S. Bethke [110], A. Betti [75a,75b], A.J. Bevan [95], M. Bhamjee [33c], S. Bhatta [145], D.S. Bhattacharya [166], P. Bhattarai [26], V.S. Bhopatkar [121], R. Bi [29,am], R.M. Bianchi [129], G. Bianco [23b,23a], O. Biebel [109], R. Bielski [123], M. Biglietti [77a], T.R.V. Billoud [132], M. Bindi [55], A. Bingul [21b], C. Bini [75a,75b], A. Biondini [93], C.J. Birch-sykes [102], G.A. Bird [20,134], M. Birman [169], M. Biros [133], T. Bisanz [49], E. Bisceglie [43b,43a], D. Biswas [141], A. Bitadze [102], K. Bjørke [125], I. Bloch [48], C. Blocker [26], A. Blue [59], U. Blumenschein [95], J. Blumenthal [101], G.J. Bobbink [114], V.S. Bobrovnikov [37], M. Boehler [54], B. Boehm [166], D. Bogavac [36], A.G. Bogdanchikov [37], C. Bohm [47a], V. Boisvert [96], P. Bokan [48], T. Bold [85a], M. Bomben [5], M. Bona [95], M. Boonekamp [135], C.D. Booth [96], A.G. Borbély [59], I.S. Bordulev [37], H.M. Borecka-Bielska [108], L.S. Borgna [97], G. Borissov [92], D. Bortoletto [126], D. Boscherini [23b], M. Bosman [13], J.D. Bossio Sola [36], K. Bouaouda [35a], N. Bouchhar [163], J. Boudreau [129], E.V. Bouhova-Thacker [92], D. Boumediene [40], R. Bouquet [5], A. Boveia [119], J. Boyd [36], D. Boye [29], I.R. Boyko [38], J. Bracinik [20], N. Brahimi [62d], G. Brandt [171], O. Brandt [32], F. Braren [48], B. Brau [103], J.E. Brau [123], R. Brener [169], L. Brenner [114], R. Brenner [161], S. Bressler [169], D. Britton [59], D. Britzger [110], I. Brock [24], G. Brooijmans [41], W.K. Brooks [137f], E. Brost [29], L.M. Brown [165,m], L.E. Bruce [61], T.L. Bruckler [126], P.A. Bruckman de Renstrom [86], B. Brüers [48], D. Bruncko [28b,*], A. Bruni [23b], G. Bruni [23b], M. Bruschi [23b], N. Bruscino [75a,75b], T. Buanes [16], Q. Buat [138], D. Buchin [110], A.G. Buckley [59], M.K. Bugge [125], O. Bulekov [37], B.A. Bullard [143], S. Burdin [93], C.D. Burgard [49], A.M. Burger [40], B. Burghgrave [8], O. Burlayenko [54], J.T.P. Burr [32], C.D. Burton [11], J.C. Burzynski [142], E.L. Busch [41], V. Büscher [101], P.J. Bussey [59], J.M. Butler [25], C.M. Buttar [59], J.M. Butterworth [97], W. Buttinger [134], C.J. Buxo Vazquez [107], A.R. Buzykaev [37], G. Cabras [23b], S. Cabrera Urbán [163], L. Cadamuro [66], D. Caforio [58], H. Cai [129], Y. Cai [14a,14e], V.M.M. Cairo [36], O. Cakir [3a], N. Calace [36], P. Calafiura [17a], G. Calderini [127], P. Calfayan [68], G. Callea [59], L.P. Caloba [82b], D. Calvet [40], S. Calvet [40], T.P. Calvet [90b], M. Calvetti [74a,74b], R. Camacho Toro [127], S. Camarda [36], D. Camarero Munoz [26], P. Camarri [76a,76b], M.T. Camerlingo [72a,72b], D. Cameron [125], C. Camincher [165], M. Campanelli [97], A. Camplani [42], V. Canale [72a,72b], A. Canesse [104], M. Cano Bret [80], J. Cantero [163], Y. Cao [162], F. Capocasa [26], M. Capua [43b,43a], A. Carbone [71a,71b], R. Cardarelli [76a], J.C.J. Cardenas [8], F. Cardillo [163], T. Carli [36], G. Carlino [72a], J.I. Carlotto [13], B.T. Carlson [129,u], E.M. Carlson [165,156a], L. Carminati [71a,71b], A. Carnelli [135], M. Carnesale [75a,75b], S. Caron [113], E. Carquin [137f], S. Carrá [71a,71b], G. Carratta [23b,23a], F. Carrio Argos [33g], J.W.S. Carter [155], T.M. Carter [52], M.P. Casado [13,j], M. Caspar [48], E.G. Castiglia [172], F.L. Castillo [4], L. Castillo Garcia [13], V. Castillo Gimenez [163], N.F. Castro [130a,130e], A. Catinaccio [36], J.R. Catmore [125], V. Cavaliere [29], N. Cavalli [23b,23a], V. Cavasinni [74a,74b], Y.C. Cekmecelioglu [48], E. Celebi [21a], F. Celli [126], M.S. Centonze [70a,70b], K. Cerny [122], A.S. Cerqueira [82a], A. Cerri [146], L. Cerrito [76a,76b], F. Cerutti [17a], B. Cervato [141], A. Cervelli [23b], G. Cesarini [53], S.A. Cetin [21d], Z. Chadi [35a], D. Chakraborty [115], M. Chala [130f], J. Chan [170], W.Y. Chan [153], J.D. Chapman [32], E. Chapon [135], B. Chargeishvili [149b], D.G. Charlton [20], T.P. Charman [95], M. Chatterjee [19], C. Chauhan [133], Y. Che [14c], S. Chekanov [6], S.V. Chekulaev [156a], G.A. Chelkov [38,a], A. Chen [106], B. Chen [151], B. Chen [165], H. Chen [14c], H. Chen [29], J. Chen [62c], J. Chen [142], M. Chen [126], S. Chen [153], S.J. Chen [14c], X. Chen [62c], X. Chen [14b,aj], Y. Chen [62a], C.L. Cheng [170], H.C. Cheng [64a], S. Cheong [143], A. Cheplakov [38], E. Cheremushkina [48], E. Cherepanova [114], R. Cherkaoui El Moursli [35e], E. Cheu [7], K. Cheung [65], L. Chevalier [135],

V. Chiarella[53], G. Chiarelli[74a], N. Chiedde[90b], G. Chiodini[70a], A.S. Chisholm[20], A. Chitan[27b], M. Chitishvili[163], M.V. Chizhov[38], K. Choi[11], A.R. Chomont[75a,75b], Y. Chou[103], E.Y.S. Chow[114], T. Chowdhury[33g], K.L. Chu[169], M.C. Chu[64a], X. Chu[14a,14e], J. Chudoba[131], J.J. Chwastowski[86], D. Cieri[110], K.M. Ciesla[85a], V. Cindro[94], A. Ciocio[17a], F. Cirotto[72a,72b], Z.H. Citron[169,n], M. Citterio[71a], D.A. Ciubotaru[27b], B.M. Ciungu[155], A. Clark[56], P.J. Clark[52], J.M. Clavijo Columbie[48], S.E. Clawson[48], C. Clement[47a,47b], J. Clercx[48], L. Clissa[23b,23a], Y. Coadou[90b], M. Cobal[69a,69c], A. Coccaro[57b], R.F. Coelho Barrue[130a], R. Coelho Lopes De Sa[103], S. Coelli[71a], H. Cohen[151], A.E.C. Coimbra[71a,71b], B. Cole[41], J. Collot[60], P. Conde Muiño[130a,130g], M.P. Connell[33c], S.H. Connell[33c], I.A. Connelly[59], E.I. Conroy[126], F. Conventi[72a,al], H.G. Cooke[20], A.M. Cooper-Sarkar[126], A. Cordeiro Oudot Choi[127], F. Cormier[164], L.D. Corpe[40], M. Corradi[75a,75b], F. Corriveau[104,ab], A. Cortes-Gonzalez[18], M.J. Costa[163], F. Costanza[4], D. Costanzo[139], B.M. Cote[119], G. Cowan[96], K. Cranmer[170], D. Cremonini[23b,23a], S. Crépé-Renaudin[60], F. Crescioli[127], M. Cristinziani[141], M. Cristoforetti[78a,78b], V. Croft[114], J.E. Crosby[121], G. Crosetti[43b,43a], A. Cueto[100], T. Cuhadar Donszelmann[160], H. Cui[14a,14e], Z. Cui[7], W.R. Cunningham[59], F. Curcio[43b,43a], P. Czodrowski[36], M.M. Czurylo[63b], M.J. Da Cunha Sargedas De Sousa[62a], J.V. Da Fonseca Pinto[82b], C. Da Via[102], W. Dabrowski[85a], T. Dado[49], S. Dahbi[33g], T. Dai[106], C. Dallapiccola[103], M. Dam[42], G. D'amen[29], V. D'Amico[109], J. Damp[101], J.R. Dandoy[128], M.F. Daneri[30], M. Danninger[142], V. Dao[36], G. Darbo[57b], S. Darmora[6], S.J. Das[29,am], S. D'Auria[71a,71b], C. David[156b], T. Davidek[133], B. Davis-Purcell[34], I. Dawson[95], H.A. Day-hall[132], K. De[8], R. De Asmundis[72a], N. De Biase[48], S. De Castro[23b,23a], N. De Groot[113], P. de Jong[114], H. De la Torre[107], A. De Maria[14c], A. De Salvo[75a], U. De Sanctis[76a,76b], A. De Santo[146], J.B. De Vivie De Regie[60], D.V. Dedovich[38], J. Degens[114], A.M. Deiana[44], F. Del Corso[23b,23a], J. Del Peso[100], F. Del Rio[63a], F. Deliot[135], C.M. Delitzsch[49], M. Della Pietra[72a,72b], D. Della Volpe[56], A. Dell'Acqua[36], L. Dell'Asta[71a,71b], M. Delmastro[4], P.A. Delsart[60], S. Demers[172], M. Demichev[38], S.P. Denisov[37], L. D'Eramo[40], D. Derendarz[86], F. Derue[127], P. Dervan[93], K. Desch[24], C. Deutsch[24], F.A. Di Bello[57b,57a], A. Di Ciaccio[76a,76b], L. Di Ciaccio[4], A. Di Domenico[75a,75b], C. Di Donato[72a,72b], A. Di Girolamo[36], G. Di Gregorio[5], A. Di Luca[78a,78b], B. Di Micco[77a,77b], R. Di Nardo[77a,77b], C. Diaconu[90b], F.A. Dias[114], T. Dias Do Vale[142], M.A. Diaz[137a,137b], F.G. Diaz Capriles[24], M. Didenko[163], E.B. Diehl[106], L. Diehl[54], S. Díez Cornell[48], C. Diez Pardos[141], C. Dimitriadi[24,161], A. Dimitrievska[17a], J. Dingfelder[24], I-M. Dinu[27b], S.J. Dittmeier[63b], F. Dittus[36], F. Djama[90b], T. Djobava[149b], J.I. Djuvsland[16], C. Doglioni[102,99], J. Dolejsi[133], Z. Dolezal[133], M. Donadelli[82c], B. Dong[107], J. Donini[40], A. D'Onofrio[77a,77b], M. D'Onofrio[93], J. Dopke[134], A. Doria[72a], N. Dos Santos Fernandes[130a], M.T. Dova[91], A.T. Doyle[59], M.A. Draguet[126], E. Dreyer[169], I. Drivas-koulouris[10], A.S. Drobac[158], M. Drozdova[56], D. Du[62a], T.A. du Pree[114], F. Dubinin[37], M. Dubovsky[28a], E. Duchovni[169], G. Duckeck[109], O.A. Ducu[27b], D. Duda[52], A. Dudarev[36], E.R. Duden[26], M. D'uffizi[102], L. Duflot[66], M. Dührssen[36], C. Dülsen[171], A.E. Dumitriu[27b], M. Dunford[63a], S. Dungs[49], K. Dunne[47a,47b], A. Duperrin[90b], H. Duran Yildiz[3a], M. Düren[58], A. Durglishvili[149b], B.L. Dwyer[115], G.I. Dyckes[17a], M. Dyndal[85a], S. Dysch[102], B.S. Dziedzic[86], Z.O. Earnshaw[146], G.H. Eberwein[126], B. Eckerova[28a], S. Eggebrecht[55], M.G. Eggleston[51], E. Egidio Purcino De Souza[127], L.F. Ehrke[56], G. Eigen[16], K. Einsweiler[17a], T. Ekelof[161], P.A. Ekman[99], S. El Farkh[35b], Y. El Ghazali[35b], H. El Jarrari[35e,148], A. El Moussaouy[35a], V. Ellajosyula[161], M. Ellert[161], F. Ellinghaus[171], A.A. Elliot[95], N. Ellis[36], J. Elmsheuser[29], M. Elsing[36], D. Emeliyanov[134], Y. Enari[153], I. Ene[17a], S. Epari[13], J. Erdmann[49],

P.A. Erland[86], M. Errenst[171], M. Escalier[66], C. Escobar[163], E. Etzion[151], G. Evans[130a], H. Evans[68], L.S. Evans[96], M.O. Evans[146], A. Ezhilov[37], S. Ezzarqtouni[35a], F. Fabbri[59], L. Fabbri[23b,23a], G. Facini[97], V. Fadeyev[136], R.M. Fakhrutdinov[37], S. Falciano[75a], L.F. Falda Ulhoa Coelho[36], P.J. Falke[24], J. Faltova[133], C. Fan[162], Y. Fan[14a], Y. Fang[14a,14e], M. Fanti[71a,71b], M. Faraj[69a,69b], Z. Farazpay[98], A. Farbin[8], A. Farilla[77a], T. Farooque[107], S.M. Farrington[52], F. Fassi[35e], D. Fassouliotis[9], M. Faucci Giannelli[76a,76b], W.J. Fawcett[32], L. Fayard[66], P. Federic[133], P. Federicova[131], O.L. Fedin[37,a], G. Fedotov[37], M. Feickert[170], L. Feligioni[90b], A. Fell[139], D.E. Fellers[123], C. Feng[62b], M. Feng[14b], Z. Feng[114], M.J. Fenton[160], A.B. Fenyuk[37], L. Ferencz[48], R.A.M. Ferguson[92], S.I. Fernandez Luengo[137f], M.J.V. Fernoux[90b], J. Ferrando[48], A. Ferrari[161], P. Ferrari[114,113], R. Ferrari[73a], D. Ferrere[56], C. Ferretti[106], F. Fiedler[101], A. Filipčič[94], E.K. Filmer[1], F. Filthaut[113], M.C.N. Fiolhais[130a,130c,d], L. Fiorini[163], W.C. Fisher[107], T. Fitschen[102], P.M. Fitzhugh[135], I. Fleck[141], P. Fleischmann[106], T. Flick[171], L. Flores[128], M. Flores[33d,ah], L.R. Flores Castillo[64a], L. Flores Sanz De Acedo[36], F.M. Follega[78a,78b], N. Fomin[16], J.H. Foo[155], B.C. Forland[68], A. Formica[135], A.C. Forti[102], E. Fortin[36], A.W. Fortman[61], M.G. Foti[17a], L. Fountas[9,k], D. Fournier[66], H. Fox[92], P. Francavilla[74a,74b], S. Francescato[61], S. Franchellucci[56], M. Franchini[23b,23a], S. Franchino[63a], D. Francis[36], L. Franco[113], L. Franconi[48], M. Franklin[61], G. Frattari[26], A.C. Freegard[95], W.S. Freund[82b], Y.Y. Frid[151], N. Fritzsche[50], A. Froch[54], D. Froidevaux[36], J.A. Frost[126], Y. Fu[62a], M. Fujimoto[118], E. Fullana Torregrosa[163,*], K.Y. Fung[64a], E. Furtado De Simas Filho[82b], M. Furukawa[153], J. Fuster[163], A. Gabrielli[23b,23a], A. Gabrielli[155], P. Gadow[48], G. Gagliardi[57b,57a], L.G. Gagnon[17a], E.J. Gallas[126], B.J. Gallop[134], K.K. Gan[119], S. Ganguly[153], J. Gao[62a], Y. Gao[52], F.M. Garay Walls[137a,137b], B. Garcia[29,am], C. García[163], A. Garcia Alonso[114], A.G. Garcia Caffaro[172], J.E. García Navarro[163], M. Garcia-Sciveres[17a], G.L. Gardner[128], R.W. Gardner[39], N. Garelli[158], D. Garg[80], R.B. Garg[143,r], J.M. Gargan[52], C.A. Garner[155], S.J. Gasiorowski[138], P. Gaspar[82b], G. Gaudio[73a], V. Gautam[13], P. Gauzzi[75a,75b], I.L. Gavrilenko[37], A. Gavrilyuk[37], C. Gay[164], G. Gaycken[48], E.N. Gazis[10], A.A. Geanta[27b], C.M. Gee[136], C. Gemme[57b], M.H. Genest[60], S. Gentile[75a,75b], S. George[96], W.F. George[20], T. Geralis[46], P. Gessinger-Befurt[36], M.E. Geyik[171], M. Ghneimat[141], K. Ghorbanian[95], A. Ghosal[141], A. Ghosh[160], A. Ghosh[7], B. Giacobbe[23b], S. Giagu[75a,75b], P. Giannetti[74a], A. Giannini[62a], S.M. Gibson[96], M. Gignac[136], D.T. Gil[85b], A.K. Gilbert[85a], B.J. Gilbert[41], D. Gillberg[34], G. Gilles[114], N.E.K. Gillwald[48], L. Ginabat[127], D.M. Gingrich[2,ak], M.P. Giordani[69a,69c], P.F. Giraud[135], G. Giugliarelli[69a,69c], D. Giugni[71a], F. Giuli[36], I. Gkialas[9,k], L.K. Gladilin[37], C. Glasman[100], G.R. Gledhill[123], M. Glisic[123], I. Gnesi[43b,g], Y. Go[29,am], M. Goblirsch-Kolb[36], B. Gocke[49], D. Godin[108], B. Gokturk[21a], S. Goldfarb[105], T. Golling[56], M.G.D. Gololo[33g], D. Golubkov[37], J.P. Gombas[107], A. Gomes[130a,130b], G. Gomes Da Silva[141], A.J. Gomez Delegido[163], R. Gonçalo[130a,130c], G. Gonella[123], L. Gonella[20], A. Gongadze[38], F. Gonnella[20], J.L. Gonski[41], R.Y. González Andana[52], S. González de la Hoz[163], S. Gonzalez Fernandez[13], R. Gonzalez Lopez[93], C. Gonzalez Renteria[17a], R. Gonzalez Suarez[161], S. Gonzalez-Sevilla[56], G.R. Gonzalvo Rodriguez[163], L. Goossens[36], P.A. Gorbounov[37], B. Gorini[36], E. Gorini[70a,70b], A. Gorišek[94], T.C. Gosart[128], A.T. Goshaw[51], M.I. Gostkin[38], S. Goswami[121], C.A. Gottardo[36], M. Gouighri[35b], V. Goumarre[48], A.G. Goussiou[138], N. Govender[33c], I. Grabowska-Bold[85a], K. Graham[34], E. Gramstad[125], S. Grancagnolo[70a,70b], M. Grandi[146], V. Gratchev[37,*], P.M. Gravila[27f], F.G. Gravili[70a,70b], H.M. Gray[17a], M. Greco[70a,70b], C. Grefe[24], I.M. Gregor[48], P. Grenier[143], C. Grieco[13], A.A. Grillo[136], K. Grimm[31], S. Grinstein[13,x], J.-F. Grivaz[66], E. Gross[169], J. Grosse-Knetter[55], C. Grud[106], J.C. Grundy[126],

L. Guan [106], W. Guan [29], C. Gubbels [164], J.G.R. Guerrero Rojas [163], G. Guerrieri [69a,69b], F. Guescini [110], R. Gugel [101], J.A.M. Guhit [106], A. Guida [18], T. Guillemin [4], E. Guilloton [167,134], S. Guindon [36], F. Guo [14a,14e], J. Guo [62c], L. Guo [48], Y. Guo [106], R. Gupta [48], S. Gurbuz [24], S.S. Gurdasani [54], G. Gustavino [36], M. Guth [56], P. Gutierrez [120], L.F. Gutierrez Zagazeta [128], C. Gutschow [97], C. Gwenlan [126], C.B. Gwilliam [93], E.S. Haaland [125], A. Haas [117], M. Habedank [48], C. Haber [17a], H.K. Hadavand [8], A. Hadef [101], S. Hadzic [110], J.J. Hahn [141], E.H. Haines [97], M. Haleem [166], J. Haley [121], J.J. Hall [139], G.D. Hallewell [90b], L. Halser [19], K. Hamano [165], H. Hamdaoui [35e], M. Hamer [24], G.N. Hamity [52], E.J. Hampshire [96], J. Han [62b], K. Han [62a], L. Han [14c], L. Han [62a], S. Han [17a], Y.F. Han [155], K. Hanagaki [83], M. Hance [136], D.A. Hangal [41,ag], H. Hanif [142], M.D. Hank [128], R. Hankache [102], J.B. Hansen [42], J.D. Hansen [42], P.H. Hansen [42], K. Hara [157], D. Harada [56], T. Harenberg [171], S. Harkusha [37], M.L. Harris [103], Y.T. Harris [126], J. Harrison [13], N.M. Harrison [119], P.F. Harrison[167], N.M. Hartman [110], N.M. Hartmann [109], Y. Hasegawa [140], A. Hasib [52], S. Haug [19], R. Hauser [107], C.M. Hawkes [20], R.J. Hawkings [36], Y. Hayashi [153], S. Hayashida [111], D. Hayden [107], C. Hayes [106], R.L. Hayes [114], C.P. Hays [126], J.M. Hays [95], H.S. Hayward [93], F. He [62a], M. He [14a,14e], Y. He [154], Y. He [127], N.B. Heatley [95], V. Hedberg [99], A.L. Heggelund [125], N.D. Hehir [95], C. Heidegger [54], K.K. Heidegger [54], W.D. Heidorn [81], J. Heilman [34], S. Heim [48], T. Heim [17a], J.G. Heinlein [128], J.J. Heinrich [123], L. Heinrich [110,ai], J. Hejbal [131], L. Helary [48], A. Held [170], S. Hellesund [16], C.M. Helling [164], S. Hellman [47a,47b], C. Helsens [36], R.C.W. Henderson[92], L. Henkelmann [32], A.M. Henriques Correia[36], H. Herde [99], Y. Hernández Jiménez [145], L.M. Herrmann [24], T. Herrmann [50], G. Herten [54], R. Hertenberger [109], L. Hervas [36], M.E. Hesping [101], N.P. Hessey [156a], H. Hibi [84], S.J. Hillier [20], J.R. Hinds [107], F. Hinterkeuser [24], M. Hirose [124], S. Hirose [157], D. Hirschbuehl [171], T.G. Hitchings [102], B. Hiti [94], J. Hobbs [145], R. Hobincu [27e], N. Hod [169], M.C. Hodgkinson [139], B.H. Hodkinson [32], A. Hoecker [36], J. Hofer [48], T. Holm [24], M. Holzbock [110], L.B.A.H. Hommels [32], B.P. Honan [102], J. Hong [62c], T.M. Hong [129], B.H. Hooberman [162], W.H. Hopkins [6], Y. Horii [111], S. Hou [148], A.S. Howard [94], J. Howarth [59], J. Hoya [6], M. Hrabovsky [122], A. Hrynevich [48], T. Hryn'ova [4], P.J. Hsu [65], S.-C. Hsu [138], Q. Hu [41], Y.F. Hu [14a,14e], S. Huang [64b], X. Huang [14c], Y. Huang [62a], Y. Huang [14a], Z. Huang [102], Z. Hubacek [132], M. Huebner [24], F. Huegging [24], T.B. Huffman [126], C.A. Hugli [48], M. Huhtinen [36], S.K. Huiberts [16], R. Hulsken [104], N. Huseynov [12,a], J. Huston [107], J. Huth [61], R. Hyneman [143], G. Iacobucci [56], G. Iakovidis [29], I. Ibragimov [141], L. Iconomidou-Fayard [66], P. Iengo [72a,72b], R. Iguchi [153], T. Iizawa [83], Y. Ikegami [83], N. Ilic [155], H. Imam [35a], M. Ince Lezki [56], T. Ingebretsen Carlson [47a,47b], G. Introzzi [73a,73b], M. Iodice [77a], V. Ippolito [75a,75b], R.K. Irwin [93], M. Ishino [153], W. Islam [170], C. Issever [18,48], S. Istin [21a,ao], H. Ito [168], J.M. Iturbe Ponce [64a], R. Iuppa [78a,78b], A. Ivina [169], J.M. Izen [45], V. Izzo [72a], P. Jacka [131,132], P. Jackson [1], R.M. Jacobs [48], B.P. Jaeger [142], C.S. Jagfeld [109], P. Jain [54], G. Jäkel [171], K. Jakobs [54], T. Jakoubek [169], J. Jamieson [59], K.W. Janas [85a], A.E. Jaspan [93], M. Javurkova [103], F. Jeanneau [135], L. Jeanty [123], J. Jejelava [149a,ae], P. Jenni [54,h], C.E. Jessiman [34], S. Jézéquel [4], C. Jia[62b], J. Jia [145], X. Jia [61], X. Jia [14a,14e], Z. Jia [14c], Y. Jiang[62a], S. Jiggins [48], J. Jimenez Pena [13], S. Jin [14c], A. Jinaru [27b], O. Jinnouchi [154], P. Johansson [139], K.A. Johns [7], J.W. Johnson [136], D.M. Jones [32], E. Jones [48], P. Jones [32], R.W.L. Jones [92], T.J. Jones [93], R. Joshi [119], J. Jovicevic [15], X. Ju [17a], J.J. Junggeburth [36], T. Junkermann [63a], A. Juste Rozas [13,x], M.K. Juzek [86], S. Kabana [137e], A. Kaczmarska [86], M. Kado [110], H. Kagan [119], M. Kagan [143], A. Kahn[41], A. Kahn [128], C. Kahra [101], T. Kaji [168], E. Kajomovitz [150], N. Kakati [169], I. Kalaitzidou [54], C.W. Kalderon [29], A. Kamenshchikov [155], S. Kanayama [154], N.J. Kang [136], D. Kar [33g], K. Karava [126], M.J. Kareem [156b], E. Karentzos [54],

I. Karkanias [152], O. Karkout [114], S.N. Karpov [38], Z.M. Karpova [38], V. Kartvelishvili [92], A.N. Karyukhin [37], E. Kasimi [152], J. Katzy [48], S. Kaur [34], K. Kawade [140], T. Kawamoto [135], E.F. Kay [36], F.I. Kaya [158], S. Kazakos [107], V.F. Kazanin [37], Y. Ke [145], J.M. Keaveney [33a], R. Keeler [165], G.V. Kehris [61], J.S. Keller [34], A.S. Kelly[97], J.J. Kempster [146], K.E. Kennedy [41], P.D. Kennedy [101], O. Kepka [131], B.P. Kerridge [167], S. Kersten [171], B.P. Kerševan [94], S. Keshri [66], L. Keszeghova [28a], S. Ketabchi Haghighat [155], M. Khandoga [127], A. Khanov [121], A.G. Kharlamov [37], T. Kharlamova [37], E.E. Khoda [138], T.J. Khoo [18], G. Khoriauli [166], J. Khubua [149b], Y.A.R. Khwaira [66], M. Kiehn [36], A. Kilgallon [123], D.W. Kim [47a,47b], Y.K. Kim [39], N. Kimura [97], A. Kirchhoff [55], C. Kirfel [24], F. Kirfel [24], J. Kirk [134], A.E. Kiryunin [110], C. Kitsaki [10], O. Kivernyk [24], M. Klassen [63a], C. Klein [34], L. Klein [166], M.H. Klein [106], M. Klein [93], S.B. Klein [56], U. Klein [93], P. Klimek [36], A. Klimentov [29], T. Klioutchnikova [36], P. Kluit [114], S. Kluth [110], E. Kneringer [79], T.M. Knight [155], A. Knue [54], R. Kobayashi [87], S.F. Koch [126], M. Kocian [143], P. Kodyš [133], D.M. Koeck [123], P.T. Koenig [24], T. Koffas [34], M. Kolb [135], I. Koletsou [4], T. Komarek [122], K. Köneke [54], A.X.Y. Kong [1], T. Kono [118], N. Konstantinidis [97], B. Konya [99], R. Kopeliansky [68], S. Koperny [85a], K. Korcyl [86], K. Kordas [152,f], G. Koren [151], A. Korn [97], S. Korn [55], I. Korolkov [13], N. Korotkova [37], B. Kortman [114], O. Kortner [110], S. Kortner [110], W.H. Kostecka [115], V.V. Kostyukhin [141], A. Kotsokechagia [135], A. Kotwal [51], A. Koulouris [36], A. Kourkoumeli-Charalampidi [73a,73b], C. Kourkoumelis [9], E. Kourlitis [6], O. Kovanda [146], R. Kowalewski [165], W. Kozanecki [135], A.S. Kozhin [37], V.A. Kramarenko [37], G. Kramberger [94], P. Kramer [101], M.W. Krasny [127], A. Krasznahorkay [36], J.W. Kraus [171], J.A. Kremer [101], T. Kresse [50], J. Kretzschmar [93], K. Kreul [18], P. Krieger [155], S. Krishnamurthy [103], M. Krivos [133], K. Krizka [20], K. Kroeninger [49], H. Kroha [110], J. Kroll [131], J. Kroll [128], K.S. Krowpman [107], U. Kruchonak [38], H. Krüger [24], N. Krumnack[81], M.C. Kruse [51], J.A. Krzysiak [86], O. Kuchinskaia [37], S. Kuday [3a], S. Kuehn [36], R. Kuesters [54], T. Kuhl [48], V. Kukhtin [38], Y. Kulchitsky [37,a], S. Kuleshov [137d,137b], M. Kumar [33g], N. Kumari [90b], A. Kupco [131], T. Kupfer[49], A. Kupich [37], O. Kuprash [54], H. Kurashige [84], L.L. Kurchaninov [156a], O. Kurdysh [66], Y.A. Kurochkin [37], A. Kurova [37], M. Kuze [154], A.K. Kvam [103], J. Kvita [122], T. Kwan [104], N.G. Kyriacou [106], L.A.O. Laatu [90b], C. Lacasta [163], F. Lacava [75a,75b], H. Lacker [18], D. Lacour [127], N.N. Lad [97], E. Ladygin [38], B. Laforge [127], T. Lagouri [137e], S. Lai [55], I.K. Lakomiec [85a], N. Lalloue [60], J.E. Lambert [165,m], S. Lammers [68], W. Lampl [7], C. Lampoudis [152,f], A.N. Lancaster [115], E. Lançon [29], U. Landgraf [54], M.P.J. Landon [95], V.S. Lang [54], R.J. Langenberg [103], O.K.B. Langrekken [125], A.J. Lankford [160], F. Lanni [36], K. Lantzsch [24], A. Lanza [73a], A. Lapertosa [57b,57a], J.F. Laporte [135], T. Lari [71a], F. Lasagni Manghi [23b], M. Lassnig [36], V. Latonova [131], A. Laudrain [101], A. Laurier [150], S.D. Lawlor [96], Z. Lawrence [102], M. Lazzaroni [71a,71b], B. Le[102], E.M. Le Boulicaut [51], B. Leban [94], A. Lebedev [81], M. LeBlanc [36], F. Ledroit-Guillon [60], A.C.A. Lee[97], S.C. Lee [148], S. Lee [47a,47b], T.F. Lee [93], L.L. Leeuw [33c], H.P. Lefebvre [96], M. Lefebvre [165], C. Leggett [17a], G. Lehmann Miotto [36], M. Leigh [56], W.A. Leight [103], W. Leinonen [113], A. Leisos [152,w], M.A.L. Leite [82c], C.E. Leitgeb [48], R. Leitner [133], K.J.C. Leney [44], T. Lenz [24], S. Leone [74a], C. Leonidopoulos [52], A. Leopold [144], C. Leroy [108], R. Les [107], C.G. Lester [32], M. Levchenko [37], J. Levêque [4], D. Levin [106], L.J. Levinson [169], M.P. Lewicki [86], D.J. Lewis [4], A. Li [5], B. Li [62b], C. Li[62a], C-Q. Li [62c], H. Li [62a], H. Li [62b], H. Li [14c], H. Li [62b], K. Li [138], L. Li [62c], M. Li [14a,14e], Q.Y. Li [62a], S. Li [14a,14e], S. Li [62d,62c,e], T. Li [5,c], X. Li [104], Z. Li [126], Z. Li [104], Z. Li [93], Z. Li [14a,14e], Z. Liang [14a], M. Liberatore [48], B. Liberti [76a], K. Lie [64c], J. Lieber Marin [82b], H. Lien [68], K. Lin [107], R.E. Lindley [7], J.H. Lindon [2], A. Linss [48], E. Lipeles [128], A. Lipniacka [16], A. Lister [164], J.D. Little [4], B. Liu [14a], B.X. Liu [142], D. Liu [62d,62c], J.B. Liu [62a], J.K.K. Liu [32], K. Liu [62d,62c], M. Liu [62a],

M.Y. Liu[62a], P. Liu[14a], Q. Liu[62d,138,62c], X. Liu[62a], Y. Liu[14d,14e], Y.L. Liu[106], Y.W. Liu[62a], J. Llorente Merino[142], S.L. Lloyd[95], E.M. Lobodzinska[48], P. Loch[7], S. Loffredo[76a,76b], T. Lohse[18], K. Lohwasser[139], E. Loiacono[48], M. Lokajicek[131,*], J.D. Lomas[20], J.D. Long[162], I. Longarini[160], L. Longo[70a,70b], R. Longo[162], I. Lopez Paz[67], A. Lopez Solis[48], J. Lorenz[109], N. Lorenzo Martinez[4], A.M. Lory[109], O. Loseva[37], X. Lou[47a,47b], X. Lou[14a,14e], A. Lounis[66], J. Love[6], P.A. Love[92], G. Lu[14a,14e], M. Lu[80], S. Lu[128], Y.J. Lu[65], H.J. Lubatti[138], C. Luci[75a,75b], F.L. Lucio Alves[14c], A. Lucotte[60], F. Luehring[68], I. Luise[145], O. Lukianchuk[66], O. Lundberg[144], B. Lund-Jensen[144], N.A. Luongo[123], M.S. Lutz[151], D. Lynn[29], H. Lyons[93], R. Lysak[131], E. Lytken[99], V. Lyubushkin[38], T. Lyubushkina[38], M.M. Lyukova[145], H. Ma[29], K. Ma[62a], L.L. Ma[62b], Y. Ma[121], D.M. Mac Donell[165], G. Maccarrone[53], J.C. MacDonald[101], R. Madar[40], W.F. Mader[50], J. Maeda[84], T. Maeno[29], M. Maerker[50], H. Maguire[139], V. Maiboroda[135], A. Maio[130a,130b,130d], K. Maj[85a], O. Majersky[48], S. Majewski[123], N. Makovec[66], V. Maksimovic[15], B. Malaescu[127], Pa. Malecki[86], V.P. Maleev[37], F. Malek[60], M. Mali[94], D. Malito[96,q], U. Mallik[80], S. Maltezos[10], S. Malyukov[38], J. Mamuzic[13], G. Mancini[53], G. Manco[73a,73b], J.P. Mandalia[95], I. Mandić[94], L. Manhaes de Andrade Filho[82a], I.M. Maniatis[169], J. Manjarres Ramos[90a,af], D.C. Mankad[169], A. Mann[109], B. Mansoulie[135], S. Manzoni[36], A. Marantis[152,w], G. Marchiori[5], M. Marcisovsky[131], C. Marcon[71a,71b], M. Marinescu[20], M. Marjanovic[120], E.J. Marshall[92], Z. Marshall[17a], S. Marti-Garcia[163], T.A. Martin[167], V.J. Martin[52], B. Martin dit Latour[16], L. Martinelli[75a,75b], M. Martinez[13,x], P. Martinez Agullo[163], V.I. Martinez Outschoorn[103], P. Martinez Suarez[13], S. Martin-Haugh[134], V.S. Martoiu[27b], A.C. Martyniuk[97], A. Marzin[36], D. Mascione[78a,78b], L. Masetti[101], T. Mashimo[153], J. Masik[102], A.L. Maslennikov[37], L. Massa[23b], P. Massarotti[72a,72b], P. Mastrandrea[74a,74b], A. Mastroberardino[43b,43a], T. Masubuchi[153], T. Mathisen[161], J. Matousek[133], N. Matsuzawa[153], J. Maurer[27b], B. Maček[94], D.A. Maximov[37], R. Mazini[148], I. Maznas[152], M. Mazza[107], S.M. Mazza[136], E. Mazzeo[71a,71b], C. Mc Ginn[29], J.P. Mc Gowan[104], S.P. Mc Kee[106], E.F. McDonald[105], A.E. McDougall[114], J.A. Mcfayden[146], R.P. McGovern[128], G. Mchedlidze[149b], R.P. Mckenzie[33g], T.C. Mclachlan[48], D.J. Mclaughlin[97], K.D. McLean[165], S.J. McMahon[134], P.C. McNamara[105], C.M. Mcpartland[93], R.A. McPherson[165,ab], S. Mehlhase[109], A. Mehta[93], D. Melini[150], B.R. Mellado Garcia[33g], A.H. Melo[55], F. Meloni[48], A.M. Mendes Jacques Da Costa[102], H.Y. Meng[155], L. Meng[92], S. Menke[110], M. Mentink[36], E. Meoni[43b,43a], C. Merlassino[126], L. Merola[72a,72b], C. Meroni[71a,71b], G. Merz[106], O. Meshkov[37], J. Metcalfe[6], A.S. Mete[6], C. Meyer[68], J-P. Meyer[135], R.P. Middleton[134], L. Mijović[52], G. Mikenberg[169], M. Mikestikova[131], M. Mikuž[94], H. Mildner[101], A. Milic[36], C.D. Milke[44], D.W. Miller[39], L.S. Miller[34], A. Milov[169], D.A. Milstead[47a,47b], T. Min[14c], A.A. Minaenko[37], I.A. Minashvili[149b], L. Mince[59], A.I. Mincer[117], B. Mindur[85a], M. Mineev[38], Y. Mino[87], L.M. Mir[13], M. Miralles Lopez[163], M. Mironova[17a], A. Mishima[153], M.C. Missio[113], T. Mitani[168], A. Mitra[167], V.A. Mitsou[163], O. Miu[155], P.S. Miyagawa[95], Y. Miyazaki[89], A. Mizukami[83], T. Mkrtchyan[63a], M. Mlinarevic[97], T. Mlinarevic[97], M. Mlynarikova[36], S. Mobius[19], K. Mochizuki[108], P. Moder[48], P. Mogg[109], A.F. Mohammed[14a,14e], S. Mohapatra[41], G. Mokgatitswane[33g], L. Moleri[169], B. Mondal[141], S. Mondal[132], G. Monig[146], K. Mönig[48], E. Monnier[90b], L. Monsonis Romero[163], J. Montejo Berlingen[13,83], M. Montella[119], F. Montereali[77a,77b], F. Monticelli[91], S. Monzani[69a,69c], N. Morange[66], A.L. Moreira De Carvalho[130a], M. Moreno Llácer[163], C. Moreno Martinez[56], P. Morettini[57b], S. Morgenstern[36], M. Morii[61], M. Morinaga[153], A.K. Morley[36], F. Morodei[75a,75b], L. Morvaj[36], P. Moschovakos[36], B. Moser[36], M. Mosidze[149b], T. Moskalets[54],

P. Moskvitina[113], J. Moss[31,o], E.J.W. Moyse[103], O. Mtintsilana[33g], S. Muanza[90b], J. Mueller[129], D. Muenstermann[92], R. Müller[19], G.A. Mullier[161], A.J. Mullin[32], J.J. Mullin[128], D.P. Mungo[155], D. Munoz Perez[163], F.J. Munoz Sanchez[102], M. Murin[102], W.J. Murray[167,134], A. Murrone[71a,71b], J.M. Muse[120], M. Muškinja[17a], C. Mwewa[29], A.G. Myagkov[37,a], A.J. Myers[8], A.A. Myers[129], G. Myers[68], M. Myska[132], B.P. Nachman[17a], O. Nackenhorst[49], A. Nag[50], K. Nagai[126], K. Nagano[83], J.L. Nagle[29,am], E. Nagy[90b], A.M. Nairz[36], Y. Nakahama[83], K. Nakamura[83], K. Nakkalil[5], H. Nanjo[124], R. Narayan[44], E.A. Narayanan[112], I. Naryshkin[37], M. Naseri[34], S. Nasri[159], C. Nass[24], G. Navarro[22a], J. Navarro-Gonzalez[163], R. Nayak[151], A. Nayaz[18], P.Y. Nechaeva[37], F. Nechansky[48], L. Nedic[126], T.J. Neep[20], A. Negri[73a,73b], M. Negrini[23b], C. Nellist[114], C. Nelson[104], K. Nelson[106], S. Nemecek[131], M. Nessi[36,i], M.S. Neubauer[162], F. Neuhaus[101], J. Neundorf[48], R. Newhouse[164], P.R. Newman[20], C.W. Ng[129], Y.W.Y. Ng[48], B. Ngair[35e], H.D.N. Nguyen[108], R.B. Nickerson[126], R. Nicolaidou[135], J. Nielsen[136], M. Niemeyer[55], J. Niermann[55,36], N. Nikiforou[36], V. Nikolaenko[37,a], I. Nikolic-Audit[127], K. Nikolopoulos[20], P. Nilsson[29], I. Ninca[48], H.R. Nindhito[56], G. Ninio[151], A. Nisati[75a], N. Nishu[2], R. Nisius[110], J-E. Nitschke[50], E.K. Nkadimeng[33g], S.J. Noacco Rosende[91], T. Nobe[153], D.L. Noel[32], T. Nommensen[147], M.B. Norfolk[139], R.R.B. Norisam[97], B.J. Norman[34], J. Novak[94], T. Novak[48], L. Novotny[132], R. Novotny[112], L. Nozka[122], K. Ntekas[160], N.M.J. Nunes De Moura Junior[82b], E. Nurse[97], J. Ocariz[127], A. Ochi[84], I. Ochoa[130a], S. Oerdek[161], J.T. Offermann[39], A. Ogrodnik[133], A. Oh[102], C.C. Ohm[144], H. Oide[83], R. Oishi[153], M.L. Ojeda[48], Y. Okazaki[87], M.W. O'Keefe[93], Y. Okumura[153], L.F. Oleiro Seabra[130a], S.A. Olivares Pino[137d], D. Oliveira Damazio[29], D. Oliveira Goncalves[82a], J.L. Oliver[160], M.J.R. Olsson[160], A. Olszewski[86], Ö.O. Öncel[54], D.C. O'Neil[142], A.P. O'Neill[19], A. Onofre[130a,130e], P.U.E. Onyisi[11], M.J. Oreglia[39], G.E. Orellana[91], D. Orestano[77a,77b], N. Orlando[13], R.S. Orr[155], V. O'Shea[59], L.M. Osojnak[128], R. Ospanov[62a], G. Otero y Garzon[30], H. Otono[89], P.S. Ott[63a], G.J. Ottino[17a], M. Ouchrif[35d], J. Ouellette[29], F. Ould-Saada[125], M. Owen[59], R.E. Owen[134], K.Y. Oyulmaz[21a], V.E. Ozcan[21a], N. Ozturk[8], S. Ozturk[21d], H.A. Pacey[32], A. Pacheco Pages[13], C. Padilla Aranda[13], G. Padovano[75a,75b], S. Pagan Griso[17a], G. Palacino[68], A. Palazzo[70a,70b], S. Palestini[36], J. Pan[172], T. Pan[64a], D.K. Panchal[11], C.E. Pandini[114], J.G. Panduro Vazquez[96], H. Pang[14b], P. Pani[48], G. Panizzo[69a,69c], L. Paolozzi[56], C. Papadatos[108], S. Parajuli[44], A. Paramonov[6], C. Paraskevopoulos[10], D. Paredes Hernandez[64b], T.H. Park[155], M.A. Parker[32], F. Parodi[57b,57a], E.W. Parrish[115], V.A. Parrish[52], J.A. Parsons[41], U. Parzefall[54], B. Pascual Dias[108], L. Pascual Dominguez[151], F. Pasquali[114], E. Pasqualucci[75a], S. Passaggio[57b], F. Pastore[96], P. Pasuwan[47a,47b], P. Patel[86], U.M. Patel[51], J.R. Pater[102], T. Pauly[36], J. Pearkes[143], M. Pedersen[125], R. Pedro[130a], S.V. Peleganchuk[37], O. Penc[36], E.A. Pender[52], H. Peng[62a], K.E. Penski[109], M. Penzin[37], B.S. Peralva[82d], A.P. Pereira Peixoto[60], L. Pereira Sanchez[47a,47b], D.V. Perepelitsa[29,am], E. Perez Codina[156a], M. Perganti[10], L. Perini[71a,71b,*], H. Pernegger[36], A. Perrevoort[113], O. Perrin[40], K. Peters[48], R.F.Y. Peters[102], B.A. Petersen[36], T.C. Petersen[42], E. Petit[90b], V. Petousis[132], C. Petridou[152,f], A. Petrukhin[141], M. Pettee[17a], N.E. Pettersson[36], A. Petukhov[37], K. Petukhova[133], A. Peyaud[135], R. Pezoa[137f], L. Pezzotti[36], G. Pezzullo[172], T.M. Pham[170], T. Pham[105], P.W. Phillips[134], G. Piacquadio[145], E. Pianori[17a], F. Piazza[71a,71b], R. Piegaia[30], D. Pietreanu[27b], A.D. Pilkington[102], M. Pinamonti[69a,69c], J.L. Pinfold[2], B.C. Pinheiro Pereira[130a], A.E. Pinto Pinoargote[135], K.M. Piper[146], A. Pirttikoski[56], C. Pitman Donaldson[97], D.A. Pizzi[34], L. Pizzimento[76a,76b], A. Pizzini[114], M.-A. Pleier[29], V. Plesanovs[54], V. Pleskot[133], E. Plotnikova[38], G. Poddar[4], R. Poettgen[99],

L. Poggioli[127], I. Pokharel[55], S. Polacek[133], G. Polesello[73a], A. Poley[142,156a], R. Polifka[132], A. Polini[23b], C.S. Pollard[167], Z.B. Pollock[119], V. Polychronakos[29], E. Pompa Pacchi[75a,75b], D. Ponomarenko[113], L. Pontecorvo[36], S. Popa[27a], G.A. Popeneciu[27d], A. Poreba[36], D.M. Portillo Quintero[156a], S. Pospisil[132], M.A. Postill[139], P. Postolache[27c], K. Potamianos[167], P.A. Potepa[85a], I.N. Potrap[38], C.J. Potter[32], H. Potti[1], T. Poulsen[48], J. Poveda[163], M.E. Pozo Astigarraga[36], A. Prades Ibanez[163], J. Pretel[54], D. Price[102], M. Primavera[70a], M.A. Principe Martin[100], R. Privara[122], T. Procter[59], M.L. Proffitt[138], N. Proklova[128], K. Prokofiev[64c], G. Proto[110], S. Protopopescu[29], J. Proudfoot[6], M. Przybycien[85a], W.W. Przygoda[85b], J.E. Puddefoot[139], D. Pudzha[37], D. Pyatiizbyantseva[37], J. Qian[106], D. Qichen[102], Y. Qin[102], T. Qiu[52], A. Quadt[55], M. Queitsch-Maitland[102], G. Quetant[56], G. Rabanal Bolanos[61], D. Rafanoharana[54], F. Ragusa[71a,71b], J.L. Rainbolt[39], J.A. Raine[56], S. Rajagopalan[29], E. Ramakoti[37], K. Ran[48,14e], N.P. Rapheeha[33g], H. Rasheed[27b], V. Raskina[127], D.F. Rassloff[63a], S. Rave[101], B. Ravina[55], I. Ravinovich[169], M. Raymond[36], A.L. Read[125], N.P. Readioff[139], D.M. Rebuzzi[73a,73b], G. Redlinger[29], A.S. Reed[110], K. Reeves[26], J.A. Reidelsturz[171,v], D. Reikher[151], A. Rej[141], C. Rembser[36], A. Renardi[48], M. Renda[27b], M.B. Rendel[110], F. Renner[48], A.G. Rennie[59], S. Resconi[71a], M. Ressegotti[57b,57a], S. Rettie[36], J.G. Reyes Rivera[107], B. Reynolds[119], E. Reynolds[17a], O.L. Rezanova[37], P. Reznicek[133], N. Ribaric[92], E. Ricci[78a,78b], R. Richter[110], S. Richter[47a,47b], E. Richter-Was[85b], M. Ridel[127], S. Ridouani[35d], P. Rieck[117], P. Riedler[36], M. Rijssenbeek[145], A. Rimoldi[73a,73b], M. Rimoldi[48], L. Rinaldi[23b,23a], T.T. Rinn[29], M.P. Rinnagel[109], G. Ripellino[161], I. Riu[13], P. Rivadeneira[48], J.C. Rivera Vergara[165], F. Rizatdinova[121], E. Rizvi[95], B.A. Roberts[167], B.R. Roberts[17a], S.H. Robertson[104,ab], M. Robin[48], D. Robinson[32], C.M. Robles Gajardo[137f], M. Robles Manzano[101], A. Robson[59], A. Rocchi[76a,76b], C. Roda[74a,74b], S. Rodriguez Bosca[63a], Y. Rodriguez Garcia[22a], A. Rodriguez Rodriguez[54], A.M. Rodríguez Vera[156b], S. Roe[36], J.T. Roemer[160], A.R. Roepe-Gier[136], J. Roggel[171], O. Røhne[125], R.A. Rojas[103], C.P.A. Roland[68], J. Roloff[29], A. Romaniouk[37], E. Romano[73a,73b], M. Romano[23b], A.C. Romero Hernandez[162], N. Rompotis[93], L. Roos[127], S. Rosati[75a], B.J. Rosser[39], E. Rossi[126], E. Rossi[72a,72b], L.P. Rossi[57b], L. Rossini[48], R. Rosten[119], M. Rotaru[27b], B. Rottler[54], C. Rougier[90a,af], D. Rousseau[66], D. Rousso[32], A. Roy[162], S. Roy-Garand[155], A. Rozanov[90b], Y. Rozen[150], X. Ruan[33g], A. Rubio Jimenez[163], A.J. Ruby[93], V.H. Ruelas Rivera[18], T.A. Ruggeri[1], A. Ruggiero[126], A. Ruiz-Martinez[163], A. Rummler[36], Z. Rurikova[54], N.A. Rusakovich[38], H.L. Russell[165], G. Russo[75a,75b], J.P. Rutherfoord[7], S. Rutherford Colmenares[32], K. Rybacki[92], M. Rybar[133], E.B. Rye[125], A. Ryzhov[44], J.A. Sabater Iglesias[56], P. Sabatini[163], L. Sabetta[75a,75b], H.F-W. Sadrozinski[136], F. Safai Tehrani[75a], B. Safarzadeh Samani[146], M. Safdari[143], S. Saha[165], M. Sahinsoy[110], M. Saimpert[135], M. Saito[153], T. Saito[153], D. Salamani[36], A. Salnikov[143], J. Salt[163], A. Salvador Salas[13], D. Salvatore[43b,43a], F. Salvatore[146], A. Salzburger[36], D. Sammel[54], D. Sampsonidis[152,f], D. Sampsonidou[123], J. Sánchez[163], A. Sanchez Pineda[4], V. Sanchez Sebastian[163], H. Sandaker[125], C.O. Sander[48], J.A. Sandesara[103], M. Sandhoff[171], C. Sandoval[22b], D.P.C. Sankey[134], T. Sano[87], A. Sansoni[53], L. Santi[75a,75b], C. Santoni[40], H. Santos[130a,130b], S.N. Santpur[17a], A. Santra[169], K.A. Saoucha[139], J.G. Saraiva[130a,130d], J. Sardain[7], O. Sasaki[83], K. Sato[157], C. Sauer[63b], F. Sauerburger[54], E. Sauvan[4], P. Savard[155,ak], R. Sawada[153], C. Sawyer[134], L. Sawyer[98], I. Sayago Galvan[163], C. Sbarra[23b], A. Sbrizzi[23b,23a], T. Scanlon[97], J. Schaarschmidt[138], P. Schacht[110], D. Schaefer[39], U. Schäfer[101], A.C. Schaffer[66,44], D. Schaile[109], R.D. Schamberger[145], C. Scharf[18], M.M. Schefer[19], V.A. Schegelsky[37], D. Scheirich[133], F. Schenck[18], M. Schernau[160], C. Scheulen[55], C. Schiavi[57b,57a], E.J. Schioppa[70a,70b],

M. Schioppa [43b,43a], B. Schlag [143,r], K.E. Schleicher [54], S. Schlenker [36], J. Schmeing [171], M.A. Schmidt [171], K. Schmieden [101], C. Schmitt [101], S. Schmitt [48], L. Schoeffel [135], A. Schoening [63b], P.G. Scholer [54], E. Schopf [126], M. Schott [101], J. Schovancova [36], S. Schramm [56], F. Schroeder [171], T. Schroer [56], H-C. Schultz-Coulon [63a], M. Schumacher [54], B.A. Schumm [136], Ph. Schune [135], A.J. Schuy [138], H.R. Schwartz [136], A. Schwartzman [143], T.A. Schwarz [106], Ph. Schwemling [135], R. Schwienhorst [107], A. Sciandra [136], G. Sciolla [26], F. Scuri [74a], C.D. Sebastiani [93], K. Sedlaczek [115], P. Seema [18], S.C. Seidel [112], A. Seiden [136], B.D. Seidlitz [41], C. Seitz [48], J.M. Seixas [82b], G. Sekhniaidze [72a], S.J. Sekula [44], L. Selem [60], N. Semprini-Cesari [23b,23a], D. Sengupta [56], V. Senthilkumar [163], L. Serin [66], L. Serkin [69a,69b], M. Sessa [76a,76b], H. Severini [120], F. Sforza [57b,57a], A. Sfyrla [56], E. Shabalina [55], R. Shaheen [144], J.D. Shahinian [128], D. Shaked Renous [169], L.Y. Shan [14a], M. Shapiro [17a], A. Sharma [36], A.S. Sharma [164], P. Sharma [80], S. Sharma [48], P.B. Shatalov [37], K. Shaw [146], S.M. Shaw [102], A. Shcherbakova [37], Q. Shen [62c,5], P. Sherwood [97], L. Shi [97], X. Shi [14a], C.O. Shimmin [172], Y. Shimogama [168], J.D. Shinner [96], I.P.J. Shipsey [126], S. Shirabe [56,i], M. Shiyakova [38,z], J. Shlomi [169], M.J. Shochet [39], J. Shojaii [105], D.R. Shope [125], S. Shrestha [119,an], E.M. Shrif [33g], M.J. Shroff [165], P. Sicho [131], A.M. Sickles [162], E. Sideras Haddad [33g], A. Sidoti [23b], F. Siegert [50], Dj. Sijacki [15], R. Sikora [85a], F. Sili [91], J.M. Silva [20], M.V. Silva Oliveira [29], S.B. Silverstein [47a], S. Simion [66], R. Simoniello [36], E.L. Simpson [59], H. Simpson [146], L.R. Simpson [106], N.D. Simpson [99], S. Simsek [21d], S. Sindhu [55], P. Sinervo [155], S. Singh [155], S. Sinha [48], S. Sinha [102], M. Sioli [23b,23a], I. Siral [36], E. Sitnikova [48], S.Yu. Sivoklokov [37,*], J. Sjölin [47a,47b], A. Skaf [55], E. Skorda [99], P. Skubic [120], M. Slawinska [86], V. Smakhtin [169], B.H. Smart [134], J. Smiesko [36], S.Yu. Smirnov [37], Y. Smirnov [37], L.N. Smirnova [37,a], O. Smirnova [99], A.C. Smith [41], E.A. Smith [39], H.A. Smith [126], J.L. Smith [93], R. Smith [143], M. Smizanska [92], K. Smolek [132], A.A. Snesarev [37], S.R. Snider [155], H.L. Snoek [114], S. Snyder [29], R. Sobie [165,ab], A. Soffer [151], C.A. Solans Sanchez [36], E.Yu. Soldatov [37], U. Soldevila [163], A.A. Solodkov [37], S. Solomon [26], A. Soloshenko [38], K. Solovieva [54], O.V. Solovyanov [40], V. Solovyev [37], P. Sommer [36], A. Sonay [13], W.Y. Song [156b], J.M. Sonneveld [114], A. Sopczak [132], A.L. Sopio [97], F. Sopkova [28b], V. Sothilingam [63a], S. Sottocornola [68], R. Soualah [116b], Z. Soumaimi [35e], D. South [48], S. Spagnolo [70a,70b], M. Spalla [110], D. Sperlich [54], G. Spigo [36], M. Spina [146], S. Spinali [92], D.P. Spiteri [59], M. Spousta [133], E.J. Staats [34], A. Stabile [71a,71b], R. Stamen [63a], M. Stamenkovic [114], A. Stampekis [20], M. Standke [24], E. Stanecka [86], M.V. Stange [50], B. Stanislaus [17a], M.M. Stanitzki [48], B. Stapf [48], E.A. Starchenko [37], G.H. Stark [136], J. Stark [90a,af], D.M. Starko [156b], P. Staroba [131], P. Starovoitov [63a], S. Stärz [104], R. Staszewski [86], G. Stavropoulos [46], J. Steentoft [161], P. Steinberg [29], B. Stelzer [142,156a], H.J. Stelzer [129], O. Stelzer-Chilton [156a], H. Stenzel [58], T.J. Stevenson [146], G.A. Stewart [36], J.R. Stewart [121], M.C. Stockton [36], G. Stoicea [27b], M. Stolarski [130a], S. Stonjek [110], A. Straessner [50], J. Strandberg [144], S. Strandberg [47a,47b], M. Strauss [120], T. Strebler [90b], P. Strizenec [28b], R. Ströhmer [166], D.M. Strom [123], L.R. Strom [48], R. Stroynowski [44], A. Strubig [47a,47b], S.A. Stucci [29], B. Stugu [16], J. Stupak [120], N.A. Styles [48], D. Su [143], S. Su [62a], W. Su [62d], X. Su [62a,66], K. Sugizaki [153], V.V. Sulin [37], M.J. Sullivan [93], D.M.S. Sultan [78a,78b], L. Sultanaliyeva [37], S. Sultansoy [3b], T. Sumida [87], S. Sun [106], S. Sun [170], O. Sunneborn Gudnadottir [161], M.R. Sutton [146], H. Suzuki [157], M. Svatos [131], M. Swiatlowski [156a], T. Swirski [166], I. Sykora [28a], M. Sykora [133], T. Sykora [133], D. Ta [101], K. Tackmann [48,y], A. Taffard [160], R. Tafirout [156a], J.S. Tafoya Vargas [66], R. Takashima [88], E.P. Takeva [52], Y. Takubo [83], M. Talby [90b], A.A. Talyshev [37], K.C. Tam [64b], N.M. Tamir [151], A. Tanaka [153], J. Tanaka [153], R. Tanaka [66], M. Tanasini [57b,57a], Z. Tao [164], S. Tapia Araya [137f], S. Tapprogge [101],

A. Tarek Abouelfadl Mohamed [107], S. Tarem [150], K. Tariq [62b], G. Tarna [90b,27b], G.F. Tartarelli [71a], P. Tas [133], M. Tasevsky [131], E. Tassi [43b,43a], A.C. Tate [162], G. Tateno [153], Y. Tayalati [35e,aa], G.N. Taylor [105], W. Taylor [156b], H. Teagle[93], A.S. Tee [170], R. Teixeira De Lima [143], P. Teixeira-Dias [96], J.J. Teoh [155], K. Terashi [153], J. Terron [100], S. Terzo [13], M. Testa [53], R.J. Teuscher [155,ab], A. Thaler [79], O. Theiner [56], N. Themistokleous [52], T. Theveneaux-Pelzer [90b], O. Thielmann [171], D.W. Thomas[96], J.P. Thomas [20], E.A. Thompson [17a], P.D. Thompson [20], E. Thomson [128], Y. Tian [55], V. Tikhomirov [37,a], Yu.A. Tikhonov [37], S. Timoshenko[37], D. Timoshyn [133], E.X.L. Ting [1], P. Tipton [172], S.H. Tlou [33g], A. Tnourji [40], K. Todome [23b,23a], S. Todorova-Nova [133], S. Todt[50], M. Togawa [83], J. Tojo [89], S. Tokár [28a], K. Tokushuku [83], O. Toldaiev [68], R. Tombs [32], M. Tomoto [83,111], L. Tompkins [143,r], K.W. Topolnicki [85b], E. Torrence [123], H. Torres [90a,af], E. Torró Pastor [163], M. Toscani [30], C. Tosciri [39], M. Tost [11], D.R. Tovey [139], A. Traeet[16], I.S. Trandafir [27b], T. Trefzger [166], A. Tricoli [29], I.M. Trigger [156a], S. Trincaz-Duvoid [127], D.A. Trischuk [26], B. Trocmé [60], C. Troncon [71a], L. Truong [33c], M. Trzebinski [86], A. Trzupek [86], F. Tsai [145], M. Tsai [106], A. Tsiamis [152,f], P.V. Tsiareshka[37], S. Tsigaridas [156a], A. Tsirigotis [152,w], V. Tsiskaridze [155], E.G. Tskhadadze [149a], M. Tsopoulou [152,f], Y. Tsujikawa [87], I.I. Tsukerman [37], V. Tsulaia [17a], S. Tsuno [83], O. Tsur[150], K. Tsuri [118], D. Tsybychev [145], Y. Tu [64b], A. Tudorache [27b], V. Tudorache [27b], A.N. Tuna [36], S. Turchikhin [38], I. Turk Cakir [3a], R. Turra [71a], T. Turtuvshin [38,ac], P.M. Tuts [41], S. Tzamarias [152,f], P. Tzanis [10], E. Tzovara [101], K. Uchida[153], F. Ukegawa [157], P.A. Ulloa Poblete [137c,137b], E.N. Umaka [29], G. Unal [36], M. Unal [11], A. Undrus [29], G. Unel [160], J. Urban [28b], P. Urquijo [105], G. Usai [8], R. Ushioda [154], M. Usman [108], Z. Uysal [21b], L. Vacavant [90b], V. Vacek [132], B. Vachon [104], K.O.H. Vadla [125], T. Vafeiadis [36], A. Vaitkus [97], C. Valderanis [109], E. Valdes Santurio [47a,47b], M. Valente [156a], S. Valentinetti [23b,23a], A. Valero [163], E. Valiente Moreno [163], A. Vallier [90a,af], J.A. Valls Ferrer [163], D.R. Van Arneman [114], T.R. Van Daalen [138], A. Van Der Graaf [49], P. Van Gemmeren [6], M. Van Rijnbach [125,36], S. Van Stroud [97], I. Van Vulpen [114], M. Vanadia [76a,76b], W. Vandelli [36], M. Vandenbroucke [135], E.R. Vandewall [121], D. Vannicola [151], L. Vannoli [57b,57a], R. Vari [75a], E.W. Varnes [7], C. Varni [17a], T. Varol [148], D. Varouchas [66], L. Varriale [163], K.E. Varvell [147], M.E. Vasile [27b], L. Vaslin[40], G.A. Vasquez [165], F. Vazeille [40], T. Vazquez Schroeder [36], J. Veatch [31], V. Vecchio [102], M.J. Veen [103], I. Veliscek [126], L.M. Veloce [155], F. Veloso [130a,130c], S. Veneziano [75a], A. Ventura [70a,70b], A. Verbytskyi [110], M. Verducci [74a,74b], C. Vergis [24], M. Verissimo De Araujo [82b], W. Verkerke [114], J.C. Vermeulen [114], C. Vernieri [143], P.J. Verschuuren [96], M. Vessella [103], M.C. Vetterli [142,ak], A. Vgenopoulos [152,f], N. Viaux Maira [137f], T. Vickey [139], O.E. Vickey Boeriu [139], G.H.A. Viehhauser [126], L. Vigani [63b], M. Villa [23b,23a], M. Villaplana Perez [163], E.M. Villhauer[52], E. Vilucchi [53], M.G. Vincter [34], G.S. Virdee [20], A. Vishwakarma [52], A. Visibile[114], C. Vittori [36], I. Vivarelli [146], V. Vladimirov[167], E. Voevodina [110], F. Vogel [109], P. Vokac [132], J. Von Ahnen [48], E. Von Toerne [24], B. Vormwald [36], V. Vorobel [133], K. Vorobev [37], M. Vos [163], K. Voss [141], J.H. Vossebeld [93], M. Vozak [114], L. Vozdecky [95], N. Vranjes [15], M. Vranjes Milosavljevic [15], M. Vreeswijk [114], R. Vuillermet [36], O. Vujinovic [101], I. Vukotic [39], S. Wada [157], C. Wagner[103], J.M. Wagner [17a], W. Wagner [171], S. Wahdan [171], H. Wahlberg [91], R. Wakasa [157], M. Wakida [111], J. Walder [134], R. Walker [109], W. Walkowiak [141], A. Wall [128], T. Wamorkar [6], A.Z. Wang [170], C. Wang [101], C. Wang [62c], H. Wang [17a], J. Wang [64a], R.-J. Wang [101], R. Wang [61], R. Wang [6], S.M. Wang [148], S. Wang [62b], T. Wang [62a], W.T. Wang [80], W. Wang [14a], X. Wang [14c], X. Wang [162], X. Wang [62c], Y. Wang [62d], Y. Wang [14c], Z. Wang [106], Z. Wang [62d,51,62c], Z. Wang [106], A. Warburton [104], R.J. Ward [20], N. Warrack [59], A.T. Watson [20], H. Watson [59], M.F. Watson [20], E. Watton [59,134], G. Watts [138], B.M. Waugh [97], C. Weber [29], H.A. Weber [18],

M.S. Weber[19], S.M. Weber[63a], C. Wei[62a], Y. Wei[126], A.R. Weidberg[126], E.J. Weik[117], J. Weingarten[49], M. Weirich[101], C. Weiser[54], C.J. Wells[48], T. Wenaus[29], B. Wendland[49], T. Wengler[36], N.S. Wenke[110], N. Wermes[24], M. Wessels[63a], K. Whalen[123], A.M. Wharton[92], A.S. White[61], A. White[8], M.J. White[1], D. Whiteson[160], L. Wickremasinghe[124], W. Wiedenmann[170], C. Wiel[50], M. Wielers[134], C. Wiglesworth[42], D.J. Wilbern[120], H.G. Wilkens[36], D.M. Williams[41], H.H. Williams[128], S. Williams[32], S. Willocq[103], B.J. Wilson[102], P.J. Windischhofer[39], F.I. Winkel[30], F. Winklmeier[123], B.T. Winter[54], J.K. Winter[102], M. Wittgen[143], M. Wobisch[98], Z. Wolffs[114], R. Wölker[126], J. Wollrath[160], M.W. Wolter[86], H. Wolters[130a,130c], A.F. Wongel[48], S.D. Worm[48], B.K. Wosiek[86], K.W. Woźniak[86], S. Wozniewski[55], K. Wraight[59], C. Wu[20], J. Wu[14a,14e], M. Wu[64a], M. Wu[113], S.L. Wu[170], X. Wu[56], Y. Wu[62a], Z. Wu[135], J. Wuerzinger[110], T.R. Wyatt[102], B.M. Wynne[52], S. Xella[42], L. Xia[14c], M. Xia[14b], J. Xiang[64c], X. Xiao[106], M. Xie[62a], X. Xie[62a], S. Xin[14a,14e], J. Xiong[17a], D. Xu[14a], H. Xu[62a], L. Xu[62a], R. Xu[128], T. Xu[106], Y. Xu[14b], Z. Xu[52], Z. Xu[14a], B. Yabsley[147], S. Yacoob[33a], N. Yamaguchi[89], Y. Yamaguchi[154], E. Yamashita[153], H. Yamauchi[157], T. Yamazaki[17a], Y. Yamazaki[84], J. Yan[62c], S. Yan[126], Z. Yan[25], H.J. Yang[62c,62d], H.T. Yang[62a], S. Yang[62a], T. Yang[64c], X. Yang[62a], X. Yang[14a], Y. Yang[44], Y. Yang[62a], Z. Yang[62a], W-M. Yao[17a], Y.C. Yap[48], H. Ye[14c], H. Ye[55], J. Ye[44], S. Ye[29], X. Ye[62a], Y. Yeh[97], I. Yeletskikh[38], B.K. Yeo[17a], M.R. Yexley[97], P. Yin[41], K. Yorita[168], S. Younas[27b], C.J.S. Young[54], C. Young[143], Y. Yu[62a], M. Yuan[106], R. Yuan[62b,l], L. Yue[97], M. Zaazoua[62a], B. Zabinski[86], E. Zaid[52], T. Zakareishvili[149b], N. Zakharchuk[34], S. Zambito[56], J.A. Zamora Saa[137d,137b], J. Zang[153], D. Zanzi[54], O. Zaplatilek[132], C. Zeitnitz[171], H. Zeng[14a], J.C. Zeng[162], D.T. Zenger Jr[26], O. Zenin[37], T. Ženiš[28a], S. Zenz[95], S. Zerradi[35a], D. Zerwas[66], M. Zhai[14a,14e], B. Zhang[14c], D.F. Zhang[139], J. Zhang[62b], J. Zhang[6], K. Zhang[14a,14e], L. Zhang[14c], P. Zhang[14a,14e], R. Zhang[170], S. Zhang[106], T. Zhang[153], X. Zhang[62c], X. Zhang[62b], Y. Zhang[62c,5], Y. Zhang[97], Z. Zhang[17a], Z. Zhang[66], H. Zhao[138], P. Zhao[51], T. Zhao[62b], Y. Zhao[136], Z. Zhao[62a], A. Zhemchugov[38], K. Zheng[162], X. Zheng[62a], Z. Zheng[143], D. Zhong[162], B. Zhou[106], H. Zhou[7], N. Zhou[62c], Y. Zhou[7], C.G. Zhu[62b], J. Zhu[106], Y. Zhu[62c], Y. Zhu[62a], X. Zhuang[14a], K. Zhukov[37], V. Zhulanov[37], N.I. Zimine[38], J. Zinsser[63b], M. Ziolkowski[141], L. Živković[15], A. Zoccoli[23b,23a], K. Zoch[56], T.G. Zorbas[139], O. Zormpa[46], W. Zou[41], L. Zwalinski[36].

[1]Department of Physics, University of Adelaide, Adelaide; Australia.
[2]Department of Physics, University of Alberta, Edmonton AB; Canada.
[3(a)]Department of Physics, Ankara University, Ankara;[(b)]Division of Physics, TOBB University of Economics and Technology, Ankara; Türkiye.
[4]LAPP, Université Savoie Mont Blanc, CNRS/IN2P3, Annecy; France.
[5]APC, Université Paris Cité, CNRS/IN2P3, Paris; France.
[6]High Energy Physics Division, Argonne National Laboratory, Argonne IL; United States of America.
[7]Department of Physics, University of Arizona, Tucson AZ; United States of America.
[8]Department of Physics, University of Texas at Arlington, Arlington TX; United States of America.
[9]Physics Department, National and Kapodistrian University of Athens, Athens; Greece.
[10]Physics Department, National Technical University of Athens, Zografou; Greece.
[11]Department of Physics, University of Texas at Austin, Austin TX; United States of America.
[12]Institute of Physics, Azerbaijan Academy of Sciences, Baku; Azerbaijan.
[13]Institut de Física d'Altes Energies (IFAE), Barcelona Institute of Science and Technology, Barcelona; Spain.

[14(a)]Institute of High Energy Physics, Chinese Academy of Sciences, Beijing;[(b)]Physics Department, Tsinghua University, Beijing;[(c)]Department of Physics, Nanjing University, Nanjing;[(d)]School of Science, Shenzhen Campus of Sun Yat-sen University;[(e)]University of Chinese Academy of Science (UCAS), Beijing; China.
[15]Institute of Physics, University of Belgrade, Belgrade; Serbia.
[16]Department for Physics and Technology, University of Bergen, Bergen; Norway.
[17(a)]Physics Division, Lawrence Berkeley National Laboratory, Berkeley CA;[(b)]University of California, Berkeley CA; United States of America.
[18]Institut für Physik, Humboldt Universität zu Berlin, Berlin; Germany.
[19]Albert Einstein Center for Fundamental Physics and Laboratory for High Energy Physics, University of Bern, Bern; Switzerland.
[20]School of Physics and Astronomy, University of Birmingham, Birmingham; United Kingdom.
[21(a)]Department of Physics, Bogazici University, Istanbul;[(b)]Department of Physics Engineering, Gaziantep University, Gaziantep;[(c)]Department of Physics, Istanbul University, Istanbul;[(d)]Istinye University, Sariyer, Istanbul; Türkiye.
[22(a)]Facultad de Ciencias y Centro de Investigaciónes, Universidad Antonio Nariño, Bogotá;[(b)]Departamento de Física, Universidad Nacional de Colombia, Bogotá; Colombia.
[23(a)]Dipartimento di Fisica e Astronomia A. Righi, Università di Bologna, Bologna;[(b)]INFN Sezione di Bologna; Italy.
[24]Physikalisches Institut, Universität Bonn, Bonn; Germany.
[25]Department of Physics, Boston University, Boston MA; United States of America.
[26]Department of Physics, Brandeis University, Waltham MA; United States of America.
[27(a)]Transilvania University of Brasov, Brasov;[(b)]Horia Hulubei National Institute of Physics and Nuclear Engineering, Bucharest;[(c)]Department of Physics, Alexandru Ioan Cuza University of Iasi, Iasi;[(d)]National Institute for Research and Development of Isotopic and Molecular Technologies, Physics Department, Cluj-Napoca;[(e)]University Politehnica Bucharest, Bucharest;[(f)]West University in Timisoara, Timisoara;[(g)]Faculty of Physics, University of Bucharest, Bucharest; Romania.
[28(a)]Faculty of Mathematics, Physics and Informatics, Comenius University, Bratislava;[(b)]Department of Subnuclear Physics, Institute of Experimental Physics of the Slovak Academy of Sciences, Kosice; Slovak Republic.
[29]Physics Department, Brookhaven National Laboratory, Upton NY; United States of America.
[30]Universidad de Buenos Aires, Facultad de Ciencias Exactas y Naturales, Departamento de Física, y CONICET, Instituto de Física de Buenos Aires (IFIBA), Buenos Aires; Argentina.
[31]California State University, CA; United States of America.
[32]Cavendish Laboratory, University of Cambridge, Cambridge; United Kingdom.
[33(a)]Department of Physics, University of Cape Town, Cape Town;[(b)]iThemba Labs, Western Cape;[(c)]Department of Mechanical Engineering Science, University of Johannesburg, Johannesburg;[(d)]National Institute of Physics, University of the Philippines Diliman (Philippines);[(e)]University of South Africa, Department of Physics, Pretoria;[(f)]University of Zululand, KwaDlangezwa;[(g)]School of Physics, University of the Witwatersrand, Johannesburg; South Africa.
[34]Department of Physics, Carleton University, Ottawa ON; Canada.
[35(a)]Faculté des Sciences Ain Chock, Réseau Universitaire de Physique des Hautes Energies - Université Hassan II, Casablanca;[(b)]Faculté des Sciences, Université Ibn-Tofail, Kénitra;[(c)]Faculté des Sciences Semlalia, Université Cadi Ayyad, LPHEA-Marrakech;[(d)]LPMR, Faculté des Sciences, Université Mohamed Premier, Oujda;[(e)]Faculté des sciences, Université Mohammed V, Rabat;[(f)]Institute of Applied Physics, Mohammed VI Polytechnic University, Ben Guerir; Morocco.
[36]CERN, Geneva; Switzerland.

[37]Affiliated with an institute covered by a cooperation agreement with CERN.
[38]Affiliated with an international laboratory covered by a cooperation agreement with CERN.
[39]Enrico Fermi Institute, University of Chicago, Chicago IL; United States of America.
[40]LPC, Université Clermont Auvergne, CNRS/IN2P3, Clermont-Ferrand; France.
[41]Nevis Laboratory, Columbia University, Irvington NY; United States of America.
[42]Niels Bohr Institute, University of Copenhagen, Copenhagen; Denmark.
[43(a)]Dipartimento di Fisica, Università della Calabria, Rende;[(b)]INFN Gruppo Collegato di Cosenza, Laboratori Nazionali di Frascati; Italy.
[44]Physics Department, Southern Methodist University, Dallas TX; United States of America.
[45]Physics Department, University of Texas at Dallas, Richardson TX; United States of America.
[46]National Centre for Scientific Research "Demokritos", Agia Paraskevi; Greece.
[47(a)]Department of Physics, Stockholm University;[(b)]Oskar Klein Centre, Stockholm; Sweden.
[48]Deutsches Elektronen-Synchrotron DESY, Hamburg and Zeuthen; Germany.
[49]Fakultät Physik , Technische Universität Dortmund, Dortmund; Germany.
[50]Institut für Kern- und Teilchenphysik, Technische Universität Dresden, Dresden; Germany.
[51]Department of Physics, Duke University, Durham NC; United States of America.
[52]SUPA - School of Physics and Astronomy, University of Edinburgh, Edinburgh; United Kingdom.
[53]INFN e Laboratori Nazionali di Frascati, Frascati; Italy.
[54]Physikalisches Institut, Albert-Ludwigs-Universität Freiburg, Freiburg; Germany.
[55]II. Physikalisches Institut, Georg-August-Universität Göttingen, Göttingen; Germany.
[56]Département de Physique Nucléaire et Corpusculaire, Université de Genève, Genève; Switzerland.
[57(a)]Dipartimento di Fisica, Università di Genova, Genova;[(b)]INFN Sezione di Genova; Italy.
[58]II. Physikalisches Institut, Justus-Liebig-Universität Giessen, Giessen; Germany.
[59]SUPA - School of Physics and Astronomy, University of Glasgow, Glasgow; United Kingdom.
[60]LPSC, Université Grenoble Alpes, CNRS/IN2P3, Grenoble INP, Grenoble; France.
[61]Laboratory for Particle Physics and Cosmology, Harvard University, Cambridge MA; United States of America.
[62(a)]Department of Modern Physics and State Key Laboratory of Particle Detection and Electronics, University of Science and Technology of China, Hefei;[(b)]Institute of Frontier and Interdisciplinary Science and Key Laboratory of Particle Physics and Particle Irradiation (MOE), Shandong University, Qingdao;[(c)]School of Physics and Astronomy, Shanghai Jiao Tong University, Key Laboratory for Particle Astrophysics and Cosmology (MOE), SKLPPC, Shanghai;[(d)]Tsung-Dao Lee Institute, Shanghai; China.
[63(a)]Kirchhoff-Institut für Physik, Ruprecht-Karls-Universität Heidelberg, Heidelberg;[(b)]Physikalisches Institut, Ruprecht-Karls-Universität Heidelberg, Heidelberg; Germany.
[64(a)]Department of Physics, Chinese University of Hong Kong, Shatin, N.T., Hong Kong;[(b)]Department of Physics, University of Hong Kong, Hong Kong;[(c)]Department of Physics and Institute for Advanced Study, Hong Kong University of Science and Technology, Clear Water Bay, Kowloon, Hong Kong; China.
[65]Department of Physics, National Tsing Hua University, Hsinchu; Taiwan.
[66]IJCLab, Université Paris-Saclay, CNRS/IN2P3, 91405, Orsay; France.
[67]Centro Nacional de Microelectrónica (IMB-CNM-CSIC), Barcelona; Spain.
[68]Department of Physics, Indiana University, Bloomington IN; United States of America.
[69(a)]INFN Gruppo Collegato di Udine, Sezione di Trieste, Udine;[(b)]ICTP, Trieste;[(c)]Dipartimento Politecnico di Ingegneria e Architettura, Università di Udine, Udine; Italy.
[70(a)]INFN Sezione di Lecce;[(b)]Dipartimento di Matematica e Fisica, Università del Salento, Lecce; Italy.
[71(a)]INFN Sezione di Milano;[(b)]Dipartimento di Fisica, Università di Milano, Milano; Italy.
[72(a)]INFN Sezione di Napoli;[(b)]Dipartimento di Fisica, Università di Napoli, Napoli; Italy.
[73(a)]INFN Sezione di Pavia;[(b)]Dipartimento di Fisica, Università di Pavia, Pavia; Italy.

[74](a)INFN Sezione di Pisa;(b)Dipartimento di Fisica E. Fermi, Università di Pisa, Pisa; Italy.
[75](a)INFN Sezione di Roma;(b)Dipartimento di Fisica, Sapienza Università di Roma, Roma; Italy.
[76](a)INFN Sezione di Roma Tor Vergata;(b)Dipartimento di Fisica, Università di Roma Tor Vergata, Roma; Italy.
[77](a)INFN Sezione di Roma Tre;(b)Dipartimento di Matematica e Fisica, Università Roma Tre, Roma; Italy.
[78](a)INFN-TIFPA;(b)Università degli Studi di Trento, Trento; Italy.
[79]Universität Innsbruck, Department of Astro and Particle Physics, Innsbruck; Austria.
[80]University of Iowa, Iowa City IA; United States of America.
[81]Department of Physics and Astronomy, Iowa State University, Ames IA; United States of America.
[82](a)Departamento de Engenharia Elétrica, Universidade Federal de Juiz de Fora (UFJF), Juiz de Fora;(b)Universidade Federal do Rio De Janeiro COPPE/EE/IF, Rio de Janeiro;(c)Instituto de Física, Universidade de São Paulo, São Paulo;(d)Rio de Janeiro State University, Rio de Janeiro; Brazil.
[83]KEK, High Energy Accelerator Research Organization, Tsukuba; Japan.
[84]Graduate School of Science, Kobe University, Kobe; Japan.
[85](a)AGH University of Krakow, Faculty of Physics and Applied Computer Science, Krakow;(b)Marian Smoluchowski Institute of Physics, Jagiellonian University, Krakow; Poland.
[86]Institute of Nuclear Physics Polish Academy of Sciences, Krakow; Poland.
[87]Faculty of Science, Kyoto University, Kyoto; Japan.
[88]Kyoto University of Education, Kyoto; Japan.
[89]Research Center for Advanced Particle Physics and Department of Physics, Kyushu University, Fukuoka ; Japan.
[90](a)L2IT, Université de Toulouse, CNRS/IN2P3, UPS, Toulouse;(b)CPPM, Aix-Marseille Université, CNRS/IN2P3, Marseille; France.
[91]Instituto de Física La Plata, Universidad Nacional de La Plata and CONICET, La Plata; Argentina.
[92]Physics Department, Lancaster University, Lancaster; United Kingdom.
[93]Oliver Lodge Laboratory, University of Liverpool, Liverpool; United Kingdom.
[94]Department of Experimental Particle Physics, Jožef Stefan Institute and Department of Physics, University of Ljubljana, Ljubljana; Slovenia.
[95]School of Physics and Astronomy, Queen Mary University of London, London; United Kingdom.
[96]Department of Physics, Royal Holloway University of London, Egham; United Kingdom.
[97]Department of Physics and Astronomy, University College London, London; United Kingdom.
[98]Louisiana Tech University, Ruston LA; United States of America.
[99]Fysiska institutionen, Lunds universitet, Lund; Sweden.
[100]Departamento de Física Teorica C-15 and CIAFF, Universidad Autónoma de Madrid, Madrid; Spain.
[101]Institut für Physik, Universität Mainz, Mainz; Germany.
[102]School of Physics and Astronomy, University of Manchester, Manchester; United Kingdom.
[103]Department of Physics, University of Massachusetts, Amherst MA; United States of America.
[104]Department of Physics, McGill University, Montreal QC; Canada.
[105]School of Physics, University of Melbourne, Victoria; Australia.
[106]Department of Physics, University of Michigan, Ann Arbor MI; United States of America.
[107]Department of Physics and Astronomy, Michigan State University, East Lansing MI; United States of America.
[108]Group of Particle Physics, University of Montreal, Montreal QC; Canada.
[109]Fakultät für Physik, Ludwig-Maximilians-Universität München, München; Germany.
[110]Max-Planck-Institut für Physik (Werner-Heisenberg-Institut), München; Germany.
[111]Graduate School of Science and Kobayashi-Maskawa Institute, Nagoya University, Nagoya; Japan.

[112]Department of Physics and Astronomy, University of New Mexico, Albuquerque NM; United States of America.
[113]Institute for Mathematics, Astrophysics and Particle Physics, Radboud University/Nikhef, Nijmegen; Netherlands.
[114]Nikhef National Institute for Subatomic Physics and University of Amsterdam, Amsterdam; Netherlands.
[115]Department of Physics, Northern Illinois University, DeKalb IL; United States of America.
[116(a)]New York University Abu Dhabi, Abu Dhabi;[(b)]University of Sharjah, Sharjah; United Arab Emirates.
[117]Department of Physics, New York University, New York NY; United States of America.
[118]Ochanomizu University, Otsuka, Bunkyo-ku, Tokyo; Japan.
[119]Ohio State University, Columbus OH; United States of America.
[120]Homer L. Dodge Department of Physics and Astronomy, University of Oklahoma, Norman OK; United States of America.
[121]Department of Physics, Oklahoma State University, Stillwater OK; United States of America.
[122]Palacký University, Joint Laboratory of Optics, Olomouc; Czech Republic.
[123]Institute for Fundamental Science, University of Oregon, Eugene, OR; United States of America.
[124]Graduate School of Science, Osaka University, Osaka; Japan.
[125]Department of Physics, University of Oslo, Oslo; Norway.
[126]Department of Physics, Oxford University, Oxford; United Kingdom.
[127]LPNHE, Sorbonne Université, Université Paris Cité, CNRS/IN2P3, Paris; France.
[128]Department of Physics, University of Pennsylvania, Philadelphia PA; United States of America.
[129]Department of Physics and Astronomy, University of Pittsburgh, Pittsburgh PA; United States of America.
[130(a)]Laboratório de Instrumentação e Física Experimental de Partículas - LIP, Lisboa;[(b)]Departamento de Física, Faculdade de Ciências, Universidade de Lisboa, Lisboa;[(c)]Departamento de Física, Universidade de Coimbra, Coimbra;[(d)]Centro de Física Nuclear da Universidade de Lisboa, Lisboa;[(e)]Departamento de Física, Universidade do Minho, Braga;[(f)]Departamento de Física Teórica y del Cosmos, Universidad de Granada, Granada (Spain);[(g)]Departamento de Física, Instituto Superior Técnico, Universidade de Lisboa, Lisboa; Portugal.
[131]Institute of Physics of the Czech Academy of Sciences, Prague; Czech Republic.
[132]Czech Technical University in Prague, Prague; Czech Republic.
[133]Charles University, Faculty of Mathematics and Physics, Prague; Czech Republic.
[134]Particle Physics Department, Rutherford Appleton Laboratory, Didcot; United Kingdom.
[135]IRFU, CEA, Université Paris-Saclay, Gif-sur-Yvette; France.
[136]Santa Cruz Institute for Particle Physics, University of California Santa Cruz, Santa Cruz CA; United States of America.
[137(a)]Departamento de Física, Pontificia Universidad Católica de Chile, Santiago;[(b)]Millennium Institute for Subatomic physics at high energy frontier (SAPHIR), Santiago;[(c)]Instituto de Investigación Multidisciplinario en Ciencia y Tecnología, y Departamento de Física, Universidad de La Serena;[(d)]Universidad Andres Bello, Department of Physics, Santiago;[(e)]Instituto de Alta Investigación, Universidad de Tarapacá, Arica;[(f)]Departamento de Física, Universidad Técnica Federico Santa María, Valparaíso; Chile.
[138]Department of Physics, University of Washington, Seattle WA; United States of America.
[139]Department of Physics and Astronomy, University of Sheffield, Sheffield; United Kingdom.
[140]Department of Physics, Shinshu University, Nagano; Japan.
[141]Department Physik, Universität Siegen, Siegen; Germany.

[142]Department of Physics, Simon Fraser University, Burnaby BC; Canada.
[143]SLAC National Accelerator Laboratory, Stanford CA; United States of America.
[144]Department of Physics, Royal Institute of Technology, Stockholm; Sweden.
[145]Departments of Physics and Astronomy, Stony Brook University, Stony Brook NY; United States of America.
[146]Department of Physics and Astronomy, University of Sussex, Brighton; United Kingdom.
[147]School of Physics, University of Sydney, Sydney; Australia.
[148]Institute of Physics, Academia Sinica, Taipei; Taiwan.
[149(a)]E. Andronikashvili Institute of Physics, Iv. Javakhishvili Tbilisi State University, Tbilisi;[(b)]High Energy Physics Institute, Tbilisi State University, Tbilisi;[(c)]University of Georgia, Tbilisi; Georgia.
[150]Department of Physics, Technion, Israel Institute of Technology, Haifa; Israel.
[151]Raymond and Beverly Sackler School of Physics and Astronomy, Tel Aviv University, Tel Aviv; Israel.
[152]Department of Physics, Aristotle University of Thessaloniki, Thessaloniki; Greece.
[153]International Center for Elementary Particle Physics and Department of Physics, University of Tokyo, Tokyo; Japan.
[154]Department of Physics, Tokyo Institute of Technology, Tokyo; Japan.
[155]Department of Physics, University of Toronto, Toronto ON; Canada.
[156(a)]TRIUMF, Vancouver BC;[(b)]Department of Physics and Astronomy, York University, Toronto ON; Canada.
[157]Division of Physics and Tomonaga Center for the History of the Universe, Faculty of Pure and Applied Sciences, University of Tsukuba, Tsukuba; Japan.
[158]Department of Physics and Astronomy, Tufts University, Medford MA; United States of America.
[159]United Arab Emirates University, Al Ain; United Arab Emirates.
[160]Department of Physics and Astronomy, University of California Irvine, Irvine CA; United States of America.
[161]Department of Physics and Astronomy, University of Uppsala, Uppsala; Sweden.
[162]Department of Physics, University of Illinois, Urbana IL; United States of America.
[163]Instituto de Física Corpuscular (IFIC), Centro Mixto Universidad de Valencia - CSIC, Valencia; Spain.
[164]Department of Physics, University of British Columbia, Vancouver BC; Canada.
[165]Department of Physics and Astronomy, University of Victoria, Victoria BC; Canada.
[166]Fakultät für Physik und Astronomie, Julius-Maximilians-Universität Würzburg, Würzburg; Germany.
[167]Department of Physics, University of Warwick, Coventry; United Kingdom.
[168]Waseda University, Tokyo; Japan.
[169]Department of Particle Physics and Astrophysics, Weizmann Institute of Science, Rehovot; Israel.
[170]Department of Physics, University of Wisconsin, Madison WI; United States of America.
[171]Fakultät für Mathematik und Naturwissenschaften, Fachgruppe Physik, Bergische Universität Wuppertal, Wuppertal; Germany.
[172]Department of Physics, Yale University, New Haven CT; United States of America.
[a] Also Affiliated with an institute covered by a cooperation agreement with CERN.
[b] Also at An-Najah National University, Nablus; Palestine.
[c] Also at APC, Université Paris Cité, CNRS/IN2P3, Paris; France.
[d] Also at Borough of Manhattan Community College, City University of New York, New York NY; United States of America.
[e] Also at Center for High Energy Physics, Peking University; China.
[f] Also at Center for Interdisciplinary Research and Innovation (CIRI-AUTH), Thessaloniki; Greece.
[g] Also at Centro Studi e Ricerche Enrico Fermi; Italy.
[h] Also at CERN, Geneva; Switzerland.

[i] Also at Département de Physique Nucléaire et Corpusculaire, Université de Genève, Genève; Switzerland.
[j] Also at Departament de Fisica de la Universitat Autonoma de Barcelona, Barcelona; Spain.
[k] Also at Department of Financial and Management Engineering, University of the Aegean, Chios; Greece.
[l] Also at Department of Physics and Astronomy, Michigan State University, East Lansing MI; United States of America.
[m] Also at Department of Physics and Astronomy, University of Victoria, Victoria BC; Canada.
[n] Also at Department of Physics, Ben Gurion University of the Negev, Beer Sheva; Israel.
[o] Also at Department of Physics, California State University, Sacramento; United States of America.
[p] Also at Department of Physics, King's College London, London; United Kingdom.
[q] Also at Department of Physics, Royal Holloway University of London, Egham; United Kingdom.
[r] Also at Department of Physics, Stanford University, Stanford CA; United States of America.
[s] Also at Department of Physics, University of Fribourg, Fribourg; Switzerland.
[t] Also at Department of Physics, University of Thessaly; Greece.
[u] Also at Department of Physics, Westmont College, Santa Barbara; United States of America.
[v] Also at Fakultät für Mathematik und Naturwissenschaften, Fachgruppe Physik, Bergische Universität Wuppertal, Wuppertal; Germany.
[w] Also at Hellenic Open University, Patras; Greece.
[x] Also at Institucio Catalana de Recerca i Estudis Avancats, ICREA, Barcelona; Spain.
[y] Also at Institut für Experimentalphysik, Universität Hamburg, Hamburg; Germany.
[z] Also at Institute for Nuclear Research and Nuclear Energy (INRNE) of the Bulgarian Academy of Sciences, Sofia; Bulgaria.
[aa] Also at Institute of Applied Physics, Mohammed VI Polytechnic University, Ben Guerir; Morocco.
[ab] Also at Institute of Particle Physics (IPP); Canada.
[ac] Also at Institute of Physics and Technology, Ulaanbaatar; Mongolia.
[ad] Also at Institute of Physics, Azerbaijan Academy of Sciences, Baku; Azerbaijan.
[ae] Also at Institute of Theoretical Physics, Ilia State University, Tbilisi; Georgia.
[af] Also at L2IT, Université de Toulouse, CNRS/IN2P3, UPS, Toulouse; France.
[ag] Also at Lawrence Livermore National Laboratory, Livermore; United States of America.
[ah] Also at National Institute of Physics, University of the Philippines Diliman (Philippines); Philippines.
[ai] Also at Technical University of Munich, Munich; Germany.
[aj] Also at The Collaborative Innovation Center of Quantum Matter (CICQM), Beijing; China.
[ak] Also at TRIUMF, Vancouver BC; Canada.
[al] Also at Università di Napoli Parthenope, Napoli; Italy.
[am] Also at University of Colorado Boulder, Department of Physics, Colorado; United States of America.
[an] Also at Washington College, Chestertown, MD; United States of America.
[ao] Also at Yeditepe University, Physics Department, Istanbul; Türkiye.
[*] Deceased